

INFORMATION TO USERS

This manuscript has been reproduced from the microfilm master. UMI films the text directly from the original or copy submitted. Thus, some thesis and dissertation copies are in typewriter face, while others may be from any type of computer printer.

The quality of this reproduction is dependent upon the quality of the copy submitted. Broken or indistinct print, colored or poor quality illustrations and photographs, print bleedthrough, substandard margins, and improper alignment can adversely affect reproduction.

In the unlikely event that the author did not send UMI a complete manuscript and there are missing pages, these will be noted. Also, if unauthorized copyright material had to be removed, a note will indicate the deletion.

Oversize materials (e.g., maps, drawings, charts) are reproduced by sectioning the original, beginning at the upper left-hand corner and continuing from left to right in equal sections with small overlaps. Each original is also photographed in one exposure and is included in reduced form at the back of the book.

Photographs included in the original manuscript have been reproduced xerographically in this copy. Higher quality 6" x 9" black and white photographic prints are available for any photographs or illustrations appearing in this copy for an additional charge. Contact UMI directly to order.

UMI

A Bell & Howell Information Company
300 North Zeeb Road, Ann Arbor MI 48106-1346 USA
313/761-4700 800/521-0600



University of Alberta

Stochastic Simulation of Concentration Fluctuations for an Effective
Toxic Load Model

by

Trevor Lloyd Hilderman



A thesis submitted to the Faculty of Graduate Studies and Research in partial
fulfillment of the requirements for the degree of Master of Science

Department of Mechanical Engineering

Edmonton, Alberta
Fall 1997



National Library
of Canada

Acquisitions and
Bibliographic Services

395 Wellington Street
Ottawa ON K1A 0N4
Canada

Bibliothèque nationale
du Canada

Acquisitions et
services bibliographiques

395, rue Wellington
Ottawa ON K1A 0N4
Canada

Your file Votre référence

Our file Notre référence

The author has granted a non-exclusive licence allowing the National Library of Canada to reproduce, loan, distribute or sell copies of this thesis in microform, paper or electronic formats.

The author retains ownership of the copyright in this thesis. Neither the thesis nor substantial extracts from it may be printed or otherwise reproduced without the author's permission.

L'auteur a accordé une licence non exclusive permettant à la Bibliothèque nationale du Canada de reproduire, prêter, distribuer ou vendre des copies de cette thèse sous la forme de microfiche/film, de reproduction sur papier ou sur format électronique.

L'auteur conserve la propriété du droit d'auteur qui protège cette thèse. Ni la thèse ni des extraits substantiels de celle-ci ne doivent être imprimés ou autrement reproduits sans son autorisation.

0-612-22604-2

University of Alberta

Library Release Form

Name of Author: Trevor Lloyd Hilderman

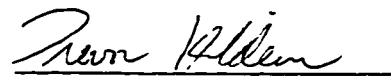
Title of Thesis: Stochastic Simulation of Concentration Fluctuations for an Effective Toxic Load Model

Degree: Master of Science

Year this Degree Granted: 1997

Permission is hereby granted to the University of Alberta to reproduce single copies of this thesis and to lend or sell such copies for private, scholarly, or scientific research purposes only.

The author reserves all other publication and other rights in association with the copyright in the thesis, and except as hereinbefore provided, neither the thesis nor any substantial portion thereof may be printed or otherwise reproduced in any material form whatever without the author's prior written permission.



Trevor Lloyd Hilderman
22 Greenborough Crescent,
Sherwood Park, Alberta,
Canada T8A 5G5

Date: Sept 30, 1997.

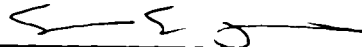
University of Alberta

Faculty of Graduate Studies and Research

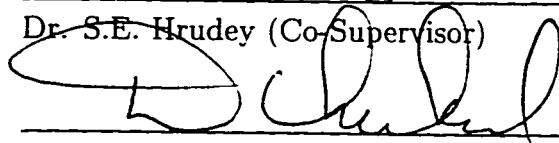
The undersigned certify that they have read, and recommend to the Faculty of Graduate Studies and Research for acceptance, a thesis entitled Stochastic Simulation of Concentration Fluctuations for an Effective Toxic Load Model submitted by Trevor Lloyd Hilderman in partial fulfillment of the requirements for the degree of Master of Science.



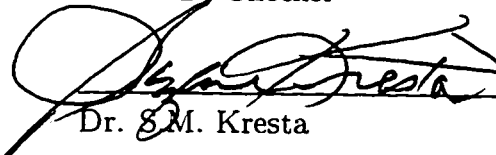
Dr. D.J. Wilson (Supervisor)



Dr. S.E. Hrudehy (Co-Supervisor)



Dr. M.D. Checkel



Dr. S.M. Kresta

Date: Sept 26/97

Abstract

This thesis presents two unpublished papers that provide tools to address two important complications in predicting the hazards caused by an atmospheric gas release: random fluctuations in exposure concentration at a fixed receptor location in a point source plume, and a lack of realistic models for estimating the acute toxicity of fluctuating concentration exposures.

A stochastic simulation of intermittent concentration fluctuations was developed from the assumption that the concentration fluctuations at a fixed receptor can be modelled as a first order Markov process. A clipped lognormal probability density function was used to describe the intermittent concentration fluctuations. The accuracy of the simulation was confirmed by comparing simulated first derivatives of concentration with respect to time and simulated concentration level upcrossing rates with measurements of concentration fluctuations in a scale model plume in a water channel.

An effective toxic load model with three receptor response parameters was proposed to provide a more realistic model of toxicity than the current exposure toxic load model that has no receptor parameters. The receptor response factors included were an uptake time constant, a recovery time constant, and a saturation concentration. This model was tested using the simulated time series produced by the stochastic model. A hydrogen sulphide exposure was considered and the effective toxic load model was found to provide more realistic estimates of the fatalities from a hydrogen sulphide release than the conventional exposure toxic load calculations.

Contents

1	Introduction	1
1.1	Simulating Concentration Fluctuations	2
1.2	Estimating Toxicity from Fluctuating Concentrations	3
1.3	Release Scenarios Considered	3
1.4	Stochastic Fluctuation Modelling	4
1.5	Toxicity Modelling	6
1.5.1	Threshold Toxicity Models	7
1.5.2	Data Based Toxicity Models	8
1.5.3	Mechanistic Biological Models	9
1.6	Hydrogen Sulphide Toxicity	11
	References	14
2	Stochastic Simulation of Intermittent Concentration Fluctuations	16
2.1	Introduction	16
2.2	Probability Distributions of Intermittent Time Series	18
2.2.1	Shifted and Clipped Lognormals	19
2.2.2	Physical Interpretation of the Shifted Lognormal	20
2.3	Stochastic Model for Fluctuations	21
2.3.1	Stochastic Differential Equation	22
2.3.2	Fokker-Planck Constraint	23
2.3.3	Functional Relations for a and b	24
2.4	Clipped Lognormal Distribution	26
2.4.1	Normalized Concentrations	27
2.4.2	Lognormal Distribution	28
2.4.3	Intermittency Factor of Clipped Lognormal	28
2.4.4	Fluctuation Intensity of Clipped Lognormal	29
2.4.5	Lognormal in c_+ Coordinates	31
2.5	Generating Stochastic Time Series	32
2.5.1	Time Scales of Intermittent and Non-Intermittent Time Series	34
2.5.2	Time Step for Molecular Diffusion Cutoff	35

2.6	Concentration Fluctuation Measurements	36
2.6.1	Water Channel Description	36
2.6.2	Data Collection and Processing	37
2.6.3	Frequency Spectrum of Experimental Data Compared to the Simulation	39
2.7	Comparison of Experimental Data and Clipped Lognormal pdf	40
2.7.1	Exceedance Probability	41
2.8	Stochastic Model Performance	41
2.8.1	Filtering the Stochastic Simulation	42
2.8.2	Time Derivative of Concentration	43
2.8.3	Concentration Level Upcrossing Rates	44
2.9	Summary and Conclusions	45
	References	63
3	A Model for Effective Toxic Load from a Hazardous Gas Release	65
3.1	Introduction	65
3.2	Exposure Toxic Load Model	69
3.2.1	Probit Method	69
3.2.2	Mean Concentration Toxic Load	70
3.2.3	Instantaneous Exposure Toxic Load	71
3.3	Effective Toxic Load	72
3.3.1	Uptake Time Constant τ_{up}	72
3.3.2	Recovery Time Constant τ_r	74
3.3.3	Saturation Concentration C_s	75
3.3.4	Effective Toxic Load Model	76
3.4	Concentration Fluctuations in Plumes	77
3.4.1	Intermittency Factor	77
3.4.2	Mean Concentration	78
3.4.3	Fluctuation Intensity	79
3.4.4	Fluctuation Time Scale	80
3.5	Parametric Study	80
3.5.1	Toxic Load Ratio (TLR)	81
3.5.2	Fluctuating Concentration Exposure Toxic Load	82
3.5.3	Uptake Time Constant	82
3.5.4	Recovery Time Constant	84
3.5.5	Saturation Concentration	85
3.6	Example for Hydrogen Sulfide Exposure	86
3.6.1	Simulated Exposure Results	87
3.6.2	Accuracy of the Toxic Load Model	88
3.7	Conclusions	90

References	101
4 Summary and Conclusions	103
4.1 Summary of the Stochastic Simulation	103
4.1.1 Conclusions from the Stochastic Simulation	105
4.2 Summary of the Effective Toxic Load Model	106
4.2.1 Conclusions from the Effective Toxic Load Model	107
References	107
A Relationship between the Deterministic and Random Terms in the Stochastic Differential Equation	108
B Clipped Lognormal Distribution	112
B.1 Lognormal Distribution in "+" Coordinates	114
B.2 Concentration Shift ϕ_{base}	115
B.3 Clipped Lognormal	115
References	118
C Integrals of the Lognormal	119
D Random Number Generation	121
D.1 Uniform Random Number Generators	121
D.2 Converting to a Gaussian Random Number	123
References	123
E Experimental Data Compared to the Clipped Lognormal pdf	124
E.1 Probability Density	125
E.2 Cumulative Probability	125
E.3 Exceedance Probability	126
References	133

List of Figures

2.1	Typical intermittent concentration fluctuation time series with low intermittency ($\gamma = 0.9$) and high intermittency ($\gamma = 0.1$).	49
2.2	Clipping procedure to produce an intermittent time series.	50
2.3	Physical model for interpreting the pdf of negative concentrations as intermittent periods of clean air (zero concentration).	51
2.4	General form of the a and b terms in the stochastic simulation	52
2.5	Boundary of clipped lognormal solutions in terms of the intermittency γ and the conditional fluctuation intensity i_p^2	53
2.6	Time scale of intermittent concentration fluctuations T_c normalized by the time scale of the pseudo-concentration time series T_{c^+} for a range of intermittency factors γ	54
2.7	Schematic diagram of the water channel shear layer generator test section.	55
2.8	Typical spectra of normalized concentration fluctuations for the experimental data and for the stochastic simulation of that experiment.	56
2.9	Conditional exceedance probability E_p for moderately intermittent fluctuations of the concentration c/C_p near the centreline of the plume at three downstream positions x/h_s	57
2.10	Conditional exceedance probability E_p for highly intermittent fluctuations of the concentration c/C_p on the outside edge of the plume at three downstream positions x/h_s	58
2.11	Normalized root mean square time derivative of concentration $(\dot{c}/C_p)T_c$ at the concentration level c/C_p near the centreline of the plume at three downstream positions x/h_s	59
2.12	Normalized root mean square time derivative of concentration $(\dot{c}/C_p)T_c$ at the concentration level c/C_p on the outside edge of the plume at three downstream positions x/h_s	60
2.13	Normalized upcrossing rate n^+T_c for moderately intermittent time series versus the normalized instantaneous concentration c/C_p near the centreline of the plume at three downstream positions x/h_s	61

2.14	Normalized upcrossing rate n^+T_c for highly intermittent time series versus the normalized instantaneous concentration c/C_p near the outside edge of the plume at three downstream positions x/h_s	62
3.1	Effects of uptake time constant τ_{up} , recovery time constant τ_r and saturation concentration C_s on the effective concentration and the calculated toxic load for a pulse of exposure concentration.	92
3.2	Examples of typical intermittent fluctuation time series.	93
3.3	Empirical relationship between intermittency factor γ and the conditional fluctuation intensity i_p^2	94
3.4	Fluctuation amplification factor TLR_{fluct} for the fluctuating exposure toxic load L	95
3.5	Ratio of $TLR_{\tau_{up}}/TLR_{\infty}$ for a range of 5 uptake time constants τ_{up}/T_c at normalized time t/τ_{up}	96
3.6	Fluctuation amplification factor TLR_{∞} of the effective toxic load model as $t \rightarrow \infty$ for a range of uptake time constants τ_{up}/T_c	97
3.7	Ratio of TLR_{τ_r}/TLR_{fluct} for 3 recovery time constants τ_r/T_c at time t/τ_r	98
3.8	Ratio of TLR_{C_s}/TLR_{fluct} as $t \rightarrow \infty$ versus the normalized saturation concentration C_s/C and the intermittency γ fluctuation intensity i_p pair.	99
3.9	Example of the effective toxic load L_{eff} predicted for a hydrogen sulphide exposure.	100
E.1	Conditional probability density p_p for moderately intermittent fluctuations of the concentration c/C_p near the centreline of the plume.	127
E.2	Conditional probability density p_p for highly intermittent fluctuations of the concentration c/C_p on the outside edge of the plume.	128
E.3	Conditional cumulative probability distribution P_p for moderately intermittent fluctuations of the concentration c/C_p near the centreline of the plume.	129
E.4	Conditional cumulative probability distribution P_p for highly intermittent fluctuations of the concentration c/C_p on the outside edge of the plume.	130
E.5	Conditional exceedance probability E_p for moderately intermittent fluctuations of the concentration c/C_p near the centreline of the plume.	131
E.6	Conditional exceedance probability E_p for highly intermittent fluctuations of the concentration c/C_p on the outside edge of the plume.	132

Nomenclature

- $a(c, t)$ deterministic term in the stochastic differential equation for the time derivative of concentration. $\text{kg}/\text{m}^3\text{s}$, see Equation (2.2)
- $b(c, t)$ random forcing function term in the stochastic differential equation for the time derivative of concentration, $\text{kg}/\text{m}^3\text{s}^{0.5}$, see Equation (2.2)
- C mean concentration including the zero concentration periods. kg/m^3
- c instantaneous concentration. kg/m^3
- \tilde{c} positive and negative concentration values produced after shifting c_{\pm} concentration by c_{base} . $\tilde{c} = c_{\pm} - c_{base}$. kg/m^3
- c' standard deviation of concentration about the mean C including the zero concentration periods. kg/m^3
- \dot{c}' root mean square of the first derivative of concentration with respect to time. $\text{kg}/\text{m}^3\text{s}$
- c_{-} pseudo-concentration coordinates used for non intermittent ($\gamma_{-} = 1.0$) stochastic simulation. kg/m^3
- c_{50+} median (50th percentile) pseudo-concentration. kg/m^3
- c_{50} median (50th percentile) concentration. kg/m^3
- c_{eff} biologically effective concentration. kg/m^3
- c_{base} concentration shift required to produce intermittency factor γ from the pseudo-concentration c_{\pm} simulated time series. kg/m^3
- C_p conditional (in-plume) mean concentration excluding zero concentration intermittent periods. kg/m^3
- c'_p standard deviation of the conditional (in-plume) concentration about the conditional mean C_p excluding the zero concentration periods. kg/m^3
- C_s saturation concentration for the modified toxic load model. kg/m^3
- D mass diffusivity. m^2/s
- d_0 displacement height of the surface roughness. m

- $E_p(c)$ conditional (in-plume) exceedance probability of observing a concentration greater than c
- f frequency. Hz
- F fraction of a population affected by an exposure. see Equation (3.1)
- F_c concentration power spectrum
- f_{cut} cutoff frequency for Kolmogorov microscale. Hz
- h_s source height above ground level. m
- i fluctuation intensity c'/C about the mean including zero concentration intermittent periods
- i_p conditional (in-plume) fluctuation intensity c'_p/C_p
- k_{cut} cutoff wave number $1/\eta$ for Kolmogorov microscale. m^{-1}
- K zero fluctuation concentration in the general form of the a term in the stochastic differential equation. see Equation (A.4)
- L exposure toxic load calculated from instantaneous exposure concentration integrated with time. $\int c^n dt$
- L_{mean} exposure toxic load calculated from the mean exposure concentration. $C^n t$
- L_{eff} effective toxic load calculated with appropriate values for τ_{up} , τ_r and C_s
- N Gaussian random number with zero mean and unity variance
- n toxic load exponent in $L = c^n t$. n is between 1.0 and 3.5 for a wide variety of common industrial chemicals.
- n^+ upcrossing rate. upcrossings/s
- n_T number of fluctuation integral time scales T_c in a simulated time series. see Equation (2.33)
- $p(c)$ probability density function (pdf) of concentration
- $p_p(c)$ conditional (in-plume) probability density function. excluding zero periods
- $P_p(c)$ conditional (in-plume) cumulative probability of observing a concentration less than c , excluding zero periods

- Pr probit. corresponding to a given level of response in an exposed population
- q zero offset constant in probit equation. see Equation (3.2)
- r constant in probit equation. see Equation (3.2)
- s constant in probit equation. see Equation (3.2)
- s standard deviation. see Equation (2.36)
- Sc Schmidt number. dimensionless ratio of mass diffusivity D to molecular viscosity ν
- t time. s
- T_{c+} Eulerian integral time scale of pseudo-concentration fluctuations. s
- T_c Eulerian integral time scale of actual intermittent concentration fluctuations. s
- t_e total exposure duration. s
- TLR toxic load ratio. dimensionless ratio of a toxic load to the toxic load calculated from the mean exposure concentration. see Equation (3.22)
- TLR_{fluct} toxic load ratio of the exposure toxic load L
- TLR_{eff} toxic load ratio of the effective toxic load L_{eff}
- TLR_{C_s} toxic load ratio of the effective toxic load L_{eff} with some saturation concentration C_s
- TLR_{τ_r} toxic load ratio of the effective toxic load L_{eff} with some recovery time constant τ_r
- $TLR_{\tau_{\text{up}}}$ toxic load ratio of the effective toxic load L_{eff} with some uptake time constant τ_{up}
- TLR_{∞} toxic load ratio as $t \rightarrow \infty$
- U wind speed, m/s, or mean flow velocity in water channel. mm/s
- u_* friction velocity in log-law velocity profile. m/s
- x downstream distance from source. m

y cross stream distance from centreline of source. m

z height above ground level. m

z_0 roughness length scale. m

Greek Symbols

ϕ dimensionless concentration, c/c_{50}

Φ total mean dimensionless concentration including zero periods. C/c_{50}

$\bar{\phi}$ positive and negative dimensionless concentration values produced after shifting ϕ_+ concentration by ϕ_{base} . $\bar{\phi} = \phi_- - \phi_{base}$

ϕ' standard deviation of dimensionless concentration about the dimensionless mean Φ including the zero concentration periods. c'/c_{50}

Φ_- mean dimensionless pseudo-concentration. C_-/c_{50+}

ϕ_- dimensionless pseudo-concentration. c_-/c_{50+}

ϕ_{50} median (50th percentile) dimensionless concentration. 1.0

ϕ_{50+} median (50th percentile) dimensionless pseudo-concentration. 1.0

ϕ_{base} dimensionless concentration shift. c_{base}/c_{50}

Φ_p conditional (in-plume) mean dimensionless concentration excluding zero periods. C_p/c_{50}

ϕ'_p standard deviation of the conditional (in-plume) dimensionless concentration about the dimensionless conditional mean Φ_p excluding the zero concentration periods. c'_p/c_{50}

γ intermittency factor. equal to fraction of the time that there are non-zero concentrations

γ_+ intermittency factor = 1.0 of the non-intermittent pseudo-concentration time series

η Kolmogorov microscale of turbulence kinetic energy dissipation. m

η_c Kolmogorov microscale of concentration. m

κ von Karman constant = 0.4

- μ mean value, see Equation (2.38)
- ν molecular viscosity, m^2/s
- σ_{l+} log standard deviation of non-intermittent pseudo-concentration lognormal pdf
- σ_y cross stream plume spread, m
- τ_{up} uptake time constant for the modified toxic load model, s
- τ_r recovery time constant for the modified toxic load model, s
- $d\zeta$ Gaussian random number in the stochastic differential equation with zero mean and variance dt , $\text{s}^{0.5}$, see Equation (2.2)

Chapter 1

Introduction

Accidental releases of industrial gases into the atmosphere can produce offensive odors, flammability and toxicity. These potential impacts can occur on-site in the occupational exposure setting or off-site where the general public will be exposed. Predicting the likely effects of an accidental gas release is important to ensure that accident prevention and risk management methods are appropriate and cost-effective.

This thesis addresses two important complications in estimating the toxic effects of an atmospheric gas release: random fluctuations in exposure concentration at a fixed receptor in a point source plume, and a lack of realistic models for predicting acute toxicity of fluctuating concentration exposures. The concentration fluctuations are important because in a typical plume the exposure concentration can range from zero (background) concentration when only clean air is present to more than 20 times the mean concentration. Exposure concentration and exposure duration are non-linearly related to the toxic effects of the release so an accurate toxicity model is required to predict the effects of these fluctuating concentrations. Two unpublished papers are presented that provide tools for dealing with these problems and improving the hazard assessment of toxic gas releases.

1.1 Simulating Concentration Fluctuations

Chapter 2 contains the first paper entitled "Stochastic Simulation of Intermittent Concentration Fluctuations". In this chapter the stochastic model of Du (1995) is extended to allow simulation of realistic intermittent concentration fluctuation time series. This new model is tested with experimental water channel saline plume dispersion data collected by Wilson, Zelt and Pittman (1991).

The stochastic simulation provides a numerical computer based model that can be used to generate multiple realizations of intermittent concentration fluctuation time series with realistic combinations of intermittency factors and fluctuation intensity. Each time series is a simulation of an actual exposure event that could be observed at a fixed receptor location.

Previous models of intermittent concentration fluctuations provided only probability distributions and statistics such as the mean, variance, skewness, and kurtosis, that have to be mathematically manipulated in combination with a hazard model to estimate the effects of a release. The stochastic simulation method provides a direct approach to the problem. All of the concentration fluctuation as well as the intermittent periods of zero concentration are directly simulated. The complex effects of fluctuations on toxicity, flammability, or odor can be tested by stepping through the generated time series with any possible hazard model. Each individual realization of an exposure scenario can be analyzed in detail and large ensembles of time series realizations can be used to generate average and "worst-case" effects.

1.2 Estimating Toxicity from Fluctuating Concentrations

Chapter 3 is the second paper entitled "A Model for Effective Toxic Load from a Hazardous Gas Release". A modified toxic load model is proposed and evaluated by applying it to intermittent concentration fluctuation time series produced by stochastic simulation.

The most widely used parameter for predicting acute toxicity is toxic load $L = C^n t$, where L is the toxic load calculated by the non linear relationship between the exposure concentration C and the exposure duration t . Because the exponent n is greater than unity for most common industrial chemicals, the large concentration fluctuations that are observed in an actual release can be very important to the overall toxicity. Most toxicity models do little to account for fluctuations except through implicit factors of safety to account for peak-to-mean ratios. The direct simulation approach allows a realistic effective toxic load model to be developed with an uptake time constant, a recovery time constant, and a saturation concentration. This effective toxic load model is then time-stepped through individual simulations of exposure event realizations so that both average effects and variability in effects can be determined.

1.3 Release Scenarios Considered

The focus of both the stochastic simulation and the toxicity model is a scenario where the release is of relatively short duration. Typical releases from industrial accidents last for a few minutes to a few hours. The extreme case would be a sour gas well

blowout that can produce substantial levels of toxic gases for several weeks, but this case has not been developed in this thesis.

Only immediately observable acute health effects will be considered. Chronic effects such as the development of cancers or other long term diseases will not be examined as they require entirely different models and methodologies.

Acute effects occur during or immediately following an exposure to the toxic chemical. These effects could range from odor annoyance to fatality. In practice, the only endpoint that can be reliably measured and documented is fatalities. Other less severe health effects are necessarily subjective and much more difficult to measure objectively. In some cases, the same sort of reactions that lead to fatality may also cause the less severe effects. It is reasonable to assume that exposure levels that cause death in a few very sensitive individuals also cause less severe effects in more resistant individuals.

A release of toxic gas will affect animals and plants in addition to the people that are exposed. Although these effects can be an issue in evaluating the overall risk posed by an industrial facility, this thesis will only consider the direct acute health effects on human beings.

1.4 Stochastic Fluctuation Modelling

The first stochastic process to be considered in detail was Brownian motion of small particles in a fluid. The Brownian motion phenomenon was discovered in 1827 by Robert Brown, but equations to describe this motion were not solved until 1905 by Einstein and Smoluchowski with a simpler derivation by Langevin in 1908. see Gardiner (1983, chap. 1).

The assumptions made to derive the equations for Brownian motion were that there are two forces acting on a Brownian particle:

- viscous drag of the fluid on the particle that causes the particle to slow to zero velocity in the absence of any external forces.
- a fluctuating force due to the random impacts of molecules of fluid on the particle. The impacts should be positive and negative with equal probability.

The viscous drag is a deterministic component based on the current velocity while the fluctuating forced caused by impacts of molecules of fluid is a random component of the motion of a Brownian particle.

To describe the concentration fluctuations at a fixed receptor location in a dispersing plume some analogous assumptions are made:

- there is some analog to drag that causes the concentration to return to a zero fluctuation value.
- the random fluctuations in concentration due to turbulence are positive and negative with equal probability.

The simplest one dimensional model for a stochastic concentration fluctuation process that includes a deterministic and a random component is given by the stochastic differential Langevin equation from Gardiner (1983):

$$dc(t) = a(c, t)dt + b(c, t)d\zeta \tag{1.1}$$

where c is the instantaneous concentration, $a(c, t)$ is a deterministic component that determines the behavior of the concentration in the absence of random fluctuations and $b(x, t)d\zeta$ is the random fluctuating component.

An inherent assumption of using an stochastic differential equation like Equation (1.1) is that the fluctuation process is an inertialess first order Markov process. A Markov process is a type of stochastic process which has no memory of previous states earlier than time $t - dt$. A first order Markov process has a derivative that has no memory of previous derivatives. It is called inertialess because the concentration “velocity” ($\partial c/\partial t$) is not correlated with previous concentration velocities.

Du (1995) proposed that a stochastic first order Markov model could be used to model the conditional (in-plume) concentration fluctuations. In this thesis, the Du (1995) model is extended to cover both the in-plume fluctuations and intermittent periods of zero concentration.

1.5 Toxicity Modelling

In order to estimate the acute health effects from a toxic gas release, a toxicity model is required. Many different toxicity models have been proposed and they can be divided into three broad classes:

1. *Threshold Models*: The simplest method of predicting toxicity is to simply set a threshold level based on experiment and observation. The threshold simply implies that above some concentration adverse effects will occur and below this concentration effects are negligible.
2. *Data Based Models*: A simple model can be devised by examining existing data on toxicity and finding an equation to fit these data. This is the approach used to define the existing non-linear toxic load models.
3. *Mechanistic Biological Models*: A biological model attempts to mathematically

describe all of the relevant biochemical reactions involved in the toxicity of a particular compound. A typical biological model, usually referred to as a pharmacokinetic model, divides the human body into several compartments and target organs and then applies rate constants to metabolic reactions and transfers between all of these compartments.

The following sections evaluate these three classes of toxicity model for use in estimating the acute effects of a toxic gas release.

1.5.1 Threshold Toxicity Models

The first level in toxicological modeling is to define a single threshold level above which harm can occur and below which no harm occurs. This is the approach generally used for standards such as occupational exposure limits and ambient air limits. For example, in Alberta, the occupational exposure limit for hydrogen sulphide is 10 parts per million (ppm) average concentration for an 8 hour exposure. Alberta Health (1988).

The problem with thresholds is that there is usually no accompanying explanation of how the threshold was determined. The value is usually set by a consensus judgement that decides what safety factor is appropriate to apply to the limited toxicity data available. A simple 10 ppm limit for an 8 hour hydrogen sulphide exposure does not give useful and necessary information to determine whether 11 ppm is much more dangerous, or if a much higher level, say 100 ppm, is tolerable for a short period of time provided that the 8 hour average stays below 10 ppm. The biggest question is how to scale this threshold to other situations. For example, is a 10 ppm exposure safe for sensitive individuals? If the concentration fluctuates widely (as it does in real

outdoor exposures) how do we determine the effects? If workers are on 12 hour shifts, how high a concentration should they be able to tolerate? Thresholds are difficult to apply to any exposure scenarios other than the simple ones that they specify and are not suitable for estimating the acute effects of a toxic gas release.

1.5.2 Data Based Toxicity Models

The second level of complexity for a toxicological model is a single equation describing the response of a population to a toxic substance. These types of models are based on data collected on the effects of the toxic substance in relation to a variety of different variables. In the case of toxic gases, the most relevant variables are usually considered to be the concentration and duration of exposure.

In the early part of the 20th century the relationships between the exposure concentration, the exposure duration, and the toxicity were examined. It had been suggested as early as 1910 that the relationship between concentration and exposure duration was non-linear, see Bliss (1940). In 1924, Haber reported on experiments on the acute lethal toxicity of several poison gases used on troops in World War I and proposed that the product of concentration and time was a constant for a given response, see Gelzleichter, Witchi and Last (1992). Haber's Law is $Ct = K$, where C is the mean exposure concentration, t is the duration of exposure, and the dose K is a constant for a given level of fatalities in the exposed population. The same percentage of fatality can be produced by proportional changes in the concentration C and the exposure duration t . Busvine (1938) proposed that the proper relationship between exposure concentration and duration was the non-linear $C^n t = L$, where n is an exponent greater than zero. This relationship has become known as the toxic load L . For values of $n < 1$ the duration of exposure is weighted heavier than the

concentration of exposure and for values of $n > 1$ the concentration is more important than the duration. If Haber's Law were true then $n = 1$.

An important study of toxic load relationships was reported by ten Berge, Zwart and Appelman (1986). In this paper, previously published data on the acute lethal toxicity of some volatile industrial chemicals were analyzed using probits. It was found that Haber's Law does not work very well in most circumstances, but that a toxic load exponent n different from unity and typically between 2.0 and 3.0 fits the available data very well. The scope of this study, that included 20 different industrial chemicals, indicates that non-linear toxic load L is a reasonable basis for a data-based population response toxicity model.

The toxic load concept has been widely used for the risk assessment of acutely toxic gases. The Center for Chemical Process Safety of the American Institute of Chemical Engineers, (CCPS, 1989), provides recommended toxic load relationships for a few common industrial chemicals. The Rijmond Report by Cremer and Warner Ltd. (1981) used toxic load to evaluate the potential risks of chlorine and ammonia exposures from industrial facilities in the town of Rijmond in Holland. Rogers (1990) recommended a toxic load model to evaluate the effects of hydrogen sulphide releases in Alberta.

1.5.3 Mechanistic Biological Models

There has been considerable work done with mechanistic models of toxicity. Recent advances in measurement techniques have allowed many different variables inside the body of an individual organism to be measured. These data, along with knowledge of the operation of chemical reactions, internal organs and systems have led to a wide range of complex toxicity models.

These types of models are often referred to as physiologically based pharmacokinetic models and they attempt to simulate the actual processes in the body that produce toxicity, including metabolic reactions and transfers between organs and systems. Andersen et al. (1980) investigated uptake rates in rats for a number of volatile organics and proposed a four compartment model for just the uptake process. Clewell, III and Andersen (1994) reviewed the pharmacokinetic modelling approach and discussed some models for styrene and dihalomethanes. Overton (1990) reported on another model for styrene that incorporates inhalation, exhalation, and metabolism in the respiratory tract tissues. Gargas, Medinsky and Andersen (1995) determined some metabolic constants for a few volatile organic compounds in rats.

The main difficulty of this approach is that the human body is extremely complex and pharmacokinetic models may be very complex. A typical pharmacokinetic model involves dividing the body up into at least two or three compartments and often many more, with rate constants for transfers between each compartment. Each model is very specific and not easily adapted to other chemicals or to the wide variability in individuals. Obtaining data for a reliable pharmacokinetic model is a major research effort. The best predictions of health effects could be obtained with a completely detailed pharmacokinetic model of the human body and all of the variations that are possible. However, at the present time this is not technically feasible, nor is it justifiable considering the large uncertainties that are present in other aspects of a hazard assessment of a toxic gas release.

1.6 Hydrogen Sulphide Toxicity

Hydrogen sulphide will be used as an example to test the effective toxic load model in the second paper. The Major Industrial Accident Council of Canada (MIACC, 1994) lists hydrogen sulphide as a “top priority” substance that has a high probability of causing off-site fatalities when stored in quantities greater than 1 tonne. Commercial uses of hydrogen sulphide include the manufacture of heavy water, purification of hydrochloric and sulphuric acids, manufacture of elemental sulphur, nylon, mercaptans and soda ash, see Environmental Protection Service (1984). Some natural sources of hydrogen sulphide are volcanic explosions, bacteria active in the decay process, and releases from areas of geothermal activity, see WHO (1981) and Young (1983).

The primary source of hydrogen sulphide in Canada is sour natural gas. Western Canadian natural gas deposits contain dissolved hydrogen sulphide in concentrations from less than 1 percent to greater than 90 percent, see Environmental Protection Service (1984); Alberta Health (1988); Reiffenstein, Hulbert and Roth (1992). In Alberta, occupational exposures are common, but accidental exposures to the public are also of concern. One memorable incident of public exposure was the Lodgepole, Alberta gas well blowout in 1982 that released large quantities of hydrogen sulphide containing sour natural gas into the atmosphere for a period of sixty-seven days, see Alberta Health (1988).

Hydrogen sulphide is a colourless toxic gas with a distinctive rotten egg odour at low concentrations. Carl Wilhelm Scheele, 1742-1786, is credited with the discovery of hydrogen sulphide although it is suspected that the first recorded observations of hydrogen sulphide poisoning were in 1713 by Bernardino Ramazzini who described painful inflammations of the eye in Parisian sewer workers. It was later discovered that

hydrogen sulphide was evolving from the sewage. see Smith (1989)

Numerous studies have been performed in an attempt to accurately quantify the effects of hydrogen sulphide on humans. Alberta Health (1988) summarizes exposure data from approximately 100 different experiments including both human exposures and animal tests. Large bibliographies of sulphur gas toxicology have been prepared by Beauchamp et al. (1984) who list over 1300 references and Prior, Lee and Toma (1985), Lee, Prior and Toma (1985), and Lee and Prior (1986) who list several thousand references. However, most of the information was obtained from animal testing and there is little information on direct human exposure. Human exposures are usually accidental and not performed under controlled conditions so there are rarely concentration measurements or other important information available to accurately quantify the doses responsible for the effects observed.

Most hydrogen sulphide toxicity information documents dangerous exposure concentrations, but gives little or no information on the exposure times required to produce the effects. Reiffenstein, Hulbert and Roth (1992) provide a summary of the basic toxicology of hydrogen sulphide, and give the concentration levels for some observed effects. It is reported that at 500 to 1000 parts per million (ppm) hydrogen sulphide is recognized as being rapidly lethal to humans and other animals, but no duration of exposure is specified.

As reported in Alberta Health (1988), Alberta has three different standards controlling the level of exposure for hydrogen sulphide. Occupational Health and Safety requires that the concentrations in the workplace not exceed 10 ppm for 8 hours. Alberta Environment has set an ambient standard of 0.01 ppm for a 1 hour average. Alberta Health has issued evacuation guidelines to facilitate handling emergency releases of hydrogen sulphide such as a gas well blowout or pipeline break. Evacuation

is mandatory if levels exceed 20 ppm. If average levels in a community exceed 10 ppm averaged over 8 hours residents would be advised to leave until the levels decrease. At levels below 10 ppm it is recommended that individuals who experience symptoms related to the hydrogen sulphide or individuals with medical conditions such as asthma or emphysema consider leaving the area until the ambient concentrations are reduced.

References

- Alberta Health (1988), *Report on H₂S Toxicity*, 65 pages.
- Andersen. M. E., Gargas. M. L., Jones. R. A., and Jenkins. L. J. (1980). Determination of the Kinetic Constants for Metabolism of Inhaled Toxicants in Vivo Using Gas Uptake Measurements. *Toxicology and Applied Pharmacology*, 54:100-116.
- Beauchamp, R. O., Bus, J. S., Popp, J. A., Boreiko. C. J., and Andjelkovich. D. A. (1984), A Critical Review of the Literature on Hydrogen Sulphide Toxicity. *CRC Critical Reviews in Toxicology*, 13(1):25-97.
- Bliss, C. I. (1940). The relation between exposure time, concentration and toxicity in experiments on insecticides. *Annals of the Entomological Society of America*, 23:721-766.
- Busvine, J. R. (1938), The toxicity of ethylene oxide to calandra oryzae, c. granaria triboleum castaneum, and cimex lectularius. *Annals of Applied Biology*, 25:605-32.
- CCPS (1989). *Guidelines for Chemical Process Quantitative Risk Analysis*. Center for Chemical Process Safety of the American Institute of Chemical Engineers.
- Clewell, III, H. J. and Andersen, M. E. (1994). Physiologically-based Pharmacokinetic Modeling and Bioactivation of Xenobiotics. *Journal of Toxicology and Industrial Health*, 10(1/2):1-24.
- Cremer and Warner Ltd. (1981). *Risk Analysis of Six Potentially Hazardous Industrial Objects in the Rijnmond Area, a Pilot Study*. Rijnmond Public Authority. Published by D. Reidel Publishing Company. Boston, U.S.A.
- Du, S. (1995). *Stochastic Models for Turbulent Diffusion*. PhD thesis, University of Alberta.
- Environmental Protection Service (1984). *Hydrogen Sulphide*. Technical Services Branch, Environmental Protection Programs Directorate, Ottawa, Ontario.
- Gardiner, C. W. (1983), *Handbook of Stochastic Methods*. Springer-Verlag.
- Gargas, M. L., Medinsky, M. A., and Andersen, M. E. (1995). Pharmacokinetic Modeling Approaches for Describing the Uptake, Systemic Distribution, and Disposition of Inhaled Chemicals. *Critical Review in Toxicology*, 25(3):237-254.
- Gelzleichter, T. R., Witchi, H., and Last, J. A. (1992). Concentration-Response Relationships of Rat Lungs to Exposure to Oxidant Air Pollutant: A Critical Test of Haber's Law for Ozone and Nitrogen Dioxide. *Toxicology and Applied Pharmacology*, 112:73-80.
- Lee, D. W. and Prior, M. G. (1986), *Toxicology of Sulphur Gases: A Bibliography*, Supplement 2. Alberta Environmental Centre.

- Lee, D. W., Prior, M. G., and Toma, D. S. (1985). Toxicology of Sulphur Gases: A Bibliography, Supplement 1, Alberta Environmental Centre.
- MIACC (1994). *MIACC Lists of Hazardous Substances*. Major Industrial Accidents Council of Canada, First Edition.
- Overton, J. H. (1990), A Respiratory Tract Dosimetry Model for Air Toxics. *Toxicology and Industrial Health*, 6(5):171-180.
- Prior, M. G., Lee, D. W., and Toma, D. S. (1985). Toxicology of Sulphur Gases: A Bibliography, Alberta Environmental Centre.
- Reiffenstein, R. J., Hulbert, W. C., and Roth, S. H. (1992). Toxicology of Hydrogen Sulphide. *Annual Review of Pharmacology and Toxicology*, pages 109-34.
- Rogers, R. E. (1990), Toxicological Justification of the Triple Shifted Rijnmond Equation, Technical report, Alberta Energy Resources Conservation Board. Appendix B, Volume 7 of the Risk Approach: An Approach for Estimating Risk to Public Safety from Uncontrolled Sour Gas Releases.
- Smith, R. P. (1989). Hydrogen Sulphide: Overview, History, Theories and Unknowns. In Prior, M., Roth, S. H., Green, F. H. Y., Hulbert, W. C., and Reiffenstein, R. J., editors. *Proceedings of International Conference on Hydrogen Sulphide Toxicity*, pages 1-13. Banff, Alberta, Canada. Sulphide Research Network.
- ten Berge, W. F., Zwart, A., and Appelman, L. M. (1986). Concentration-time mortality response relationship of irritant and systemically acting vapours and gases. *Journal of Hazardous Materials*, 13:301-309.
- WHO (1981), *Hydrogen Sulfide*. United Nations Environment Program, the International Labour Organization, and the World Health Organization. Geneva. Environmental Health Criteria 19.
- Wilson, D. J., Zelt, B. W., and Pittman, W. E. (1991). Statistics of Turbulent Fluctuation of Scalars in a Water Channel. Technical report. Department of Mechanical Engineering, University of Alberta, Edmonton, Alberta.
- Young, M. R. (1983), Study Trip to Rotorua, New Zealand. Technical report. Amoco Canada Petroleum Company Ltd., in Hydrogen Sulphide and Health Report.

Chapter 2

Stochastic Simulation of Intermittent Concentration Fluctuations

2.1 Introduction

The inhomogeneous mixing of a point source plume of contaminant produces large fluctuations in contaminant concentration at a fixed receptor. The instantaneous concentrations can range from zero (background) concentration to more than 20 times the mean concentration. Two examples of typical time series of concentration fluctuation are shown in Figure 2.1.

Toxicity, flammability and odor effects have a strong non-linear dependence on concentration. For example, ten Berge, Zwart and Appelman (1986) analyzed many animal experiments for 20 different acutely toxic gases and found that fatalities a function of concentration C^n where $n = 1.0$ to 3.5 . Most chemicals had an exponent n value in the range of 2.0 to 3.0 . The Center for Chemical Process Safety of the American Institute of Chemical Engineers (CCPS, 1989) recommends similar non-linear models for predicting acute toxicity from common industrial chemicals.

If the exponent $n = 1$ then the high concentrations are no more important than the low concentrations and the only variable determining toxicity is the mean concentration C . However, if $n > 1$, as it is for many substances, then concentration fluctuations increase the toxicity of the exposure because the high concentrations become much more important than low concentrations. In a typical point source gas plume where the fluctuation standard deviation c' is often several times larger than the mean concentration C these large fluctuations have a significant effect on the predicted toxic hazard from a gas release.

The current body of work on concentration fluctuations, reviewed in Wilson (1995), approaches the problem both experimentally and with theoretical models to predict the variance, skewness, kurtosis and other statistics of the fluctuations. Recent work by Yee et al. (1993, 1994, 1995) recognizes that the evaluation of toxic hazards from a release requires additional information on concentration level recurrence time intervals, intermittency, and level-crossing statistics in addition to the probability distributions and higher order concentration moments. The stochastic time series simulation proposed in the present study can be used to evaluate all of these statistical measures from user specified values of the mean, variance, intermittency and fluctuation time scale.

In this study, a time series of simulated intermittent concentration fluctuations is generated directly as a first order "inertialess" Markov process. The stochastic model used to produce these intermittent time series is an extension of a conditional (non-intermittent) model by Du (1995). The objective of this study is to generate an ensemble of realistic random time series of intermittent concentration fluctuations that can be applied directly to a hazard model. This direct simulation approach allows the user to see the effect of each realization of an ensemble and to apply

complex hazard models that cannot be used if only the overall statistics are known.

2.2 Probability Distributions of Intermittent Time Series

A probability distribution, in the form of a probability density function (pdf), is a key input to the proposed stochastic simulation. The pdf constrains the fluctuating concentrations to ensure the correct mean, variance, and intermittency in the simulated time series.

Probability distributions of intermittent concentration fluctuations usually focus on the conditional in-plume concentrations with the intermittent periods described by a delta function at zero concentration. Wilson (1995, chap. 5) examined several different distributions and recommended the lognormal as the best fit to a wide variety of data. The choice of the lognormal is supported by water channel experimental data analyzed by Yee, Wilson and Zelt (1993), although Yee et al. (1995) analyzed full scale atmospheric data and concluded that the gamma distribution provided a better fit than the lognormal. The gamma distribution sometimes provides a better fit to concentrations less than the mean while the lognormal fits better for concentrations greater than the mean. Du (1995) used both the gamma and the lognormal distribution in a stochastic model for the conditional concentration upcrossing rate and found that there was little difference between the distributions.

In the present study, a clipped lognormal pdf is used to describe the intermittent concentration fluctuations and to meet the requirements for the stochastic simulation of intermittent time series.

2.2.1 Shifted and Clipped Lognormals

The primary restriction on the choice of the pdf is that it must describe both the in-plume concentrations and the zero concentration intermittent periods. The probability of obtaining a non-zero concentration must be equal to the intermittency factor γ and the probability of obtaining a zero concentration must be equal to $(1 - \gamma)$. A simple delta function cannot be used to account for the zero periods because the stochastic model becomes mathematically trapped in a delta function and the time series of concentration will not go above zero after hitting zero concentration.

To meet the pdf requirements, the stochastic simulation is implemented in pseudo-concentration coordinates c_+ where the subscript “+” denotes parameters related to these pseudo-concentrations. Step 1 in Figure 2.2 shows the pseudo-concentration c_+ time series and pdf. In c_+ coordinates, the concentration fluctuations are represented by a complete lognormal distribution with only positive concentrations and an intermittency factor $\gamma_+ = 1.0$. There are no intermittent periods in c_+ .

After a simulated time series is generated, the concentrations are shifted by a value of c_{base} to give positive and negative concentrations \tilde{c} where:

$$\tilde{c} = c_+ - c_{\text{base}} \tag{2.1}$$

In \tilde{c} coordinates, the probability of obtaining a positive concentration is equal to the intermittency factor γ and the probability of obtaining a negative concentration is $(1 - \gamma)$. The magnitude of the negative concentration is interpreted as inversely proportional to the likelihood of obtaining a positive concentration in the next time step. The shifted lognormal is shown in Step 2 of Figure 2.2 for a typical time series and the corresponding pdf.

Negative concentrations are clearly unrealistic, so the final step in interpreting the

simulation is to clip all of the negative concentrations and replace them with a delta function at zero concentration. The result is a clipped lognormal that has only real concentrations $c \geq 0$. The final intermittent time series and pdf are shown in Step 3 of Figure 2.2.

2.2.2 Physical Interpretation of the Shifted Lognormal

A physical interpretation of the shifted lognormal is that the concentration fluctuations and the intermittent periods are part of the same physical mixing process as shown in Figure 2.3. Eddies with some positive concentration of contaminant flow by a point and cause the non-zero concentration fluctuations. Similarly, eddies of clean air flowing by the same point cause the intermittent periods. The positive concentrations of the shifted lognormal describe the contaminated eddies while the negative concentrations describe the clean air eddies. The magnitude of the negative shifted concentration \bar{c} in Figure 2.3 is inversely proportional to likelihood that the concentration will be non-negative in the next time step. The larger the negative concentration \bar{c} , the larger the eddy of clean air and the less likely that that a concentration greater than zero will occur in the next time step.

After the shifting is complete, all of the negative concentration values are converted to zero concentration intermittent periods and the result is a clipped lognormal pdf of concentration. Clipped distributions have been used to describe concentration fluctuations, but not with this interpretation. For example, Lewellen and Sykes (1986) used a clipped normal pdf to describe intermittent plumes from a power plant, but their interpretation did not attach any significance to the missing negative concentrations and was simply a fit to the available data. As pointed out by Wilson (1995, p. 46), the clipped normal is not appropriate for general use because its functional

form can only produce in-plume fluctuation intensities less than 1.0. Typical in-plume fluctuation intensities in a point source plume range from 0.5 and 2.0, with most of the values greater than unity, making the clipped normal an inappropriate choice.

2.3 Stochastic Model for Fluctuations

Du (1995) developed a numerical stochastic model to predict upcrossing rates of conditional (in-plume) concentration fluctuation time series. The limitation of this model is that it does not account for intermittent periods of zero (background) concentration that are observed experimentally.

In the present study, the Du (1995) model is extended to include the simulation of the intermittent periods. The basic assumptions of their model are that:

- the probability distribution of concentration is independent of spatial position (and therefore travel time) in the plume.
- Eulerian concentration fluctuations are produced by a first order Markov process that can be described by a stochastic differential equation, and by the equivalent Fokker-Planck equation for the time dependent evolution of the concentration probability distribution.
- the derivative of concentration is dependent on the current instantaneous concentration.
- concentration fluctuations are statistically stationary.

The intermittent stochastic simulation is implemented with a lognormal distribution in non-intermittent pseudo-concentration c_+ coordinates so that all the simulated

concentrations are greater than zero as discussed in Section 2.2 and shown in Figure 2.2. All parameters calculated from this time series of pseudo-concentrations will be denoted by the subscript “+”.

2.3.1 Stochastic Differential Equation

Experimental evidence from Yee et al. (1993) and water channel data presented later in this paper shows that the root mean square concentration derivative \hat{c}' increases with the concentration level at which it is measured. This requires a stochastic model for the time series of concentration fluctuations to have a deterministic component that changes dc_+/dt as concentration c_+ increases along with the usual random component. This first-order Markov (inertialess) concentration fluctuation process at a fixed location in a dispersing plume can be described by the one dimensional stochastic differential Langevin equation:

$$\frac{dc_+}{dt} = a(c_+, t) + b(c_+, t) \frac{d\zeta}{dt} \quad (2.2)$$

where $a(c_+, t)$ is the deterministic portion of the time derivative dependent on the concentration c_+ and time t and $b(c_+, t)d\zeta$ is a random forcing function where $d\zeta$ is a Gaussian random number with a mean of zero and variance dt .

The Langevin equation, discussed in detail by Gardiner (1983, pp. 80–83) and Durbin (1983), is used to describe a wide variety of continuous stochastic processes. Originally, the equation was developed to describe the position of Brownian particles in a fluid, see Gardiner (1983, chap. 1). It has also been applied to the modelling of concentration fluctuations in the Lagrangian sense by tracking the random flights of particles emanating from a point, see Wilson and Sawford (1996). Here, we apply the Langevin equation in an Eulerian sense by assuming that the measured concentration

at a single point can be modelled as a continuous Markov process.

2.3.2 Fokker-Planck Constraint

It is assumed that the pdf of concentration c_+ is stationary, but a useful constraint between the a and b terms can be derived by first assuming that the pdf of concentration does change with time. Durbin (1983) provides a detailed derivation of the deterministic relationship for the time evolution of the pdf in a Markov process. The basic procedure is to consider a pdf of concentration c_+ at time t . By definition, a Markov process has no memory of previous states and this translates to the requirement that the pdf at some time t depends only on the pdf at time $t - dt$ and some transition probability between concentration c_+ at time t and concentration $c_+ - dc_+$ at time $t - dt$. Integrating over all possible dc_+ values and substituting moments calculated for the stochastic process from Equation (2.2) produces a deterministic equation describing the time evolution of the probability density function $p(c_+)$, as given in Du (1995)

$$\frac{\partial p}{\partial t} = -\frac{\partial(ap)}{\partial c_+} + \frac{1}{2} \frac{\partial^2(b^2p)}{\partial c_+^2} \quad (2.3)$$

Equation (2.3) is the one dimensional Fokker-Planck equation. Additional discussion can be found in Gardiner (1983, chap. 5). The Fokker-Planck equation constrains the evolution of the probability distribution of concentration with the relationship between the a and b terms.

Stationarity requires that a , b and the pdf p do not change with time. With this assumption $\partial p/\partial t = 0$ and Equation (2.3) can be integrated once to yield:

$$\frac{d(b^2p)}{dc_+} = 2ap \quad (2.4)$$

Following Du (1995) integrating (2.4) to solve for b^2 in terms of a produces

$$b^2 = \frac{2}{p} \int_{c_+}^{\infty} -ap \, dc_+ \quad (2.5)$$

Equation (2.5) is a deterministic relationship between the pseudo concentration time series generation parameters a and b in Equation (2.2) and the probability density function p that is specified by the user.

2.3.3 Functional Relations for a and b

The a term governs the deterministic part of the fluctuation process. In the absence of random fluctuations, a determines the behavior of the concentration derivative. Yee et al. (1993) found that the first derivative of concentration with respect to time is strongly dependent on the current concentration. That is, large derivatives are observed at extreme concentrations relative to the mean, while small derivatives generally occur near the mean. Here, we assume that in the absence of random fluctuations the instantaneous concentration c_+ will return to the well mixed mean concentration C_+ at a rate dependent upon the magnitude of the current difference between c_+ and C_+ .

The model proposed by Du (1995) for the non-zero (conditional) part of the concentration time series assumed a non-linear relationship for the deterministic a term and found that the results were not too sensitive to the non-linearity. For the present study we postulate the linear form of the a term:

$$a = \frac{C_+ - c_+}{T_{c_+}} \quad (2.6)$$

Calculation of the integral time scale from the time series that are generated by the model confirms that the input time scale T_{c_+} is the integral time scale of the

pseudo-concentration fluctuation process. The fluctuating time series produced by the simulation is inertialess, so T_{c_+} may be rescaled to any value without changing the physical basis of the time series. The exact T_{c_+} value used for simulation is not important and it is nominally set to unity.

The pdf $p(c_+)$ must be specified to complete the model. In this study, $p(c_+)$ is a lognormal distribution as discussed in Section 2.2. The value of the b term is calculated by substituting the pdf and the definition of a from equation (2.6) into equation (2.5).

In the absence of concentration fluctuations, Equation (2.6) produces a derivative that will drive the pseudo-concentration to the well-mixed mean value C_- . This return-to-mean assumption is required to produce the correct random component b . The b term must go to zero at concentration $c_- = 0$ to ensure that no negative c_- concentrations will be produced by the stochastic differential equation (2.2). Appendix A provides additional detail on the a term necessary to produce an appropriate b term. The general forms of a and b calculated with a lognormal $p(c_+)$ are shown in Figure 2.4.

For a highly intermittent time series, the pseudo-mean C_+ can be a negative concentration after the shifting necessary to produce the intermittent periods. With this in mind, C_+ should be interpreted as a representative concentration that includes the effects of both the intermittent zero periods and the non-zero fluctuations. If C_- is less than zero concentration after shifting, it implies that the clean air eddies dominate the fluctuation process.

2.4 Clipped Lognormal Distribution

The lognormal is well documented in both Aitchison and Brown (1957) and Crow and Shimizu (1988) who also include some information on clipped or truncated lognormals. The clipped lognormal is not widely used and some discussion of its basic statistics and application to the stochastic model is required. A full lognormal pdf in c_{\perp} coordinates is used for the stochastic simulation as explained in Section 2.2, but the clipped lognormal in c coordinates must have the correct statistics for the final intermittent time series.

There are two sets of statistics that can be considered for an intermittent time series. Conditional statistics exclude the intermittent periods of zero concentration and are denoted by a subscript “ p ”. The total statistics include the zero periods as well as the non-zero concentrations and have no subscript. For example, C is the mean concentration including the zero periods, while C_p is the conditional mean concentration that excludes the zeroes, where uppercase symbols denote mean values.

To use the clipped distribution in the stochastic simulation, the c_{\perp} lognormal distribution must be chosen so that after it is clipped by c_{base} as shown in Figure 2.2 the desired intermittency factor γ and the conditional fluctuation intensity i_p^2 are obtained. The intermittency factor γ is defined as the fraction of the total time during which the concentration is greater than zero. The conditional fluctuation intensity i_p^2 is defined as:

$$i_p^2 = \frac{c_p'^2}{C_p^2} \quad (2.7)$$

where $c_p'^2$ is the conditional variance of the concentration and C_p is the conditional mean.

Appendix B details all the steps in calculating the statistics of the clipped log-

normal and the important results are listed below. The integrals of the lognormal distribution required for these derivations are presented in Appendix C.

2.4.1 Normalized Concentrations

The analysis of the clipped lognormal is simplified by normalizing all concentrations by the median concentration c_{50} that includes all of the zero concentration periods to produce dimensionless concentrations denoted by ϕ .

$$\phi = \frac{c}{c_{50}} \quad (2.8)$$

$$\Phi = \frac{C}{c_{50}} \quad (2.9)$$

$$\Phi_p = \frac{C_p}{c_{50}} \quad (2.10)$$

$$\phi' = \frac{c'}{c_{50}} \quad (2.11)$$

$$\phi'_p = \frac{c'_p}{c_{50}} \quad (2.12)$$

where ϕ is the instantaneous dimensionless concentration, Φ is the mean dimensionless concentration, Φ_p is the conditional (in-plume) mean dimensionless concentration, ϕ' is the standard deviation of the dimensionless concentration, and ϕ'_p is the conditional standard deviation of dimensionless concentration excluding the zero periods. By definition, $\phi_{50} = 1$ is the median dimensionless concentration.

In pseudo-concentration “+” coordinates all concentrations are normalized by the median concentration c_{50+} of the pseudo-concentration time series:

$$\phi_+ = \frac{c_+}{c_{50+}} \quad (2.13)$$

$$\Phi_+ = \frac{C_+}{c_{50+}} \quad (2.14)$$

$$\phi'_+ = \frac{c'_+}{c_{50+}} \quad (2.15)$$

where ϕ_+ is the instantaneous dimensionless pseudo-concentration, Φ_+ is the mean dimensionless pseudo-concentration, ϕ'_+ is the standard deviation of the dimensionless pseudo-concentration, and by definition the median dimensionless pseudo-concentration is $\phi_{50+} = 1$.

2.4.2 Lognormal Distribution

First, consider the non-intermittent lognormal distribution in pseudo-concentration “+” coordinates. The lognormal probability density function (pdf) is:

$$p(\phi_+) = \frac{1}{\sqrt{2\pi}\sigma_{l+}\phi_+} \exp\left(-\frac{\ln^2\left(\frac{\phi_+}{\phi_{50+}}\right)}{2\sigma_{l+}^2}\right) \quad (2.16)$$

with a mean

$$\Phi_+ = \exp\left(\frac{\sigma_{l+}^2}{2}\right) \quad (2.17)$$

and variance

$$\phi_+^{\prime 2} = \Phi_+^2(\exp(\sigma_{l+}^2) - 1) \quad (2.18)$$

This is the lognormal distribution that will be implemented in the stochastic model. For this distribution, the log standard deviation σ_{l+} must be chosen to give the correct fluctuation intensity after the distribution is shifted by ϕ_{base} and all of the negative concentrations are clipped.

2.4.3 Intermittency Factor of Clipped Lognormal

To obtain the desired intermittency factor γ the lognormal distribution is shifted by ϕ_{base} to transform the simulated time series from strictly positive concentrations ϕ_+

to $\tilde{\phi}$ with positive and negative concentrations, where the negative values represent the intermittent periods of zero concentration.

$$\tilde{\phi} = \phi_+ - \phi_{\text{base}} \quad (2.19)$$

The shift ϕ_{base} must be chosen so that the probability of observing a concentration greater than zero is equal to the user-specified intermittency factor γ .

$$\gamma = \int_{\phi_{\text{base}}}^{\infty} p(\phi_+) d(\phi_+) \quad (2.20)$$

Using Equation (2.16) in Equation (2.20) and solving for γ in terms of the two unknowns ϕ_{base} and σ_{l+}

$$\gamma = \frac{1}{2} \left(1 - \text{erf} \left(\frac{\ln(\phi_{\text{base}})}{\sqrt{2}\sigma_{l+}} \right) \right) \quad (2.21)$$

2.4.4 Fluctuation Intensity of Clipped Lognormal

In addition to the intermittency factor γ , the conditional fluctuation intensity i_p^2 is required to fully describe the clipped lognormal. After shifting the non-intermittent pseudo-concentrations ϕ_+ by ϕ_{base} , all of the negative $\tilde{\phi}$ concentrations are transformed to a delta function at zero concentration with probability $(1 - \gamma)$. This leaves only positive and zero concentrations for the actual normalized dimensionless concentration ϕ .

The full time series mean Φ of the clipped lognormal is derived in Appendix B as:

$$\Phi = \frac{\exp\left(\frac{\sigma_{l+}^2}{2}\right)}{2} \left(1 - \text{erf} \left(\frac{\ln \phi_{\text{base}} - \sigma_{l+}^2}{\sqrt{2}\sigma_{l+}} \right) \right) - \frac{\phi_{\text{base}}}{2} \left(1 - \text{erf} \left(\frac{\ln \phi_{\text{base}}}{\sqrt{2}\sigma_{l+}} \right) \right) \quad (2.22)$$

with a second moment $\overline{\phi^2}$

$$\begin{aligned} \overline{\phi^2} = & \frac{\exp(2\sigma_{l+}^2)}{2} \left(1 - \operatorname{erf} \left(\frac{\ln \phi_{\text{base}} - 2\sigma_{l+}^2}{\sqrt{2}\sigma_{l+}} \right) \right) \\ & - \phi_{\text{base}} \exp \left(\frac{\sigma_{l+}^2}{2} \right) \left(1 - \operatorname{erf} \left(\frac{\ln \phi_{\text{base}} - \sigma_{l+}^2}{\sqrt{2}\sigma_{l+}} \right) \right) \\ & + \frac{\phi_{\text{base}}^2}{2} \left(1 - \operatorname{erf} \left(\frac{\ln \phi_{\text{base}}}{\sqrt{2}\sigma_{l+}} \right) \right) \end{aligned} \quad (2.23)$$

The conditional moments including only non-zero in-plume concentration periods (denoted by a subscript “p”) are related by the definition of the intermittency factor γ to the full time series moments by:

$$\gamma \overline{\phi_p^n} = \overline{\phi^n} \quad (2.24)$$

By definition, the second moment $\overline{\phi^2}$ is related to the mean Φ and the second moment about the mean ϕ'^2 by:

$$\overline{\phi^2} = \Phi^2 + \phi'^2 \quad (2.25)$$

The conditional fluctuation intensity i_p^2 is defined as

$$i_p^2 = \frac{\phi_p'^2}{\Phi_p^2} \quad (2.26)$$

with equations (2.24), (2.25) and (2.26):

$$i_p^2 = \frac{\overline{\phi^2}}{\Phi^2} - 1 \quad (2.27)$$

Using the definitions of the moments $\overline{\phi^2}$ from Equation (2.23) and Φ from Equation (2.22) in Equation (2.27) gives an implicit relation for the input i_p^2 in terms of the unknowns ϕ_{base} and σ_{l+} .

2.4.5 Lognormal in c_+ Coordinates

Equations (2.21) and (2.27) can be used to calculate ϕ_{base} and σ_{l+} in terms of the user input fluctuation intensity i_p^2 and intermittency factor γ . Because these are implicit relationships, ϕ_{base} and σ_{l+} must be found numerically. This was accomplished using a simple iterative bisection method.

The numerical solution for equations (2.27) and (2.21) does not converge for all possible values of i_p^2 and γ . Figure 2.5 shows the lower boundary of solutions possible for given i_p^2 and γ combinations. Although the vertical axis in Figure 2.5 ends at $i_p^2 = 3.0$, values as high as $i_p^2 = 10^4$ were checked and found to have solutions. Fortunately, the presence of this lower boundary of solutions does not cause any problem because real plumes are well within the valid range. The solid line in Figure 2.5 shows an empirical relationship suggested by Wilson (1995, p. 52) for typical i_p^2 versus γ values in atmospheric plumes.

With the solution for σ_{l+} and ϕ_{base} , the value of the dimensionless conditional mean Φ_p can be calculated. The value of the median concentration c_{50+} can be found from the definition in (2.9) with the user input conditional mean concentration C_p

$$c_{50+} = \frac{C_p}{\Phi_p} \quad (2.28)$$

Using this value of c_{50+} the value of c_{base} is

$$c_{\text{base}} = \phi_{\text{base}} c_{50+} \quad (2.29)$$

The log standard deviation σ_{l+} is the same in both the dimensionless ϕ_+ coordinates and the dimensioned c_+ coordinates.

The c_{50+} and σ_{l+} values are the required parameters for the c_+ lognormal pdf:

$$p(c_+) = \frac{1}{\sqrt{2\pi}\sigma_{l+}c_+} \exp\left(-\frac{\ln^2\left(\frac{c_+}{c_{50+}}\right)}{2\sigma_{l+}^2}\right) \quad (2.30)$$

and the c_{base} value is used after the simulated time series is generated to clip the time series and the pdf.

2.5 Generating Stochastic Time Series

The stochastic differential equation (2.2) is solved numerically by using a forward difference:

$$c_{+(n+1)} = c_{+(n)} + a_n \Delta t + b_n \sqrt{\Delta t} N_n \quad (2.31)$$

where $c_{+(n-1)}$ is the instantaneous c_+ concentration at time t_{n-1} . $c_{+(n)}$ is the instantaneous concentration at time t_n . Δt is the time increment, and N_n is a Gaussian random number with zero mean and unity variance. The $\sqrt{\Delta t}$ in equation (2.31) arises from the original definition of the random fluctuation process in equation (2.2). The Gaussian random number $d\zeta$ has a mean of zero and a variance dt and the units of $d\zeta$ are $\sqrt{\text{time}}$. In equation (2.31) the Gaussian random number is normalized by $\sqrt{\Delta t}$ because it is more convenient to generate random numbers with mean 0 and variance 1. This leaves a $\sqrt{\Delta t}$ in the numerator of the second term of equation (2.31).

A uniform distribution of random numbers was generated with a shift register sequence generator as discussed by Maier (1991) and Carter (1994). For stochastic simulations it is important that the period of the random number generator is large because millions of random numbers are required for a single simulation. Repeating a short sequence of random numbers does not produce the same result as individual

random numbers. The period of the shift register generator is approximately 9×10^{74} . That is, the random sequences do not repeat until 9×10^{74} numbers have been generated so there are no repeating sequences in the simulation. The Box-Muller (1958) transformation was used to obtain the Gaussian distributed random number \mathcal{N}_n from the uniform distribution. Appendix D provides additional computational detail on the random number generator.

The simple linear form of the a term is Equation (2.6) and the b term is found from Equation (2.5) by substituting in the definition of the a term from Equation (2.6) and the pdf $p(c_+)$ from Equation (2.30).

$$b^2 = \frac{C_+ \sqrt{2\pi} \sigma_{l+} c_+}{T_c} \exp\left(\frac{\ln^2\left(\frac{c_+}{c_{50+}}\right)}{2\sigma_{l+}^2}\right) \left(\operatorname{erf}\left(\frac{\ln\left(\frac{c_+}{c_{50+}}\right)}{\sqrt{2}\sigma_{l+}}\right) - \operatorname{erf}\left(\frac{\ln\left(\frac{c_-}{c_{50+}}\right) - \sigma_{l+}^2}{\sqrt{2}\sigma_{l+}}\right)\right) \quad (2.32)$$

The parameters c_{50+} and σ_{l+} are calculated from the user input intermittency factor γ and the input conditional fluctuation intensity i_p^2 as discussed in Section 2.4.

The conditional mean C_{p+} and time scale T_{c+} were arbitrarily set to unity to generate fully normalized time series. Because the simulation is an inertialess Markov process there is no sensitivity to the length of the time step (i.e. to the “acceleration” $\partial^2 c_+ / \partial t^2$) and the output of the simulation can be scaled to match the time scale and mean concentration of any desired time series. The Δt time step was set to $0.01 T_{c-}$ giving one hundred time steps per time scale.

Each run of the simulation was started at the median concentration c_{50+} and then allowed to run for $10 T_{c+}$ to eliminate the effects of picking the same starting point for each simulation. The random number generator was seeded based on the time that the computer program was started.

The simulation was run for a total of at least 5000 integral time scales to allow a sufficient length of time to produce the rare peak concentrations that define the tail of the pdf of concentration where $c_+ \gg C_+$. The following equation gave a reasonable estimate for the number of time scales, n_T , needed for each simulation realization.

$$n_T \simeq \frac{5000i_p}{(\gamma + 0.1)} \quad (2.33)$$

with the input fluctuation intensity i_p and intermittency factor γ . The number of time scales n_T varies inversely with γ because as the intermittency factor decreases there are fewer excursions above the zero concentration level in a given length of time, so a longer duration is required to ensure that a sufficient amount of non-zero data are generated. Similarly, as i_p increases, the fluctuations become larger and additional time is required to capture all of the rare events. The factor of 0.1 in the denominator was added to put an upper bound on the number of time scales in each simulation as the intermittency factor γ becomes very small.

2.5.1 Time Scales of Intermittent and Non-Intermittent Time Series

The time scale of the non-intermittent pseudo-concentration fluctuations was set to $T_{c_+} = 1.0$ for the stochastic simulation. The time scale T_c of the actual fluctuations of the intermittent concentration c is not equal to 1.0 after clipping. The clipping process removes all of the fluctuations below c_{base} and replaces them with zero periods. This should make the time scale longer, but clipping also produces sharp high frequency cutoffs that decrease the time scale T_c . It is not obvious which of these factors dominates.

Figure 2.6 shows the variation in the actual time scales T_c calculated from the

clipped intermittent time series as compared to the T_{c+} time scale. In general, the time scale T_c of the intermittent concentration fluctuations is shorter than the time scale T_{c+} of the non-intermittent concentrations. This relationship can be approximated as a function of the intermittency factor $T_c/T_{c+} = 0.78 + 0.23\gamma$. The variability between realizations is quite large as demonstrated by the error bars in Figure 2.6. Fortunately, this is not a difficult problem to deal with since the inertialess nature of the Markov simulation allows the time scale T_c to be rescaled to match the time scale of any real process. It is important to use T_c when rescaling the time series and not T_{c+} because there can be as much as a 40% difference between the two values.

2.5.2 Time Step for Molecular Diffusion Cutoff

The stochastic simulation produces a time series of concentration fluctuations with the appearance that it has been sampled at a frequency of $1/\Delta t$. Since the purpose of the simulation is to simulate atmospheric releases, a brief calculation was required to check that this sampling frequency did not exceed the frequencies that are possible in the real atmosphere due the limits imposed by diffusion and viscosity.

In the atmosphere, the mass diffusivity D of most gases is about the same as the molecular viscosity ν of the air. Therefore, the Schmidt number $Sc \approx 1$, and the Kolmogorov microscale of concentrations is approximately equal to the Kolmogorov microscale for turbulence kinetic energy dissipation $\eta_c \simeq \eta$. A typical value is $\eta \simeq 0.001\text{m}$ that gives a cutoff wavenumber of $k_{\text{cut}} = 1/\eta = 1000 \text{ m}^{-1}$. With $k_{\text{cut}} = 2\pi f_{\text{cut}}/U$ and a typical windspeed of $U = 2 \text{ m/s}$ this corresponds to a cutoff frequency of about $f_{\text{cut}} = 300 \text{ Hz}$ with frequency rolloff beginning at about $0.2f_{\text{cut}} = 60 \text{ Hz}$.

The stochastic model samples at 100 samples per time scale. For typical atmo-

spheric time scale of $T_c = 100$ seconds, the sampling rate is only 1 Hz, about 2 orders of magnitude below the Kolmogorov cutoff. No physical limitations on fluctuation frequency were present in the stochastic simulation of atmospheric concentration fluctuations.

2.6 Concentration Fluctuation Measurements

The water channel facility, shown in Figure 2.7, in the Mechanical Engineering Department at the University of Alberta was used to collect the concentration fluctuation data. The experimental time series used for verification and development of the stochastic model were measured by Wilson, Zelt and Pittman (1991). The measurement equipment and technique is documented in the Ph.D. thesis by Zelt (1992) and discussed in Yee, Wilson and Zelt (1993).

2.6.1 Water Channel Description

The water channel is a recirculating system with a total volume of about 4300 litres driven by a pair of recirculating pumps. Both pumps discharge into a settling chamber in the lower part of the inlet tank. The flow from the settling chamber is directed through turning vanes and flow straighteners to remove any pump generated turbulence.

The test section in Figure 2.7 has a width of 680 mm and a length of about 5000 mm. The floor of the water channel was covered with an uniform roughness array of in-line cylinders 1.9 mm high and 4.5 mm diameter on 8.0 mm centers in the cross-stream and downstream directions. A boundary layer trip of solid bars to generate large scale turbulence and a low wall to increase the turbulence near ground

level were placed in the channel to enhance the development of the neutrally stable boundary layer. When run at a depth of 300 mm in the test section, the rough bottom boundary layer had a thickness of $H = 150$ mm giving a scale factor of approximately 3300:1 as compared to a neutral atmosphere.

The mean velocity profile of the shear layer in the water channel agreed closely with the log law profile:

$$\frac{U}{u_*} = \frac{1}{\kappa} \ln \left(\frac{z - d_0}{z_0} \right) \quad (2.34)$$

where U is the mean flow velocity, $u_* = 14.6$ mm/s is the friction velocity, $\kappa = 0.4$ is the von Karman constant, $d_0 = 1.5$ mm is the displacement height of the surface roughness, $z_0 = 0.15$ mm is the roughness length scale and z is the height above ground level.

A downstream facing isokinetic source from a 3.45 mm ID tube at a position 2030 mm downstream from the beginning of the channel emitted saline tracer solution at a height $h_s = 52$ mm above the bottom of the channel into a mean velocity of 210mm/s at the source height. The tracer was a neutrally buoyant mixture of water, ethanol and 50g/l salt emitted with a flow rate of 2.0 ml/s.

2.6.2 Data Collection and Processing

The concentration fluctuation data were obtained with a rake of 8 electrical conductivity probes mounted with the probe tips 20 mm apart. Each probe had a spatial resolution of about 1 mm. Throughout the experiments the probe response was corrected for background buildup and electronic drift in the output. Each fluctuation time series consisted of 125,000 points sampled at 250 points per second for a total sample time of 500 seconds. At 3300:1 scale this corresponded to samples spaced

about 3 m apart in the wind direction. The concentration measurements were normalized by the source concentration and stored as 16-bit integer values.

After the data set was collected it was processed to correct for the probe response time constant that produced a -3dB rolloff frequency of 35 Hz. Deconvolution of the digital signals from the probes with the inverse of a first order impulse response function enhanced the effective frequency response to 105 Hz, equivalent to a spatial resolution of about 0.3 mm in the water channel or about 1 m in the atmosphere at a scale of 3300:1.

A zero concentration threshold was set at 8.0 times the background noise level to eliminate the effect of noise on the measured intermittency. This threshold corresponds to about $0.09C_p$ and was determined empirically by analyzing time series with no source emission and adjusting the threshold to find the required 100% zero period intermittency.

The data were collected by Wilson, Zelt and Pittman (1991) at three downstream positions $x/h_s = 9.0, 19$ and 29 . Measurements were taken at various positions y across the width of the plume at each of these downstream locations. In the present study, only data taken at the source height $z = h_s$ with intermittency factors $\gamma > 0.01$ were used. The restriction on the intermittency factor ensured that there were a sufficient number non-zero data points to generate reasonable probability distribution histograms.

2.6.3 Frequency Spectrum of Experimental Data Compared to the Simulation

There is one potential problem with attempting to match the experimental water channel data with the stochastic simulation. As Wilson, Zelt and Pittman (1991) note, for salt into water the mass diffusivity D is much smaller than the molecular viscosity of the fluid ν and the Schmidt number $Sc = \nu/D \gg 1$. The effect of this large Schmidt number is that velocity driven straining of the concentration field decays before molecular diffusion smears out the concentration fluctuations. This can be seen in the spectrum of concentration fluctuations shown in Figure 2.8 where the water channel data follow the viscous-convective Batchelor spectrum with $F_c \propto f^{-1}$ at high frequencies f . The shape of the concentration spectrum of the stochastic simulation is determined by the assumption of a first order Markov process that produces $F_c \propto f^{-2}$ at high frequencies. Not shown in Figure 2.8 is the spectrum of concentration fluctuations in the atmosphere where $D \approx \nu$ so $Sc \approx 1$ and at high frequencies $F_c \propto f^{-5/3}$, see Wilson (1995, pp. 143-146).

The important implication of this spectral mismatch between the stochastic simulation and the experimental data is that there should be more high frequencies in the water channel data than in the stochastic simulation, even if the fluctuation intensities are the same. Higher peak concentrations might be expected in the water channel data. Comparison of the experimental data and the stochastic simulation indicated that the effect of this spectral mismatch is small. When the stochastic model is used for atmospheric concentration fluctuations the effect should be even smaller as the first order Markov spectrum $F_c \propto f^{-2}$ provides a much closer match to the $F_c \propto f^{-5/3}$ spectrum expected in the atmosphere.

2.7 Comparison of Experimental Data and Clipped Lognormal pdf

A key input to the stochastic model is the probability density function (pdf) of concentration. In the previous sections it was assumed that the clipped lognormal distribution can be used to describe intermittent concentration fluctuations. To demonstrate that this assumption is reasonable, the experimental water channel concentration probability distribution was compared to the clipped lognormal probability distribution. For this comparison only conditional (in-plume) concentrations were considered, so all concentrations were normalized by the conditional mean concentration C_p . The theoretical clipped lognormal distributions were given the same intermittency factor γ and conditional fluctuation intensity i_p^2 as the experimental data sets.

Several different forms of the probability distribution of concentration were examined including the probability density function (pdf) which is the form of the probability distribution used directly in the simulation, the cumulative probability distribution function (cdf) which emphasizes the low concentration levels less than the mean, and the exceedance probability distribution function which emphasizes the high concentrations greater than the mean. Plots of all of these forms of the probability distribution are contained in Appendix E. Only the exceedance plots are presented in this paper in Figures 2.9 and 2.10. All of these probability distributions prove only one point, that the clipped lognormal is a good choice for describing the water channel experimental data. Additional probability distribution shapes such as the gamma or clipped lognormal were not evaluated because the clipped lognormal provided a good fit and other distributions are much more difficult to manipulate mathematically with the shifting and clipping processes necessary to produce intermittent time series.

2.7.1 Exceedance Probability

In most hazardous releases the high concentrations greater than the mean are the most important, so the most relevant information is contained in the exceedance probability plots. Figures 2.9 and 2.10 show the normalized conditional exceedance probability $E_p(c/C_p)$ defined as the probability of finding a concentration greater than c/C_p

$$E_p\left(\frac{c}{C_p}\right) = \int_{\frac{c}{C_p}}^{\infty} p_p\left(\frac{c}{C_p}\right) d\left(\frac{c}{C_p}\right) \quad (2.35)$$

The log-log plots of exceedance probability emphasize the high concentrations $c > C_p$. Agreement with the experimental data set is within a few percent up to $E_p = 0.1$, that is the 90th percentile concentration. At the 99th percentile concentration or $E_p = 0.01$, the error is within a factor of two, even when the intermittency factor γ is very small and there are measurable concentrations only 1% of the total time. All of the plots go to $E_p = 0.00001$ that gives the concentration that is exceeded only 0.001% of the time during which there is a measurable concentration. This low probability means that there are at only 1 or 2 events in the entire experimental data set that exceeded that concentration. It is difficult to evaluate the fit at these high concentration, low probability values, because only 125,000 data points were recorded in each experimental time series.

2.8 Stochastic Model Performance

To determine if the stochastic model is an accurate simulation of the intermittent concentration fluctuation time series, the output of the stochastic simulation is compared to data generated from the water channel experiments. The first derivative of

concentration with respect to time and the upcrossing rate are two outputs that can be used to test the stochastic simulation. The correct distribution of concentration values is guaranteed by the input clipped lognormal pdf that matches the statistics of the data set, but the derivative of concentration and the upcrossing rate are recurrence statistics that will only agree with the experimental data if the simulation produces the correct fluctuations.

2.8.1 Filtering the Stochastic Simulation

To compare time derivatives and upcrossing rates, the simulated time series and the experimental time series must have the same high frequency cutoff. Each stochastic model time series is generated with 100 time steps per time scale T_c . When this time step is adjusted to match the experimental data time scale of about $T_c = 0.027$ seconds the effective sampling rate of the simulation is about 3700 Hz. Because the frequency response of the experimental probes was only about 105 Hz, the stochastic simulation was filtered with a sixth order Butterworth digital filter to limit the high frequency components in the simulation to 105 Hz.

The filter was applied to the simulated time series after it was clipped by setting all of the negative concentration values to zero. This approximates the way the experimental probes filter the concentration fluctuations in the water channel data. Filtering affects the length of the intermittent periods because it removes the high frequency transients and the short zero periods and causes the intermittency factor $\gamma \rightarrow 1.0$ as the cutoff frequency decreases. To recover the intermittent periods in the experimental data a “zero” cutoff was defined by Wilson, Zelt and Pittman (1991) at 8 standard deviations above the background noise level. An equivalent cutoff of $0.09C_p$ was applied to the stochastic simulation after filtering to match the experimental

data processing that discarded concentration measurements below the probe noise threshold.

2.8.2 Time Derivative of Concentration

One of the important assumptions in the stochastic model is that the magnitude of the derivative of concentration is dependent on the current concentration through the deterministic term $a(c_+, t)$ in Equation (2.2). Figures 2.11 and 2.12 show that the water channel measurements confirm the field observations of Yee et al. (1993), with the rms (root mean square) concentration derivation \check{c}' exhibiting a very strong dependence on the concentration level c/C_p at which it was measured.

Figures 2.11 and 2.12 compare the stochastic simulation rms time derivative of concentration \check{c}' with the rms time derivative of concentration for the water channel data. The time derivative of concentration was calculated as the change in concentration over one time step. The normalized rms time derivative of concentration $\check{c}'T_c/C_p$ is plotted against the concentration level c/C_p for a range of downstream positions. Figure 2.11 shows points near the centreline of the plume and Figure 2.12 shows points near the outside edge of the plume. The stochastic simulation line in Figures 2.11 and 2.12 is the mean of 10 independent simulated time series.

Figures 2.11 and 2.12 demonstrate that the stochastic model, Equation (2.31), gives a good estimate of the rms time derivative of concentration \check{c}' . Even though there is a wide range in fluctuation intensities and intermittency factors the stochastic model produces the correct \check{c}' within about a factor of 2. This confirms that the linear assumption for the a term in the stochastic model in conjunction with the assumption of a clipped lognormal is a reasonable model for the time derivatives of concentration.

There some evidence of a gradual evolution of the \check{c}' profiles with downstream dis-

tance in the experimental data set that does not occur in the stochastic model. Close to the source at $x/h_s = 9.0$ the stochastic simulation overestimates the derivative of concentration. At a downstream distance of $x/h_s = 19$ the stochastic simulation derivative is close to the experimental data and at the far downstream location with $x/h_s = 29$ the derivative is underestimated.

Some of the difference between the experimental data and the stochastic simulation can be accounted for by the different frequency rolloff rates of the experiments and the simulation as discussed in Section 2.6. The derivatives at high concentration levels $c/C_p > 10$ are underestimated by the stochastic model. This would be expected because the experimental data has more high frequency fluctuations and higher peak concentrations than the simulation.

2.8.3 Concentration Level Upcrossing Rates

An upcrossing is counted each time the concentration in the time series exceeds a threshold value while the derivative of concentration is positive (i.e. the concentration is increasing). The upcrossing rate is a measure of the average frequency of the fluctuations that exceed a particular concentration level. The upcrossing rate n^+ is not an input to the model so simulating the correct upcrossing rate demonstrates that the simulation produces the correct frequencies of fluctuations for each concentration level. Du's (1995) model was originally proposed to estimate the upcrossing rates for conditional time series of concentration fluctuations, ignoring all of the intermittent periods. In the present study, the total upcrossing rates including the intermittent periods of zero concentration was simulated.

In Figures 2.13 and 2.14 the results from a single experimental water channel run are shown. The stochastic simulation line is the mean of 10 realizations. Since

this is a stochastic model each realization is different and the dotted lines on the plot indicate a 2 standard deviation multiplicative range of run to run variation calculated as follows:

$$\begin{aligned} \text{upper bound} &= \mu \left(1 + 2 \frac{s}{\mu} \right) \\ \text{lower bound} &= \frac{\mu}{\left(1 + 2 \frac{s}{\mu} \right)} \end{aligned} \quad (2.36)$$

where μ is the mean of the upcrossing rate n^+T_c and s is the standard deviation of the 10 simulated time series. The upcrossing rates match well for the wide range in intermittencies and fluctuation intensities. The maximum difference is about a factor of 2 from the mean of the 10 simulation runs and within about 50% of the 2 standard deviation range of run to run variability.

As in the case of the time derivatives of concentration, there is some evidence of the spectral mismatch between the data and the stochastic simulation and there is also evidence of evolution of the experimental plume with downstream distance. As expected, there are more higher frequency fluctuations in the experimental data and the upcrossing rates at high concentrations $c/C_p > 10$ are underestimated by the simulation. At the far downstream location $x/h_s = 29$ the stochastic simulation consistently underestimates the upcrossing rate. At the locations closer to the source for $x/h_s = 9.0$ and 19, the upcrossing rate is overestimated at low concentrations and underestimated at high concentrations.

2.9 Summary and Conclusions

In this study it was demonstrated that intermittent concentration fluctuation time series at a fixed receptor in a dispersing point source plume can be simulated as a

first order inertialess Markov stochastic process. The input parameters required for the simulation are:

- intermittency factor γ
- conditional fluctuation intensity i_p^2 .
- probability distribution $p(c)$ for the intermittent time series.

Simulated time series are generated with a normalized mean concentration $c/C_p = 1$ so they can be scaled to any mean concentration. The inertialess Markov process allows the time scale of the generated time series T_c to be scaled to match any fluctuation time scale.

The stochastic simulation cannot handle intermittent time series directly, so some manipulation and interpretation of the simulated time series is required to produce the necessary intermittency. The key assumption is that intermittent periods of zero concentration are part of the same physical mixing process as the periods of non-zero concentration. This assumption allows the simulated non-intermittent time series to be shifted by a concentration c_{base} to give positive and negative concentrations \bar{c} . The positive concentrations are interpreted as actual fluctuations while the negative concentrations are interpreted as periods of zero concentration where the magnitude of the negative concentration represents the likelihood of obtaining a non-zero concentration in the next time step. The result is an intermittent time series represented by a clipped probability distribution. In this study, the lognormal distribution was used for the simulation. After shifting and clipping the resultant probability distribution of intermittent concentration fluctuations was a clipped lognormal with a delta function at zero concentration representing the intermittent periods.

The clipped lognormal was tested with experimental data from Wilson, Zelt and Pittman (1991) water channel experiments and found to provide a good fit to these data. There was some evidence of evolution of the experimental plume with downstream distance that does not occur in the stochastic model, but the effect was small. No effect of intermittency, fluctuation intensity or cross stream distance on the pdf was observed.

The stochastic simulation accuracy was demonstrated by comparing the first derivative of concentration with respect to time and the upcrossing statistics of the simulation with the experimental data over a range of intermittency factors $\gamma = 0.7$ to 0.01 and fluctuation intensities $i_p^2 = 2.2$ to 7.5. In all cases, the root mean square derivative of concentration and the mean upcrossing rate from the simulation were within a factor of two of the experimental upcrossing rate.

The advantages of the stochastic model are that it can be used to produce time series with any realistic combination of intermittency and fluctuation intensity and it can generate large ensembles of random time series with identical means, variances, and intermittencies. The same sort of data could be generated experimentally, but experiments are expensive and time consuming and the results cannot be controlled as carefully to examine a range of different means, variances and intermittencies. Each simulated time series represents an individual realization of the event and complex hazard models can be time stepped through simulated releases to observe the effects of realization to realization variability as well as large ensemble averages.

In its present form, the stochastic simulation is useful for generating time series to evaluate hazardous effects. However, some additional work may be required to make this model more realistic near ground level. All data used in the present study were taken at the source emission height, but near ground level, where most receptor

exposures occur, the mixing is complicated by large shearing forces and the current form of the stochastic simulation may not work as well. Additional experimental and theoretical work is required to further develop and validate this stochastic model.

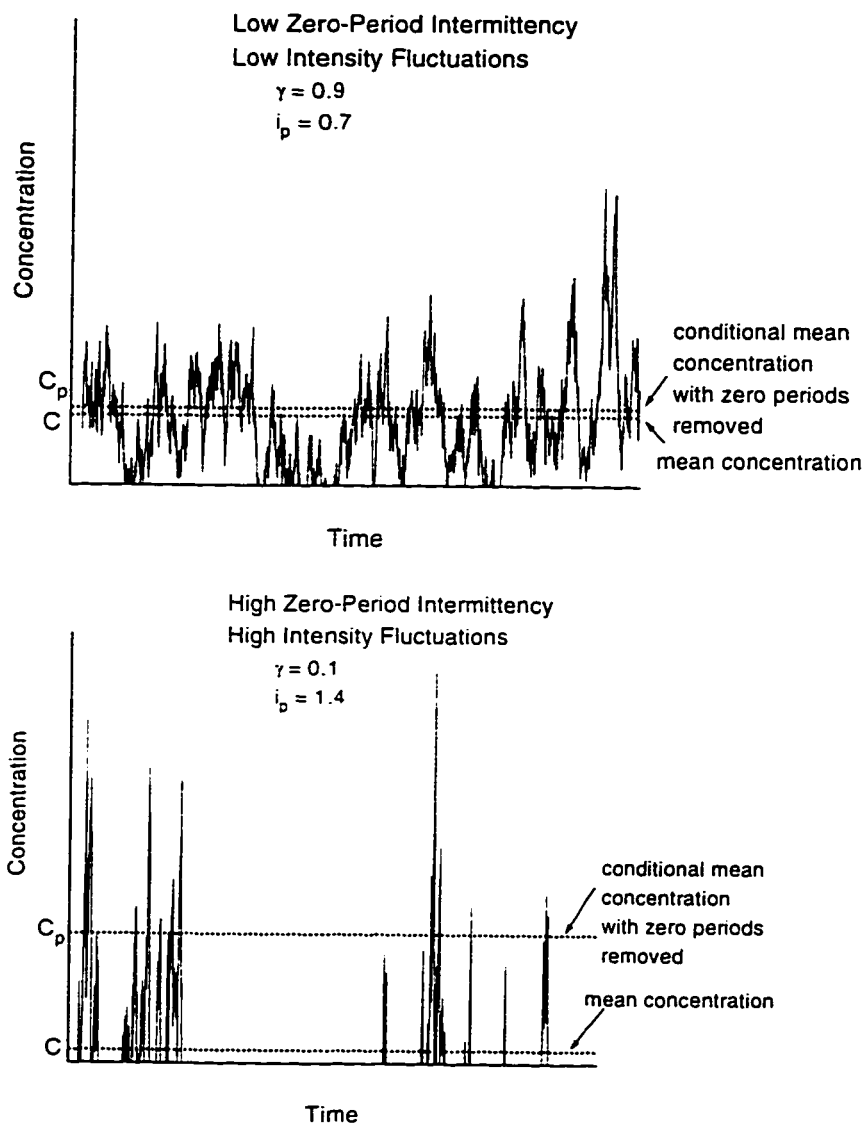
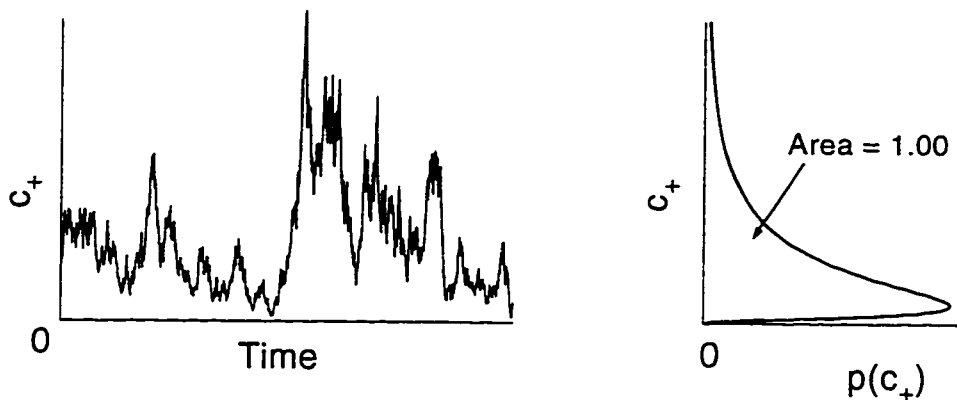
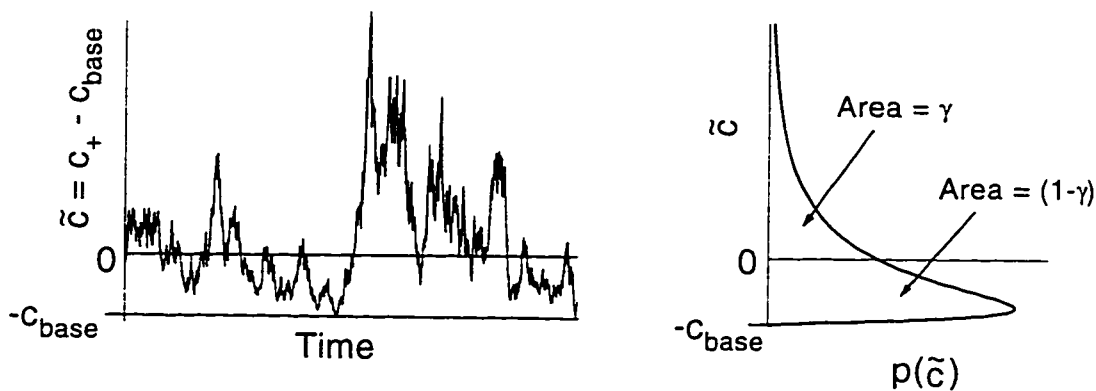


Figure 2.1: Typical intermittent concentration fluctuation time series with low intermittency ($\gamma = 0.9$) and high intermittency ($\gamma = 0.1$).

Step 1: Simulation in c_+ coordinates, with no intermittency ($\gamma_+ = 1.00$)



Step 2: Baseline shift by c_{base} to produce intermittency



Step 3: Clipping to obtain intermittency factor γ and concentration c

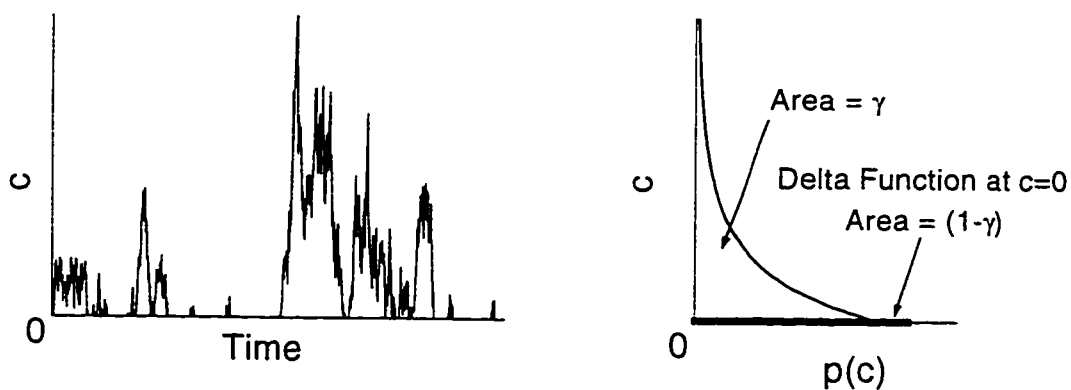


Figure 2.2: Clipping procedure to produce an intermittent time series.

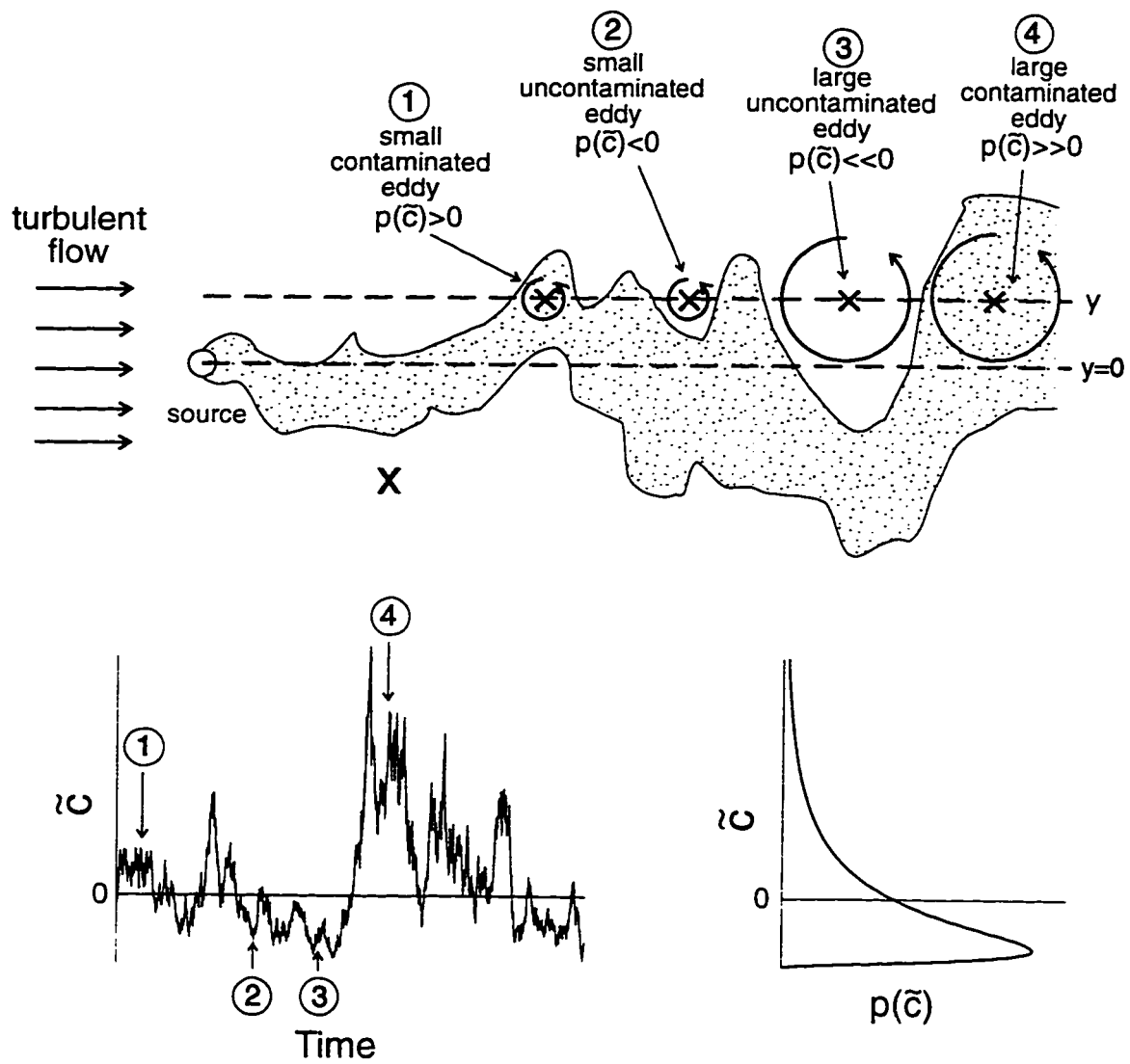
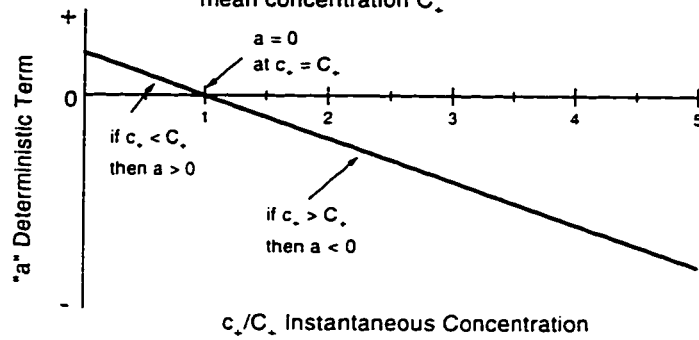


Figure 2.3: Physical model for interpreting the pdf of negative concentrations as intermittent periods of clean air (zero concentration).

Stochastic Differential Equation for Concentration Fluctuation

$$\frac{dc}{dt} = a + b \frac{d\zeta}{dt}$$

"a" is a deterministic restoring "force" to pull fluctuations back to well-mixed mean concentration C_e .



"b" is multiplied by the Gaussian random number $d\zeta$ to obtain the random fluctuations.

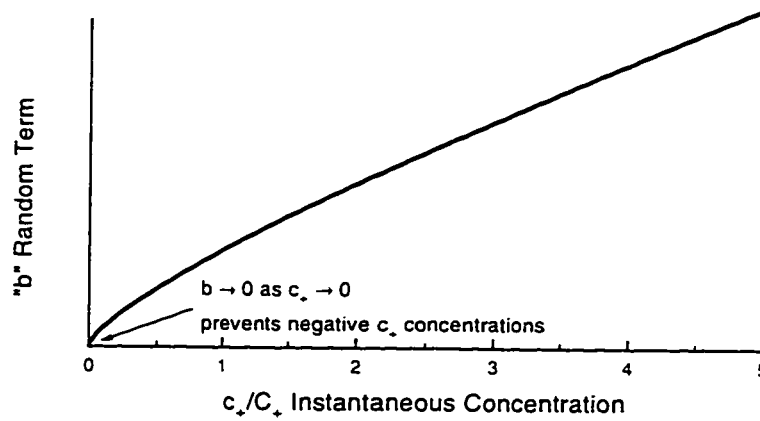


Figure 2.4: General form of the a and b terms in the stochastic simulation

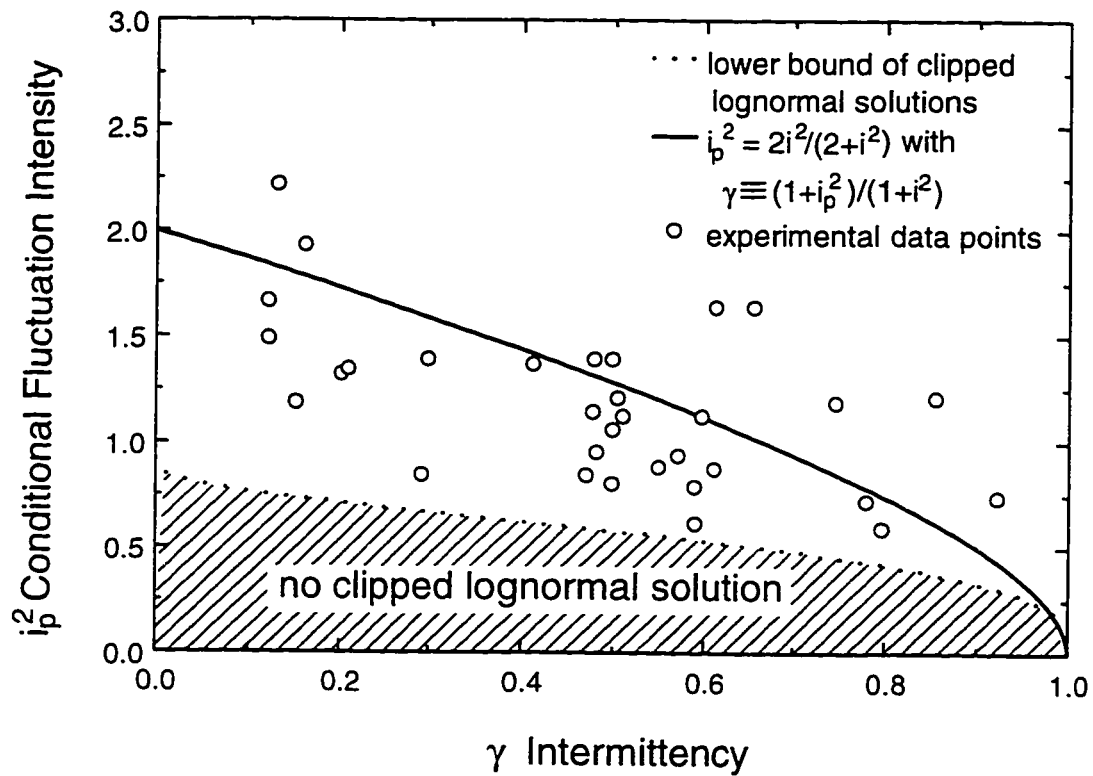


Figure 2.5: Boundary of clipped lognormal solutions in terms of the intermittency γ and the conditional fluctuation intensity i_p^2 . The solid line is the empirical relationship between i_p^2 and γ suggested by Wilson (1995) after considering the experimental data points from full scale and laboratory scale experiments. Experimental data points from Mylne and Mason (1991) and Fackrell and Robins (1982)

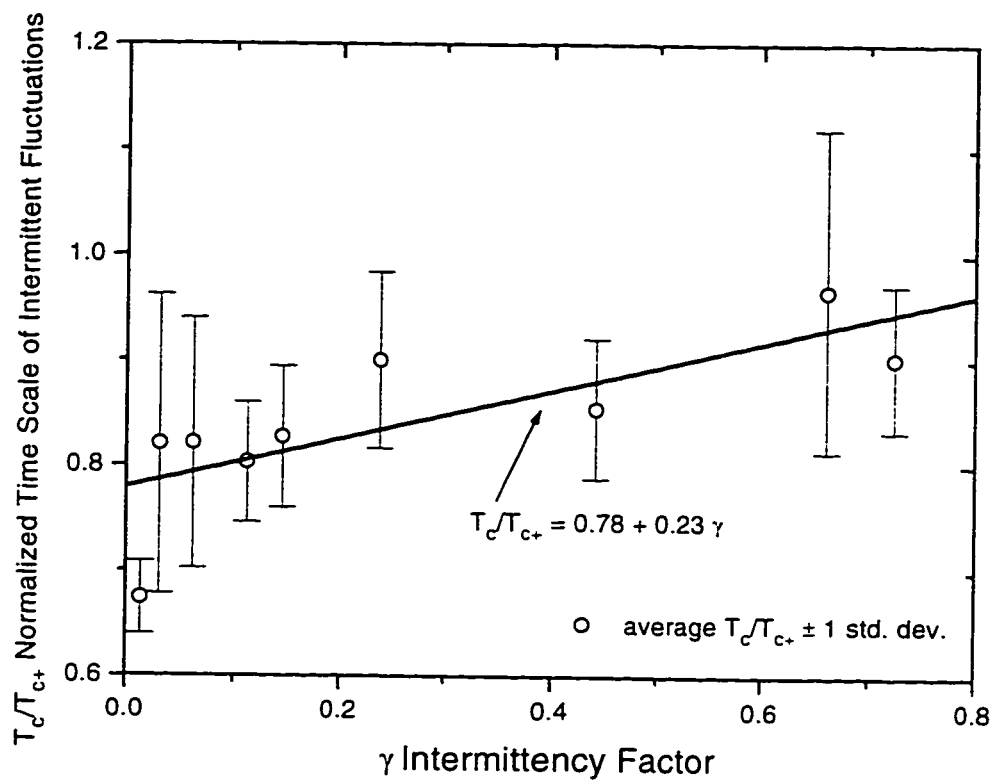


Figure 2.6: Time scale of intermittent concentration fluctuations T_c normalized by the time scale of the pseudo-concentration time series T_{c+} for a range of intermittency factors γ .

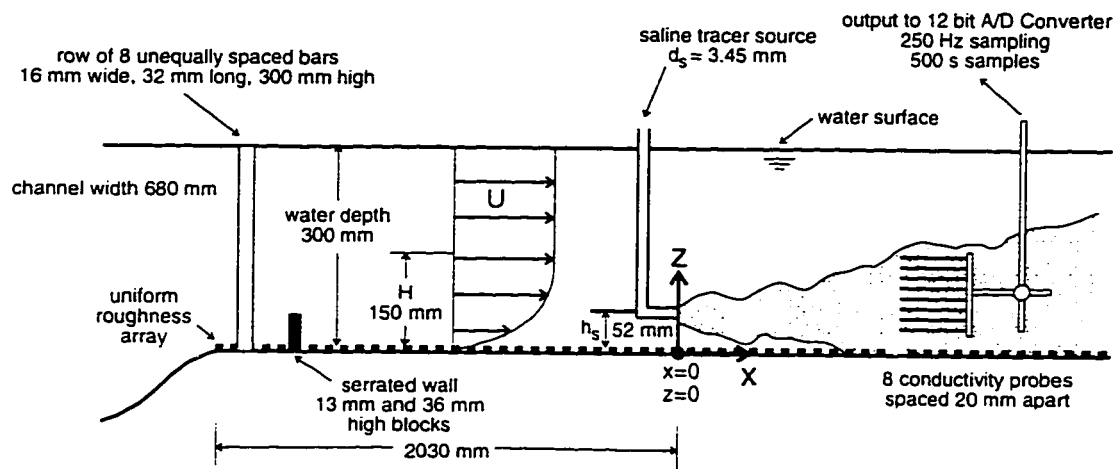


Figure 2.7: Schematic diagram of the water channel shear layer generator test section.

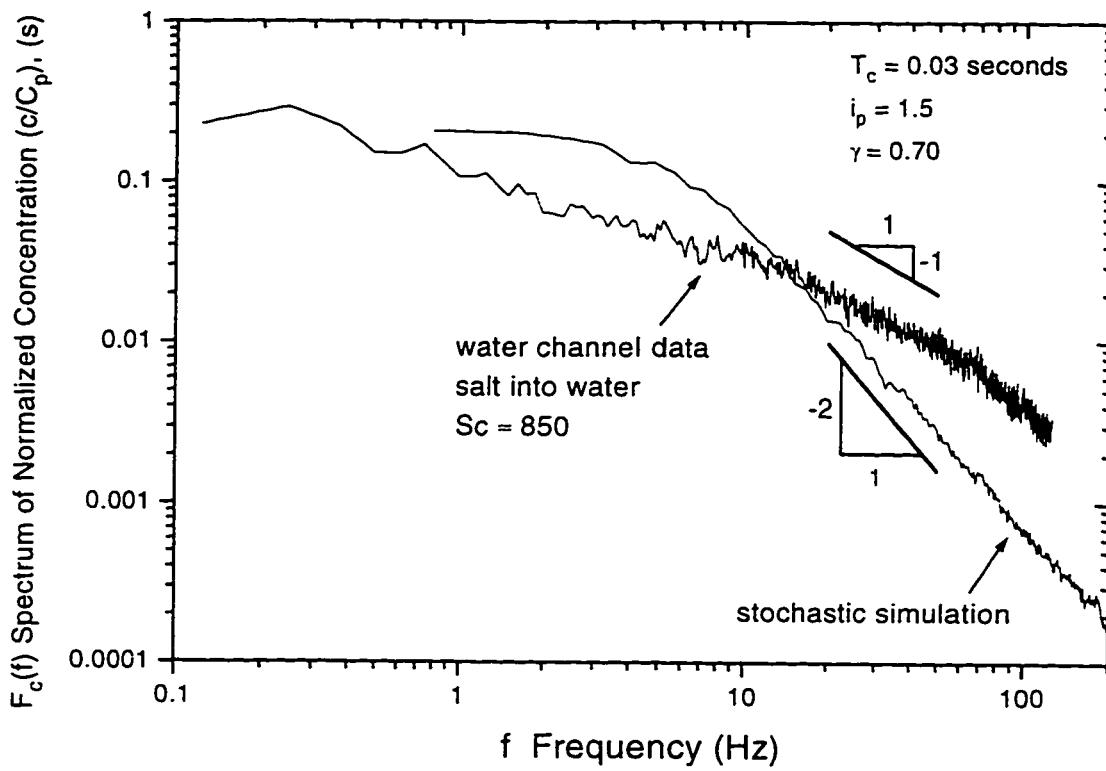


Figure 2.8: Typical spectra of normalized concentration fluctuations for the experimental data and for the stochastic simulation of that experiment.

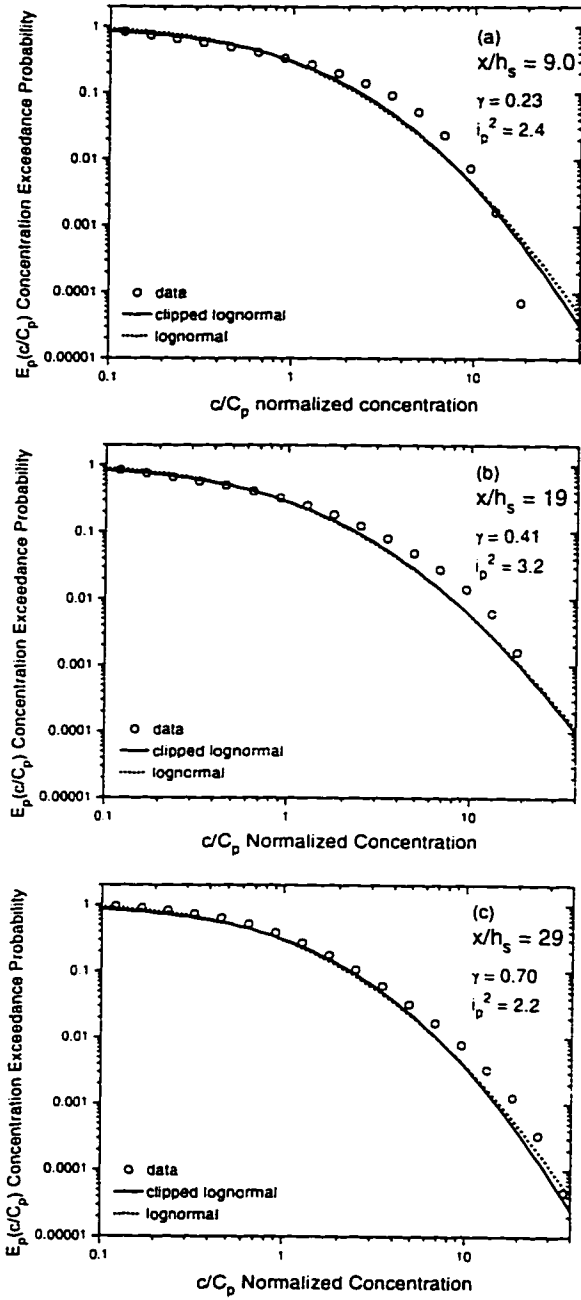


Figure 2.9: Conditional exceedance probability E_p for moderately intermittent fluctuations of the concentration c/C_p near the centreline of the plume at three downstream positions x/h_s . Cross stream distance from source (a) $y/\sigma_y = 0.3$ (b) $y/\sigma_y = 0.25$ (c) $y/\sigma_y = 0.18$

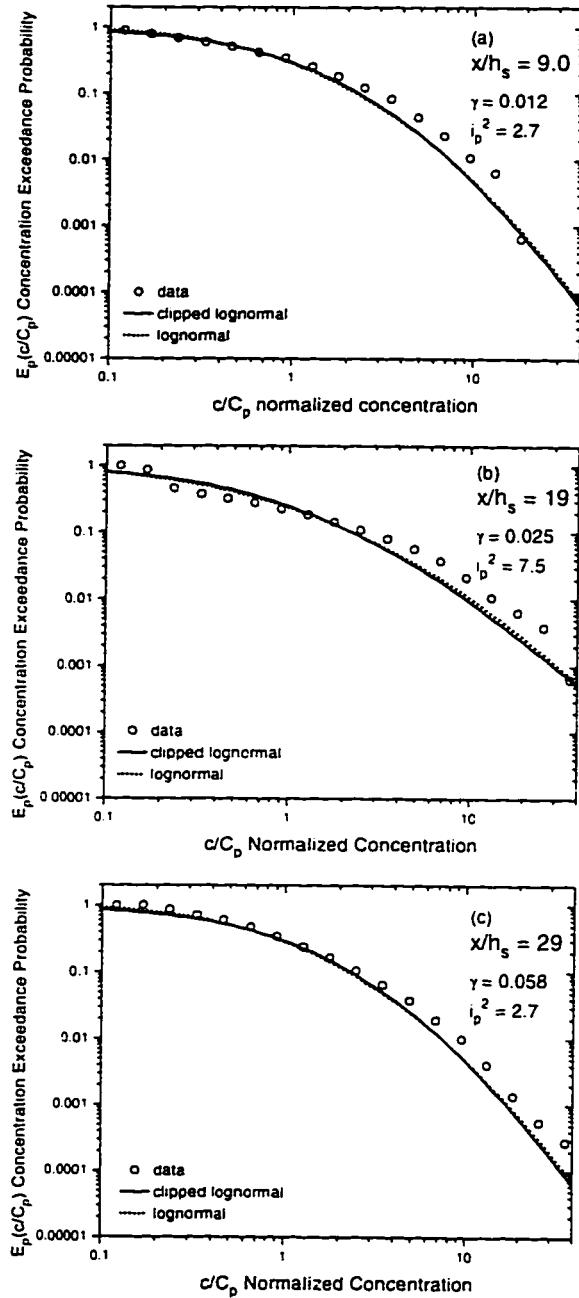


Figure 2.10: Conditional exceedance probability E_p for highly intermittent fluctuations of the concentration c/C_p on the outside edge of the plume at three downstream positions x/h_s . Cross stream distance from source (a) $y/\sigma_y = 4.1$ (b) $y/\sigma_y = 4.8$ (c) $y/\sigma_y = 2.8$

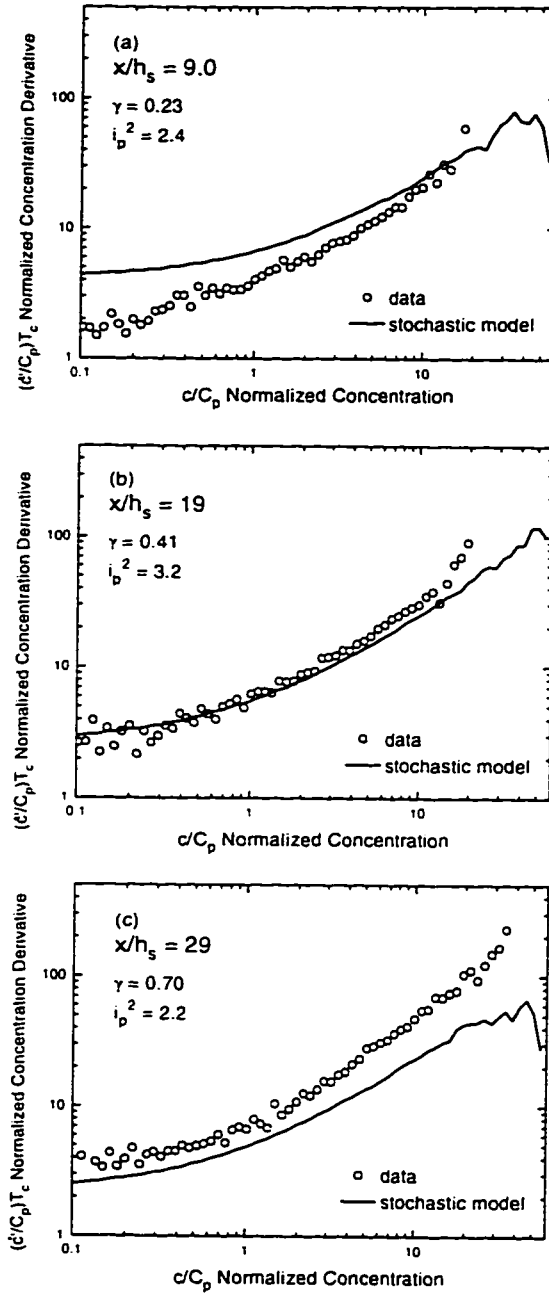


Figure 2.11: Normalized root mean square time derivative of concentration $(\dot{c}'/C_p)T_c$ at the concentration level c/C_p near the centreline of the plume at three downstream positions x/h_s . Cross stream distance from source (a) $y/\sigma_y = 0.30$ (b) $y/\sigma_y = 0.25$ (c) $y/\sigma_y = 0.18$

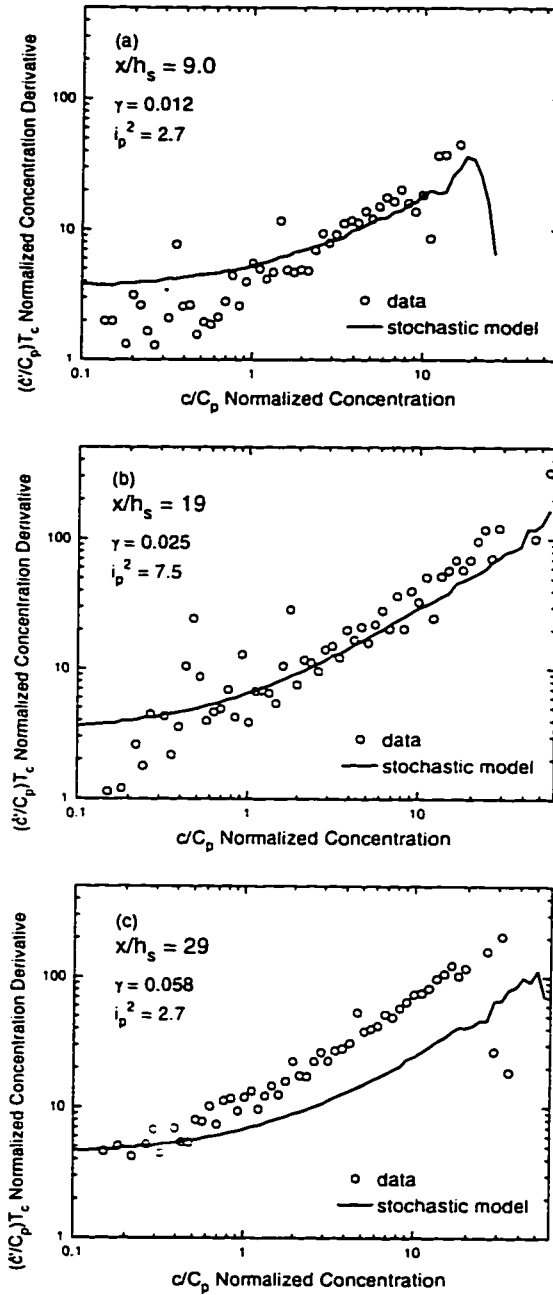


Figure 2.12: Normalized root mean square time derivative of concentration $(\partial c / \partial t)_{T_c}$ at the concentration level c / C_p on the outside edge of the plume at three downstream positions x / h_s . Cross stream distance from source (a) $y / \sigma_y = 4.1$ (b) $y / \sigma_y = 4.8$ (c) $y / \sigma_y = 2.8$

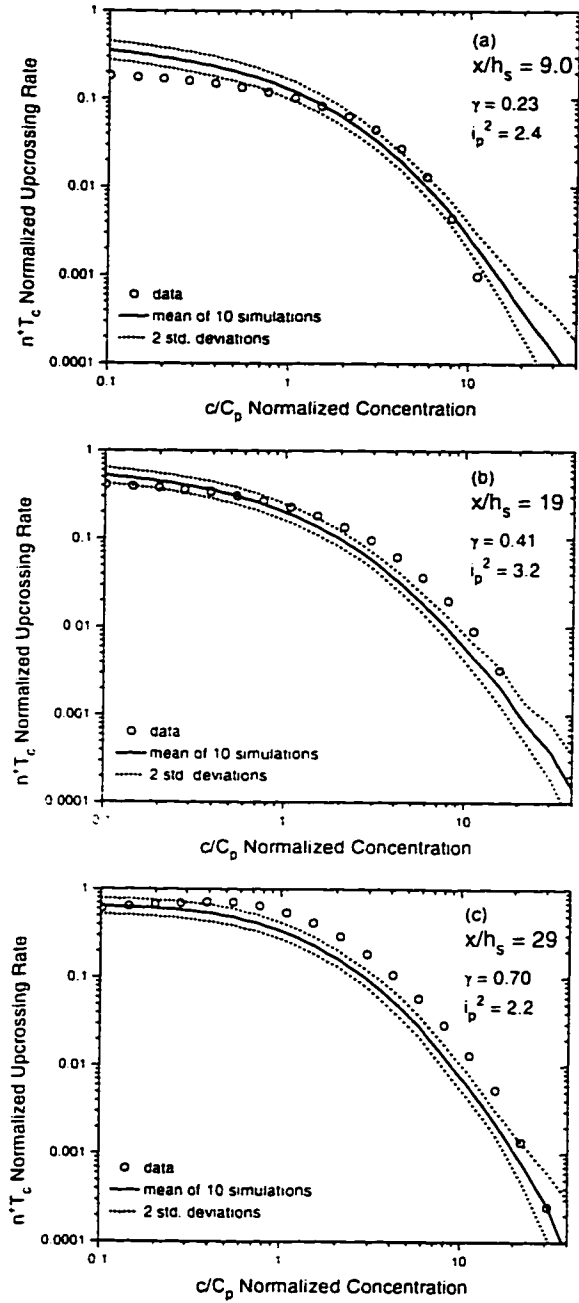


Figure 2.13: Normalized upcrossing rate $n^+ T_c$ for moderately intermittent time series versus the normalized instantaneous concentration c/C_p near the centreline of the plume at three downstream positions x/h_s . Cross stream distance from source (a) $y/\sigma_y = 0.30$ (b) $y/\sigma_y = 0.25$ (c) $y/\sigma_y = 0.18$

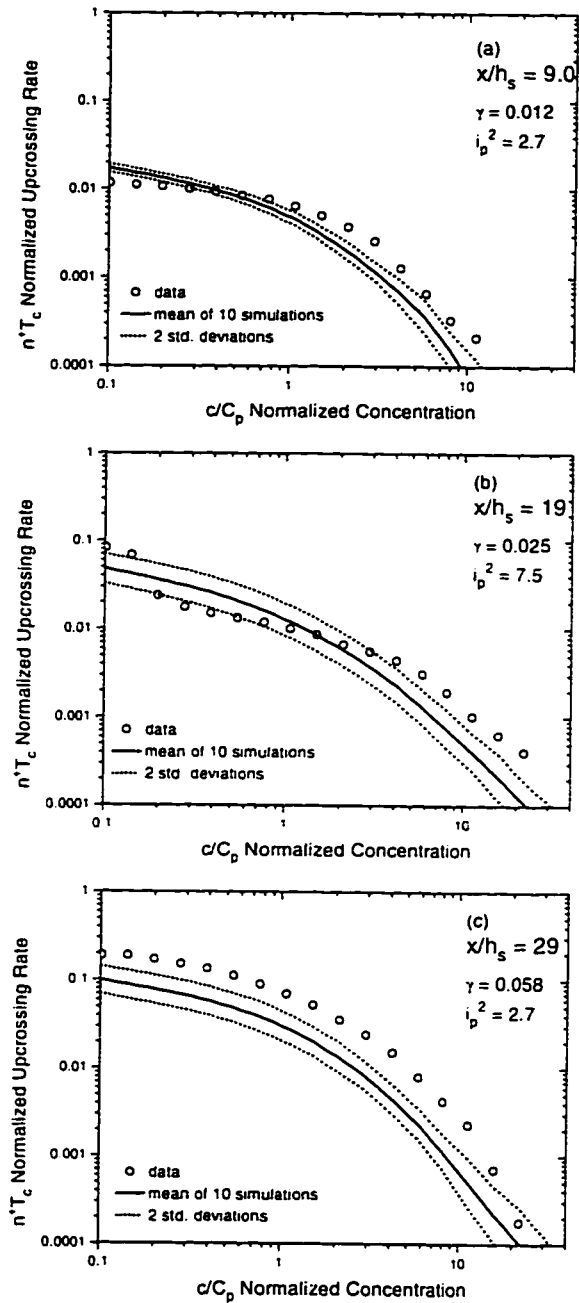


Figure 2.14: Normalized upcrossing rate n^+T_c for highly intermittent time series versus the normalized instantaneous concentration c/C_p near the outside edge of the plume at three downstream positions x/h_s . Cross stream distance from source (a) $y/\sigma_y = 4.1$ (b) $y/\sigma_y = 4.8$ (c) $y/\sigma_y = 2.8$

References

- Aitchison, J. and Brown, J. A. C. (1957), *The Lognormal Distribution*. Cambridge University Press.
- Box, G. E. P. and Muller, M. F. (1958), A note on the generation of random normal deviates, *Annals of Mathematical Statistics*, 29:610–611.
- Carter, E. F. (1994), The Generation and Application of Random Numbers, *Forth Dimensions*, 16(1.2):67–72.
- CCPS (1989), *Guidelines for Chemical Process Quantitative Risk Analysis*. Center for Chemical Process Safety of the American Institute of Chemical Engineers.
- Crow, E. L. and Shimizu, K. (1988), *Lognormal Distributions: Theory and Applications*, Marcel Dekker Inc.
- Du, S. (1995), *Stochastic Models for Turbulent Diffusion*. PhD thesis. University of Alberta.
- Durbin, P. A. (1983), Stochastic Differential Equations and Turbulent Dispersion. Technical report, National Aeronautics and Space Administration. NASA Reference Publication 1103.
- Fackrell, J. E. and Robins, A. G. (1982). Concentration Fluctuations and Fluxes in Plumes from Point Sources in a Turbulent Boundary Layer. *Journal of Fluid Mechanics*, 117:1–26.
- Gardiner, C. W. (1983). *Handbook of Stochastic Methods*. Springer-Verlag.
- Lewellen, W. S. and Sykes, R. I. (1986), Analysis of concentration fluctuations from lidar observations of atmospheric plumes, *American Meteorological Society*, pages 1145–1154.
- Maier, W. L. (1991), A Fast Pseudo Random Number Generator. *Dr. Dobb's Journal*, pages 152–157.
- Mylne, K. R. and Mason, P. (1991). Concentration fluctuation measurements in a dispersing plume at a range of up to 1000 m. *Quarterly Journal of the Royal Meteorological Society*, 117:177–206.
- ten Berge, W. F., Zwart, A., and Appelman, L. M. (1986). Concentration-time mortality response relationship of irritant and systemically acting vapours and gases, *Journal of Hazardous Materials*, 13:301–309.
- Wilson, D. J. (1995), *Concentration Fluctuations and Averaging Time in Vapor Clouds*, Center for Chemical Process Safety of the American Institute of Chemical Engineers.

- Wilson, D. J., Zelt, B. W., and Pittman, W. E. (1991), Statistics of Turbulent Fluctuation of Scalars in a Water Channel, Technical report. Department of Mechanical Engineering, University of Alberta, Edmonton, Alberta.
- Wilson, J. D. and Sawford, B. L. (1996), Review of Lagrangian Stochastic Models for Trajectories in the Turbulent Atmosphere. *Boundary-Layer Meteorology*, 78:191-210.
- Yee, E., Chan, R., Kosteniuk, P. R., Chandler, G. M., Bilotft, C. A., and Bowers, J. F. (1994), Experimental Measurements of Concentration Fluctuations and Scales in a Dispersing Plume in the Atmospheric Surface Layer Obtained Using a Very Fast Response Concentration Detector, *Journal of Applied Meteorology*, 33:996-1016.
- Yee, E., Chan, R., Kosteniuk, P. R., Chandler, G. M., Bilotft, C. A., and Bowers, J. F. (1995). Measurements of Level-Crossing Statistics of Concentration Fluctuations in Plumes Dispersing in the Atmospheric Surface Layer. *Boundary-Layer Meteorology*, 73:53-90.
- Yee, E., Kosteniuk, P. R., Chandler, G. M., Bilotft, C. A., and Bowers, J. F. (1993a). Recurrence Statistics of Concentration Fluctuations in Plumes within a Near-neutral Atmospheric Surface Layer. *Boundary-Layer Meteorology*, 66:127-153.
- Yee, E., Wilson, D. J., and Zelt, B. W. (1993b). Probability distributions of concentration fluctuations of a weakly diffusive passive plume in a turbulent boundary layer. *Boundary-Layer Meteorology*, 64:321-354.
- Zelt, B. W. (1992), *Concentration Fluctuations and their Probability Distributions in Laboratory Plumes*. PhD thesis. University of Alberta, Edmonton, Alberta.

Chapter 3

A Model for Effective Toxic Load from a Hazardous Gas Release

3.1 Introduction

The hazard posed by an acutely toxic gas release depends non-linearly upon the exposure concentration and the exposure duration. At a fixed receptor location in a dispersing atmospheric gas plume, random turbulent dilution and dispersion processes cause wide fluctuations in the instantaneous concentrations from zero (background) levels to greater than 20 times the mean concentration. These large fluctuations coupled with the non-linearity of toxicity with exposure concentration can have a large effect on the toxic response from a release.

Acutely toxic chemicals cause effects ranging from annoyance caused by an offensive odor to fatality. All of these effects are important, but in practice only serious injury or fatalities can be reliably measured and reported. Less severe effects are necessarily subjective and difficult to quantify. Variability in individual susceptibility

means that there are variable levels of response. At low doses only sensitive individuals respond while much higher doses are required to affect the resistant individuals. In some cases, the same sort of reactions leading to fatality may also cause the less severe effects so that dose levels that cause only a small fraction of population fatalities will cause less severe effects in the resistant individuals. In this study, the acute toxicity of a gas is evaluated in terms of the level of fatal response.

The limited information available for creating acute toxicity models consists mostly of experiments in which laboratory animals were exposed to constant concentrations for a fixed period of time and the number of fatalities were recorded. In these experiments, the only independent variables were the mean exposure concentration and the exposure duration.

In 1924, Haber reported experiments with various military poison gases and proposed that the appropriate parameter for describing fatal toxicity was $K = Ct$, where K is some constant value for a given level of fatalities, C is the mean exposure concentration, and t is the exposure duration, see Gelzleichter, Witchi and Last (1992). Haber's law predicts the same level of response provided the product of concentration and time is the same. For example, doubling the exposure concentration would cause the same level of fatalities in half the exposure time. If Haber's law were true, concentration fluctuations would not affect the outcome of a gas release and the mean concentration would be sufficient to predict toxicity.

Busvine (1938) proposed that the toxic response of insecticides was better fit by a non-linear parameter with the exposure concentration and time $C^n t$ where C is the mean exposure concentration, t is the exposure duration, and n is an exponent that is constant for a particular chemical. This parameter is now more widely known as the toxic load $L = C^n t$. The exponent n in the toxic load relationship is typically

found by analyzing experimental data using the probit method first proposed by Bliss (1934a,b). A complete discussion of the probit method is given by Finney (1971).

The toxic load concept and probit relationships have been applied in many studies of acutely toxic gases. Cremer and Warner (1982) applied toxic load to the risk analysis of an industrial facility in Rijnmond Holland. Withers and Lees (1985a,b, 1987) used toxic load to evaluate the effects of chlorine releases. The Center for Chemical Process Safety of the American Institute of Chemical Engineers (CCPS, 1989) lists probit relationships to use for evaluating the hazard of many common industrial gases.

A thorough investigation of acutely toxic gas exposure experiments by ten Berge, Zwart and Appelman (1986) determined that the exponent n in the toxic load parameter is between 1.0 and 3.5 for a wide variety of industrial gases and the most common values of n are between 2 and 3. This non-linear relationship between the effects of concentration, duration and toxic load means that doubling the exposure concentration has the same effect as increasing the exposure time by a factor of 4 to 8. In an atmospheric exposure to a point source plume with concentrations fluctuating between 0 and more than 20 times the mean concentration, this calculated non-linear effect on toxicity is very large.

There have been attempts to deal with the toxicity of fluctuating concentrations by simplifying the fluctuating time series. Griffiths and Megson (1984), Griffiths and Harper (1985) and Griffiths (1991) modelled fluctuating concentrations as a series of constant peak level square concentration pulses and zero concentration intermittent periods. Ride (1984) modelled the fluctuations as uniform spherical eddies of contaminated air suspended inside a cloud of clean air. The problem with both of these approaches is that they oversimplify the exposure concentration fluctuations

and do not include physically realistic limitations on the receptor absorption rates or recovery from previous exposure.

Some recent work has incorporated receptor dependent factors into the toxicity calculations. Ride (1995) notes that the uptake of toxic chemicals is not instantaneous and not all of the high frequency fluctuations are important for toxicity. Saltzman (1996) does not specifically consider toxic load, but does examine the effect that a sine wave fluctuating concentration has on toxicity and notes that the important frequencies of fluctuations are related to the biological half-life of the chemical. However, receptor frequency response is only one of several interacting factors important to the toxic response.

In the present study, the exposure toxic load model is modified by accounting for three receptor response factors: an uptake time constant, a recovery time constant, and a saturation concentration. Applying these factors, the exposure toxic load is converted to an effective toxic load. This effective toxic load model is used in conjunction with realistic simulated time series of concentration fluctuations in a point source plume. Ensemble averages for a wide range of the uptake, recovery, and saturation will be examined to determine their effect on the effective toxic load. A hydrogen sulphide exposure example is considered to examine the effects of realistic receptor response parameters on a realistic exposure. The objective of this study is to demonstrate that the definition of toxic load can be modified to produce more realistic estimates of fatal toxicity.

3.2 Exposure Toxic Load Model

3.2.1 Probit Method

The toxic load equation can be derived from experimental data that are fit using the probit method of Finney (1971). The probit method, first proposed by Bliss (1934a,b), is a way of linearizing a cumulative normal distribution of population response to some toxic exposure variable. One probit unit, Pr , is equal to one standard deviation of the normal distribution. The median or 50th percentile response was defined arbitrarily as $Pr=5.0$ by Bliss. A probit value of $Pr=4.0$ is one standard deviation below the median at a cumulative probability of 16%. That is, it is expected that 16% of the population responds to a toxic load that produces a probit value of 4.0. Similarly, 84% of the population would be expected to respond to a toxic load that produces a probit of $Pr=6.0$, one standard deviation above the mean. The fraction F of the population responding to a toxic exposure can be calculated from the probit value Pr using the following relationship

$$F = \frac{1}{2} \left(\operatorname{erf} \left(\frac{Pr - 5}{\sqrt{2}} \right) + 1 \right) \quad (3.1)$$

where erf is the error function.

For acutely toxic gases it is observed that the logarithm of the toxic load L follows a normal distribution. This implies that the population response level follows a lognormal distribution with L . Toxic load $L = c^n t$ is the combination of two variables, the concentration c and the exposure duration t . To find the value of n for a particular chemical both variables must be considered using a two dimensional probit relationship:

$$Pr = q + r \ln c + s \ln t \quad (3.2)$$

where q is the offset from zero, r is the coefficient of the logarithm of concentration, and s is the coefficient of the logarithm of time. The logarithms in Equation (3.2) produce the required lognormal distribution of response with toxic load. For each experiment the probit of response is recorded along with the logarithm of the concentration c and the logarithm of exposure duration t . The linear two dimensional relationship is solved to give the coefficients q , r , and s .

The toxic load relationship is obtained by combining the last two terms of Equation (3.2):

$$\text{Pr} = q + s \ln c^n t \quad (3.3)$$

where n is the toxic load exponent equal to r/s from Equation (3.2) and the toxic load L is defined as

$$L = c^n t \quad (3.4)$$

In terms of the toxic load L , Equation (3.3) can be rewritten as:

$$\text{Pr} = q + s \ln L \quad (3.5)$$

To determine the proportion of a population responding to a release, the toxic load L is calculated and then Equation (3.5) is used to determine the probit value Pr . The percentage fatalities is obtained from the Pr value and Equation (3.1).

3.2.2 Mean Concentration Toxic Load

In animal experiments, the exposure is in controlled conditions at a constant concentration for a set period of time. In this case, there are no fluctuations in concentration and the instantaneous exposure concentration c is constant with time over the entire

exposure duration t_e . With $c = C$, the mean concentration, the appropriate variables to calculate the toxic load L_{mean} are

$$L_{\text{mean}} = C^n t_e \quad (3.6)$$

The calculation of L_{mean} is the original definition of toxic load. Note that L_{mean} is not the mean toxic load, but rather is a representative toxic load based on the mean concentration C .

The toxic load of a fluctuating exposure concentration could also be calculated with the mean concentration C and the exposure duration t_e . If $n = 1$, the effect of concentration is linear and this is a reasonable approach, but it still does not take into account any uptake, recovery or saturation processes. For most chemicals, where $n > 1$, the mean concentration toxic load L_{mean} misses the important non-linear effects of the concentration fluctuations as well as any limitations on receptor response.

3.2.3 Instantaneous Exposure Toxic Load

In the risk assessment literature, the definition of toxic load has been extended, without any toxicological justification, to include time varying exposure concentrations, see Ride (1984) and ten Berge, Zwart and Appelman (1986):

$$L = \int_0^{t_e} c^n dt \quad (3.7)$$

where c is the exposure concentration as a function of time. This definition of the toxic load L is the total fluctuating exposure toxic load, and is the most useful toxic load for real exposure scenarios. If the toxic load exponent n is greater than 1 then the exposure toxic load L will be larger than the toxic load calculated with the mean exposure concentration L_{mean} .

The exposure toxic load does not take into account any physically realistic limitations on the fluctuations that will determine the effective toxic load that produces fatalities. In Equation (3.7) it is implicitly assumed that:

- uptake of any exposure concentration is instantaneous.
- recovery does not occur, so toxic load increases indefinitely with time and repeated exposures.
- saturation of biological uptake pathways does not occur.

None of these assumptions are justifiable for real exposures and responses.

3.3 Effective Toxic Load

In this study, the problems with calculating the toxic load for fluctuating concentrations are addressed by adding three receptor response parameters:

- uptake time constant τ_{up}
- recovery time constant τ_r
- saturation concentration C_s

With these parameters an effective toxic load L_{eff} is calculated instead of the exposure toxic load.

3.3.1 Uptake Time Constant τ_{up}

The uptake rate of a toxic gas determines how much of the exposure concentration is available to cause damage. We define an effective concentration c_{eff} that is a function of the exposure concentration c and the uptake time constant τ_{up} .

Toxic gases have many possible absorption routes and mechanisms, so there are many possible models of uptake that could be considered. For example, if the gas is a contact irritant, it acts directly on the nose, throat and lung tissue and the relevant effective concentration is the concentration measured in the airways. If it is assumed that each breath fills the lungs with a uniform well-mixed concentration then the effective concentration is the average concentration during the breath. If the toxic gas acts on internal organs it must first be absorbed into the bloodstream through the alveoli in the lungs and the effective concentration is the concentration in the bloodstream. This bloodstream concentration depends on absorption rates and transfer mechanisms between the lungs and the blood. Absorption of a toxic gas through the skin would involve different mechanisms and rates. The uptake process is complex and is gas specific.

In this study, we assume that all of the complex absorption processes that control the effective concentration can be approximated by a simple first order response function. Using the standard equation for a first order response:

$$\frac{dc_{\text{eff}}}{dt} = \frac{c - c_{\text{eff}}}{\tau_{\text{up}}} \quad (3.8)$$

where c_{eff} is the effective concentration, c is the instantaneous exposure concentration, and τ_{up} is the uptake time constant.

The uptake time constant τ_{up} simply filters the exposure concentration fluctuation time series. Rapid changes in concentration are attenuated so c_{eff} fluctuates more slowly than the external exposure concentration. Figure 3.1 illustrates the effect of an uptake time constant with a on an exposure pulse of concentration. The toxic load L_{eff} in this fluctuating exposure accumulates based on the effective concentration c_{eff} and not the external instantaneous exposure concentration c . The uptake time constant

reduces the rate of change of concentration, and so reduces the rate of increase of effective toxic load as well as reducing the final effective toxic load accumulated as compared to the toxic load L calculated using an instantaneous uptake assumption as in Equation (3.7).

3.3.2 Recovery Time Constant τ_r

By definition, no repair or recovery processes are accounted for in exposure toxic load. As a consequence, even a very small exposure concentration will produce a large toxic load if the exposure time is long. This is unrealistic because the atmosphere contains trace concentrations of many toxic gases, but no measurable effects occur in the general population. Even at much higher concentrations there are few or no measurable effects for many chemicals. For example, Young (1983) discusses the case of the people of Rotorua, New Zealand who live in an area with a large amount of geothermal activity and who are routinely exposed to levels of 0.5 to 1.0 ppm of hydrogen sulphide without any apparent ill effects. A standard toxic load exposure calculation using Equation (3.7) would predict that everyone in Rotorua would be dead.

As with uptake, recovery is a complex process involving a number of different biological mechanisms. One method of recovery is elimination of the toxic substance by excretion or metabolic reactions that convert it to a less toxic material. This type of recovery would be based primarily on the internal concentration. Another recovery mechanism is the repair of damaged tissue, with recovery rate dependent on the type of tissue damaged and its repair mechanisms. Repair might occur at a constant rate or at a rate dependent on the amount of damage.

For our model, we arbitrarily chose a recovery rate dependent on the damage

level, which was assumed to be linearly proportional to the current effective toxic load. This assumption makes the recovery process a first order process with recovery time constant τ_r :

$$\frac{dL_{\text{eff}}}{dt} = c_{\text{eff}}^n - \frac{L_{\text{eff}}}{\tau_r} \quad (3.9)$$

Equation (3.9) produces an exponential decrease in the effective toxic load with time to simulate recovery. Because recovery is the most complex of the three receptor responses, alternative recovery models, such as a constant rate recovery independent of damage level, are equally plausible. The objective of this study was to include some recovery mechanism, because accounting for any recovery, even with a simplistic approximation, has a profound effect on estimated fatalities.

Figure 3.1 shows the effect of the recovery time constant with a simple pulse of concentration. If $\tau_r < \infty$ there is some recovery from any toxic load accumulated. This causes a reduction in the total toxic load accumulated and a gradual reduction in the toxic load during periods of zero concentration.

3.3.3 Saturation Concentration C_s

Biological reactions are often limited by the availability of enzymes or reaction sites for the toxicant. To address this issue we propose a saturation concentration C_s that is incorporated into the effective toxic load model:

$$\frac{dL_{\text{eff}}}{dt} = \frac{c_{\text{eff}}^n}{1 + \frac{c_{\text{eff}}^n}{C_s^n}} \quad (3.10)$$

This relationship follows the well-documented Michaelis-Menten enzyme reaction kinetics, see Pratt and Taylor (1990, p.302) .

The saturation concentration C_s simply clips off high concentration peaks and reduces the effective toxic load L_{eff} compared to having no saturation concentration. A simple example of a saturation concentration is shown in Figure 3.1.

3.3.4 Effective Toxic Load Model

The complete effective toxic load model for L_{eff} incorporates an uptake time constant τ_{up} , a recovery time constant τ_r and a saturation concentration C_s . The easiest way to present the model is with two differential equations. First, the uptake time constant τ_{up} is used to calculate the effective concentration c_{eff}

$$\frac{dc_{\text{eff}}}{dt} = \frac{c - c_{\text{eff}}}{\tau_{\text{up}}} \quad (3.11)$$

and then c_{eff} , τ_r and C_s are used to calculate the rate of increase of effective toxic load L_{eff}

$$\frac{dL_{\text{eff}}}{dt} = \left(\frac{c_{\text{eff}}^n}{1 + \frac{c_{\text{eff}}^n}{C_s^n}} \right) - \frac{L_{\text{eff}}}{\tau_r} \quad (3.12)$$

Equations (3.11) and (3.12) can be expressed numerically in time steps of Δt as:

$$c_{\text{eff}(n+1)} = c_{\text{eff}(n)} + \left(\frac{c - c_{\text{eff}(n)}}{\tau_{\text{up}}} \right) \Delta t \quad (3.13)$$

$$L_{\text{eff}(n+1)} = L_{\text{eff}(n)} + \Delta t \left(\frac{c_{\text{eff}(n+1)}^n}{1 + \frac{c_{\text{eff}(n+1)}^n}{C_s^n}} \right) - \frac{L_{\text{eff}(n)}}{\tau_r} \Delta t \quad (3.14)$$

For the case of instantaneous uptake ($\tau_{\text{up}} = 0.0$), no recovery ($\tau_r = \infty$), and no saturation level ($C_s = \infty$) equations (3.11) and (3.12) reduce to the original definition of exposure toxic load toxic load integrated with time over a fluctuating concentration time series as in Equation (3.7).

$$\frac{dL_{\text{eff}}}{dt} = c^n = \frac{dL}{dt} \quad \text{if } \tau_{\text{up}} = 0, \tau_r = \infty, C_s = \infty \quad (3.15)$$

The numerical toxic load model given by equations (3.13) and (3.14) can be applied directly to experimental or numerically generated time series of concentration fluctuations.

3.4 Concentration Fluctuations in Plumes

The effective toxic load model L_{eff} is most useful when applied directly to a concentration time series. Figure 3.2 shows two examples of typical intermittent exposure concentration fluctuation time series that can be described using four parameters:

- intermittency factor γ
- mean concentration C
- conditional fluctuation intensity i_p
- integral time scale of concentration fluctuations T_c

Highly intermittent plumes are characterized by short bursts of high concentration interspersed with long periods of zero concentration. Plumes with a low intermittency are characterized by much smaller fluctuations about the mean concentration.

3.4.1 Intermittency Factor

The intermittency factor γ is defined as the fraction of the total exposure time t_e during which the concentrations are greater than zero (background) concentration. In practice, the cutoff for zero concentration is set by the measurement instrument at some concentration slightly greater than zero or equal to the atmospheric background concentration of the particular chemical. For analysis purposes, all non-measurable

or background concentrations in the fluctuating time series will be treated as zero concentrations.

With the intermittency concept, two different sets of statistics can be calculated for a given time series. Conditional (in-plume) statistics apply only to the non-zero measurable concentrations and are denoted by a subscript "p". The total statistics include all of the zero concentrations as well as the in-plume concentrations and have no subscript.

3.4.2 Mean Concentration

The mean concentration C is the average concentration over the entire duration of the exposure, including the zero periods:

$$C = \int_0^{t_e} c dt \quad (3.16)$$

where c is the instantaneous concentration at time t , and t_e is the total exposure time.

A conditional mean concentration C_p is calculated by including only the non-zero (in-plume) concentrations where:

$$C_p = \frac{C}{\gamma} \quad (3.17)$$

The total mean concentration C is the most sensible concentration to use for comparing two different fluctuation time series. It is the easiest concentration to measure because it is a long term average and is insensitive to the probe response time. Virtually all dispersion models are based on time averaged mass flux balances in a dispersing plume and they provide estimates of only the time or ensemble mean exposure concentration for a particular spatial position.

3.4.3 Fluctuation Intensity

The conditional fluctuation intensity i_p is defined as

$$i_p = \frac{c'_p}{C_p} \quad (3.18)$$

where c'_p is the conditional (in-plume) standard deviation of the concentration. The total fluctuation intensity i includes the zero concentrations and is defined:

$$i = \frac{c'}{C} \quad (3.19)$$

where c' is the standard deviation including the zeroes. The conditional fluctuation intensity i_p and the total fluctuation intensity i are related to each other through the intermittency factor γ by the exact equation:

$$\gamma = \frac{1 + i_p^2}{1 + i^2} \quad (3.20)$$

A derivation of this relationship can be found in Wilson (1995, p. 139).

The conditional fluctuation intensity i_p is used as the parameter of interest because it is easier to interpret than the total fluctuation intensity and is less much sensitive to the intermittency factor γ . The conditional intensity gives an indication of how large the fluctuations are when measurable (non-zero) concentrations are present. If i_p increases, peak concentrations and exposure toxic load will both be higher.

The total time series fluctuation intensity i is less informative because it includes the intermittent periods of zero concentration. If i increases it could be due to either a smaller intermittency factor or an increase in the fluctuation intensity, so two pieces of information are required to decide if the peak concentrations increase.

Any combination of conditional fluctuation intensity i_p , fluctuation intensity i , and intermittency factor γ that satisfies Equation (3.20) is possible, but it has been

observed that in dispersing atmospheric plumes there is some relationship between i^2 and i_p^2 . Wilson (1995, p. 52, p. 139) suggests the following empirical equation determined from a variety of laboratory and full scale plumes:

$$i_p^2 \simeq \frac{2i^2}{2 + i^2} \quad (3.21)$$

Equation (3.21) can be combined with equation (3.20) to determine the relationship between the intermittency factor γ and i_p as illustrated in Figure 3.3.

3.4.4 Fluctuation Time Scale

The time scale T_c is the integral autocorrelation fluctuation time scale of the turbulent concentration fluctuations. The shorter the T_c , the faster the fluctuation process occurs. In the atmosphere, the fluctuation time scale varies depending on the wind speed, atmospheric turbulence, downstream position, height above the ground and distance from the centreline of the plume. Using an approximation for the fluctuation time scale near ground level given by Wilson (1995, p. 104) T_c is typically 10 to 100 seconds for receptor locations a few hundred meters downwind of a point source.

3.5 Parametric Study

Each effective toxic load parameter τ_{up} , τ_r , and C_s was studied by applying the effective toxic load model calculation L_{eff} to an ensemble of random time series of intermittent concentration fluctuations generated with the stochastic simulation technique presented in Chapter 2. Using the relationship between the conditional fluctuation intensity i_p and the intermittency factor γ from Figure 3.3 a realistic range of intermittency factors $\gamma = 0.1, 0.5$ and 0.9 and the corresponding conditional fluctuation

intensities $i_p = 1.4, 1.1$ and 0.7 were tested with the toxic load exponents $n = 1, 2$ and 3 . Ensembles of 100 random time series were generated for each intermittency factor γ and conditional fluctuation intensity i_p pair.

Large ensembles were required to find stable values for highly intermittent fluctuations. Even with 100 realizations there was still significant variability and the plotted lines are not smooth. The implication is that the realization to realization variability is large and that there can be a large difference between the ensemble average level of toxic response and the actual toxic response of a real release that will have only a single realization. This has important implications for estimating the “worst-case” scenario in a risk assessment.

The objective of this parametric study was to determine the range of τ_{up} , τ_r , and C_s that produced a significant effect on the effective toxic load. The effective toxic load L_{eff} calculated from Equations (3.11) and (3.12) is significantly different from either the exposure toxic load L_{mean} calculated with the mean concentration as in Equation (3.4) or the fluctuating exposure toxic load L calculated from the integrated instantaneous exposure concentration as in Equation (3.7).

3.5.1 Toxic Load Ratio (TLR)

For the parametric study of the effective toxic load it is convenient to normalize by the mean concentration exposure toxic load L_{mean} calculated from Equation (3.6) This toxic load ratio TLR is similar to that defined by Ride (1984). The TLR is:

$$TLR = \frac{L_{eff}}{L_{mean}} \quad (3.22)$$

The TLR can also be thought of as an amplification factor for the toxic load caused by the fluctuating concentration.

3.5.2 Fluctuating Concentration Exposure Toxic Load

Consider the case where there is instantaneous uptake ($\tau_{up} = 0$), no recovery ($\tau_r = \infty$) and no saturation level ($C_s = \infty$). The effective toxic load from Equations (3.11) and (3.12) reduces to the fluctuating exposure toxic load L from Equation (3.7). Figure 3.4 shows the toxic load ratio TLR_{fluct} produced by calculating the exposure toxic load with no uptake time constant, no recovery and no saturation.

If the toxic load exponent $n = 1$, the effect of concentration is linear and the fluctuations have no effect on the exposure toxic load. The mean concentration toxic load L_{mean} is correct for this situation. If $n > 1$ the concentration has a non-linear effect and the fluctuations become very important. For example, if $n = 3$ and the intermittency factor is 0.1 with the corresponding fluctuation intensity of 1.4 the TLR_{fluct} amplification factor is about 1500. That is, the fluctuations cause an exposure toxic load 1500 times larger than the toxic load predicted from the mean concentration.

The additional time constants and saturation levels of the effective toxic load model L_{eff} will moderate these TLR_{fluct} amplification factors with realistic limitations on the uptake rate, recovery from the exposure, and a saturation level.

3.5.3 Uptake Time Constant

The uptake time constant τ_{up} was studied by setting the recovery time constant $\tau_r = \infty$ (no recovery) and the saturation concentration $C_s = \infty$ (no saturation). In Figure 3.5 the toxic load ratio with some uptake time constant $TLR_{\tau_{up}}$ was calculated and normalized by the steady state TLR_{∞} that occurs as time $t \rightarrow \infty$. This $TLR_{\tau_{up}}/TLR_{\infty}$ value was plotted against the elapsed time t normalized by the uptake time constant τ_{up} . Figure 3.6 is the value of that steady state toxic load ratio TLR_{∞}

as function of the uptake time constant τ_{up} , the intermittency factor and fluctuation intensity pair (γ, i_p) , and the toxic load exponent n .

Figure 3.5 shows the normalized rate at which the $TLR_{\tau_{up}}$ approaches some steady state value TLR_{∞} . A simple approximation function for this relationship is:

$$\frac{TLR_{\tau_{up}}}{TLR_{\infty}} = \left(1 - \exp \left(-\frac{t}{\tau_{up}} \right) \right)^n \quad (3.23)$$

For all n values, after about $5\tau_{up}$ the $TLR_{\tau_{up}}$ is within about 20% of TLR_{∞} .

Figure 3.6 shows the difference between a fast τ_{up} and a slow τ_{up} and demonstrates the importance of the toxic load exponent n . If the uptake rate is slow, say $\tau_{up} > 100T_c$, all fluctuations are removed by the filtering effect of τ_{up} and the $TLR_{\infty} \simeq 1$. This means that the fluctuations have no enhancing effect because the uptake is so slow and $L_{eff} \simeq L_{mean}$. If the uptake rate is rapid, say $\tau_{up} < 0.01T_c$, then the uptake is effectively instantaneous as the TLR_{∞} values are approximately equal to the TLR_{fluct} values in Figure 3.4 and $L_{eff} \simeq L$.

A typical exposure scenario can be considered to help interpret the information in Figures 3.5 and 3.6. In an atmospheric exposure near ground level a few hundred meters from the source the time scale of the concentration fluctuations is $T_c \simeq 100$ seconds. If the uptake rate for a human was $\tau_{up} \simeq 1$ second, after about $5\tau_{up} \simeq 5$ seconds, the $TLR_{\tau_{up}}$ will be near its steady state value of TLR_{∞} . If the toxic load exponent is $n = 3$ and the fluctuations have a low intermittency factor $\gamma = 0.1$ with a fluctuation intensity of $i_p = 1.4$ then $TLR_{\infty} = 1500$ and the effective toxic load L_{eff} accumulated is about 1500 times larger than the mean concentration exposure toxic load L_{mean} . Even if the uptake rate of the gas were much slower, on the order of 100 seconds $TLR_{\infty} \simeq 500$ and $L_{eff} \simeq 500L_{mean}$.

3.5.4 Recovery Time Constant

The recovery time constant τ_r was isolated by setting the saturation concentration $C_s = \infty$ (no saturation) and the uptake time constant $\tau_{up} = 0$ (instantaneous uptake). In Figure 3.7 the toxic load ratio with some recovery time constant TLR_{τ_r} is normalized by the toxic load ratio that would be calculated with $\tau_r = \infty$ (no recovery) which is equal to the toxic load ratio of the fluctuating exposure toxic load $\text{TLR}_{\text{fluct}}$ as shown in Figure 3.4.

Figure 3.7 shows the decay of the toxic load with time. This decay rate is independent of γ , i_p , and n and is only a function of the elapsed time. After about $10\tau_r$ the TLR_{τ_r} is less than 10% of the $\text{TLR}_{\text{fluct}}$ with no recovery. This relationship can be well approximated by:

$$\frac{\text{TLR}_{\tau_r}}{\text{TLR}_{\text{fluct}}} = 1 - \exp\left(-\frac{\tau_r}{t}\right) \quad (3.24)$$

The recovery time constant always makes the effective toxic load L_{eff} less than the fluctuating exposure toxic load L calculated from Equation (3.7). If the total exposure time is long enough the TLR_{τ_r} amplification factor can be less than 1.0.

For a typical example, consider the hydrogen sulphide biological half life of 20 minutes from Saltzman (1996). This corresponds to a recovery time constant τ_r of about 30 minutes. The toxic load exponent n for hydrogen sulphide is about 2.5. Assume that the exposure is in a moderately intermittent point source plume with $\gamma = 0.5$ and $i_p = 1.1$. If the total exposure time is less than 30 minutes, the recovery time constant has no effect, and $\text{TLR}_{\tau_r}/\text{TLR}_{\text{fluct}}$ is approximately unity so $L_{\text{eff}} \simeq L \simeq 10L_{\text{mean}}$. If the exposure goes on for longer than 300 minutes or 5 hours $L_{\text{eff}} < L_{\text{mean}}$ with significant recovery occurring during the exposure.

3.5.5 Saturation Concentration

The saturation concentration C_s was isolated by setting $\tau_{up} = 0.0$ (instantaneous uptake) and $\tau_r = \infty$ (no recovery). Unlike uptake and recovery, saturation is not a time dependent process. The saturation concentration simply cuts off peak concentrations and has a constant effect throughout the exposure. Because concentration controls the rate of increase of the toxic load, C_s also limits the maximum uptake rate. Figure 3.8 shows the effect of C_s on concentration peaks by comparing the toxic load ratio with some saturation concentration TLR_{C_s} , with the toxic load ratio TLR_{fluct} calculated from the fluctuating exposure concentration. The TLR_{C_s} , amplification factor is independent of the elapsed time, but does depend on the toxic load exponent n , and the (γ, i_p) pair.

If the saturation concentration is very high, that is greater than 100 times the mean concentration $C_s > 100C$, then it has little effect and the TLR_{C_s} , amplification factor is approximately equal to the fluctuating exposure toxic load ratio TLR_{fluct} . As C_s becomes small, more of the high concentration peaks are cut off. If the saturation concentration is approximately equal to the mean concentration then the fluctuation peaks are all removed and the TLR_{C_s} is very small.

Values of the saturation concentration are difficult to find in the literature for any toxic gases. Consider an exposure to an average concentration of 10 ppm of hydrogen sulphide where $n \simeq 2.5$. From Figure 3.8, if the saturation levels are low, on the order of 100 ppm, then the TLR_{C_s}/TLR_{fluct} is about 0.05 for the highly intermittent case with $\gamma = 0.1$. This means that the fluctuations would only amplify the toxic load of the mean concentration by about a factor of 5. The conservative assumption is that the saturation level is very high and therefore the saturation concentration does little to reduce the effects of high peak concentrations.

3.6 Example for Hydrogen Sulfide Exposure

The effective toxic load model is intended to be used by applying it directly to a realistic fluctuating time series. The limited parametric study in Section 3.5 demonstrated the effects of each individual factor τ_{up} , τ_r and C_s , but it is not clear how these receptor response factors interact in a realistic exposure. To demonstrate that these factors are significant the following exposure scenario of hydrogen sulphide gas was considered and the results are shown in Figure 3.9:

- mean concentration $C = 10$ ppm. This is the 8 hour average concentration allowed for occupational exposure in Alberta (Alberta Health, 1988).
- two intermittency factor and fluctuation intensity pairs to simulate a wide range of exposure conditions from near the plume centreline with $\gamma = 0.9$ and $i_p = 0.7$ to the highly intermittent edges of the plume where $\gamma = 0.1$ and $i_p = 1.4$.
- fluctuation time scale $T_c = 100$ seconds is a typical time scale for fluctuations in the atmosphere.
- fatal toxic load calculated from the probit model given by Rogers (1990) for predicting fatalities for human exposures in Alberta. The probit equation is:

$$\text{Pr} = -36.2 + 2.366 \ln c^{2.5} t \quad (3.25)$$

where Pr is the probit value, c is the concentration in ppm, and t is the time in seconds. The toxic load equation from this probit relationship is $L = c^{2.5} t$. Using Equation (3.25) the exposure toxic load required to produce a certain level of fatalities can be calculated. At Pr=3.72 we expect 10% fatalities in the population, $L_{10} = 2.1 \times 10^7$ ppm^{2.5}s. At Pr=5 we expect 50% fatalities and $L_{50} = 3.7 \times 10^7$ ppm^{2.5}s.

- uptake time constant τ_{up} was determined by making the conservative assumption that the uptake rate is governed primarily by the inhalation rate. It is estimated that τ_{up} is about 1 second. Given that the uptake is treated as a first order process this means that the effective concentration c_{eff} would reach 95% of the external concentration c after 3 time constants or 3 seconds (approximately the time for a deep breath).
- recovery time constant τ_r was based on the biological half life of hydrogen sulphide given by Saltzman (1996) of “less than 20 minutes”. This corresponds to a recovery time constant of $\tau_r \simeq 30$ minutes.
- saturation concentration C_s has not been documented in the literature. A conservative assumption of $C_s = 5000$ ppm was used for this simulated hydrogen sulphide exposure.

3.6.1 Simulated Exposure Results

For each intermittency and fluctuation intensity pair 10 separate random realizations were created with the stochastic model and the average effective toxic load L_{eff} was calculated using Equations (3.13) and (3.14). Figure 3.9 shows the results of these calculations. For comparison, L_{mean} from Equation (3.6) calculated using the mean exposure concentration of 10 ppm and the fluctuating exposure toxic load L from Equation (3.7) are also plotted in Figure 3.9. The L_{10} and L_{50} lines indicate the toxic load necessary to cause 10% and 50% fatalities according to Rogers (1990). In these examples only the average toxic loads have been considered, with curves smoothed through variations caused by the small ensemble of 10 realizations. Worst case scenarios could be evaluated by considering a number of random realizations and

finding the time at which the toxic load first exceeds a dangerous level.

If the total exposure time is short, $t < 600$ seconds, then the effective load L_{eff} is approximately equal to the fluctuating exposure toxic load L . The additional parameters of the effective toxic load model have little effect for very short duration exposures. At longer times it is apparent that the exposure toxic load calculated from the mean concentration L_{mean} and the fluctuating exposure toxic load L without any receptor response parameters both increase steadily with time while L_{eff} levels off after approximately 2000 seconds or 30 minutes when the effect of the increasing toxic load caused by uptake is balanced by the recovery process.

3.6.2 Accuracy of the Toxic Load Model

It is difficult to determine the accuracy of any of the methods of calculating the toxic load because there is no direct experimental data available for human or animal exposures to fluctuating concentrations. However, more general information on the toxicity of hydrogen sulphide can be used to estimate which of the toxic load calculation approaches is more realistic.

Figure 3.9 (a) has a mean concentration of 10 ppm, an intermittency factor of $\gamma = 0.9$ and fluctuation intensity $i_p = 0.7$. This relatively constant exposure with small fluctuations about the mean meets the requirements of a safe occupational exposure level according to Alberta Health (1988). The toxic load calculated with the effective toxic load model L_{eff} indicates that not even 10% fatalities would occur with this type of exposure and the toxic load would level off at a relatively safe level. Calculation of the mean concentration exposure toxic load L_{mean} and the fluctuating concentration exposure toxic load L indicate at least 10% fatalities after 30,000 to 60,000 seconds or 8 to 16 hours of exposure. It is inconceivable that the allowable

occupational exposure limit would be set at a level that would produce fatalities, so in this particular case we conclude that the effective toxic load L_{eff} is a more realistic estimation of the actual effects of the release.

In contrast, Figure 3.9 (b) shows a highly intermittent exposures with $\gamma = 0.1$ and $i_p = 1.4$. The time averaged concentration is still 10 ppm, so these fluctuations would meet the Alberta occupational exposure limits. Other exposure limits for hydrogen sulphide have been defined in an attempt to cover some fluctuating situations. For example, the immediate danger to life and health limit (IDLH) is 300 ppm set by the National Institute for Occupational Safety and Health (NIOSH) in the United States, see Environmental Protection Service (1984). There is no time factor given with this value. The exposures in Figure 3.9 (b) do exceed 300 ppm for times as long as $1T_c = 100$ seconds despite the fact the average concentration is only 10 ppm.

In Figure 3.9 (b), the fluctuating exposure toxic load L produces 50% fatalities in about 10 minutes, the effective toxic load L_{eff} indicates up to 50% fatalities within about 30 minutes and the toxic load calculated with the mean concentration L_{mean} predicts 50% fatalities after approximately 28 hours. The fatalities would be caused by exceeding the high concentration levels long enough to cause adverse effects. With large fluctuations it seems reasonable that this could occur relatively quickly. The 28 hour estimate of L_{mean} is probably too long, while the 30 minute estimate of L_{eff} is more reasonable.

With these two simple example release scenarios it seems that the effective toxic load L_{eff} is a more realistic estimation of the fatal response from a hydrogen sulphide release than the mean exposure toxic load L_{mean} or the fluctuating exposure toxic load L_{fluct} .

3.7 Conclusions

The effective toxic load model presented in this study adds three additional receptor response parameters to the standard toxic load model: an uptake time constant τ_{up} , a recovery time constant τ_r , and a saturation concentration C_s . These additional parameters are used to correct the exposure toxic load model which is based on constant concentration and fixed duration exposures to laboratory animals. Real exposure scenarios are much different than these experimental exposures and include large fluctuations about the mean concentration and intermittent periods of zero concentration clean air.

The parametric study demonstrated that the receptor parameters make a significant difference to the toxic load that is calculated for a fluctuating exposure. The simple methods of calculating exposure toxic load using the mean exposure concentration, or even using the instantaneous fluctuating concentration, produce different toxic load levels than those calculated with the effective toxic load model.

Two realistic example hydrogen sulphide exposures were considered to determine the accuracy of the effective toxic load model. There is no direct data available for human exposures to fluctuating concentrations, but some simple concentration exposure standards were used to determine which toxic load model is more realistic. For a low intermittency low fluctuation intensity plume the effective toxic load model agreed with the Alberta occupational exposure limits while the exposure toxic loads predicted unrealistically high fatalities. For a highly intermittent high fluctuation intensity exposure which would exceed the immediate danger to life and health level, all toxic load models predict fatalities, but the effective toxic load model predicted up to 50% fatalities within 30 minutes while the mean concentration exposure toxic load

model required 28 hours to cause fatality. The effective toxic load model provides more consistently realistic estimates of toxicity for a wide range of intermittent fluctuating exposures.

The effective toxic load model is a significant advancement over the standard exposure toxic load calculations because it incorporates some simple receptor response parameters and produces more realistic estimates of fatalities from a fluctuating exposure. Although the ideal toxicity model would be a complete physiologically based pharmacokinetic model of the human body for each specific toxic gas, at the present time this is not technically feasible. The effective toxic load model provides a method of accounting for some of the most important receptor response factors and improving the hazard assessment of toxic releases.

The weakest link in the present effective toxic load model is the simplified recovery process which is difficult to justify in toxicological terms. Future work should test alternative models for recovery and applying the effective toxic load model to toxic gases other than hydrogen sulphide.

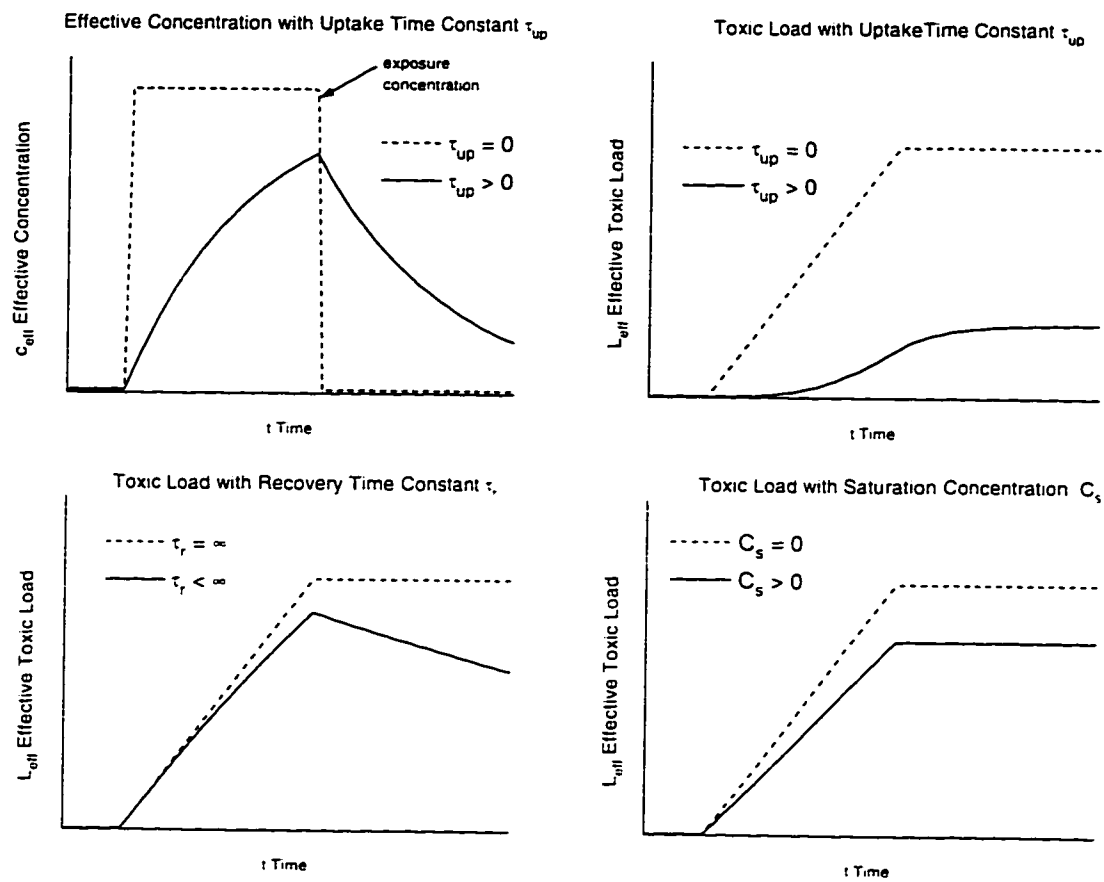


Figure 3.1: Effects of uptake time constant τ_{up} , recovery time constant τ_r and saturation concentration C_s on the effective concentration and the calculated toxic load for a pulse of exposure concentration.

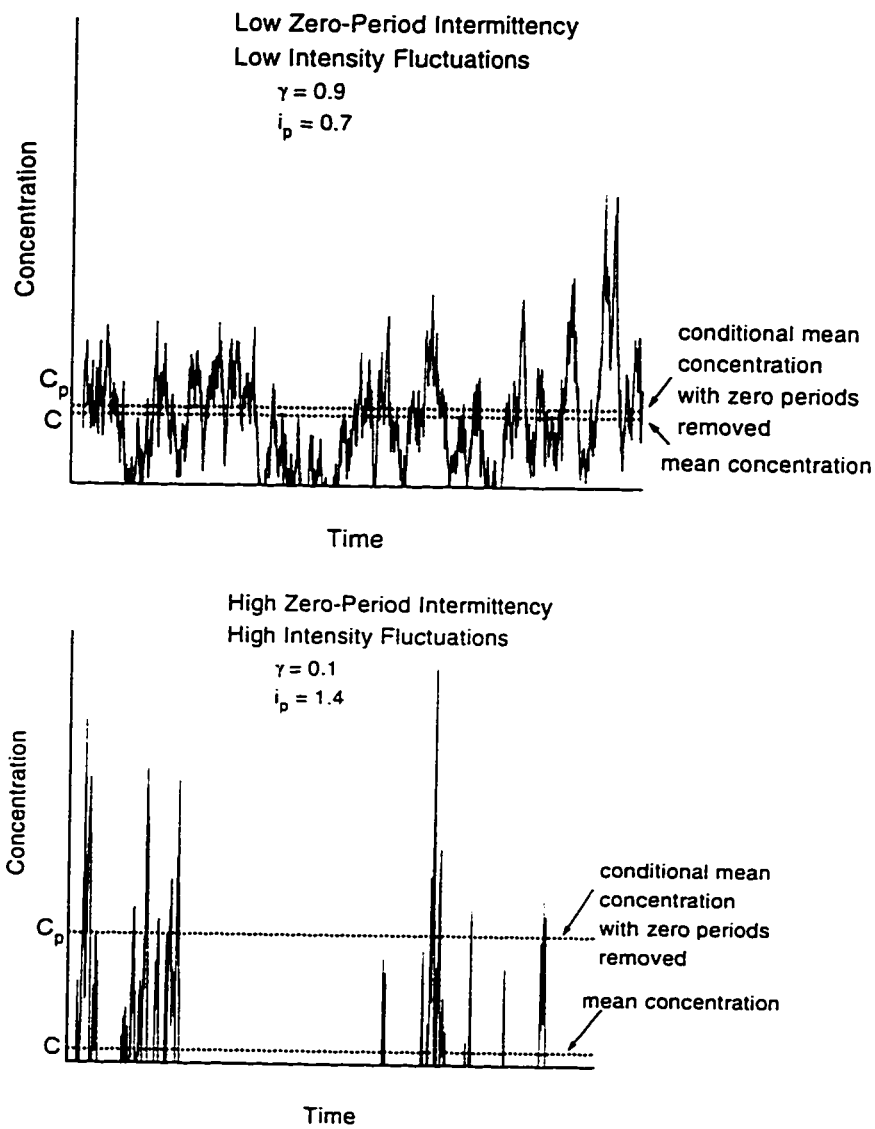


Figure 3.2: Examples of typical intermittent fluctuation time series.

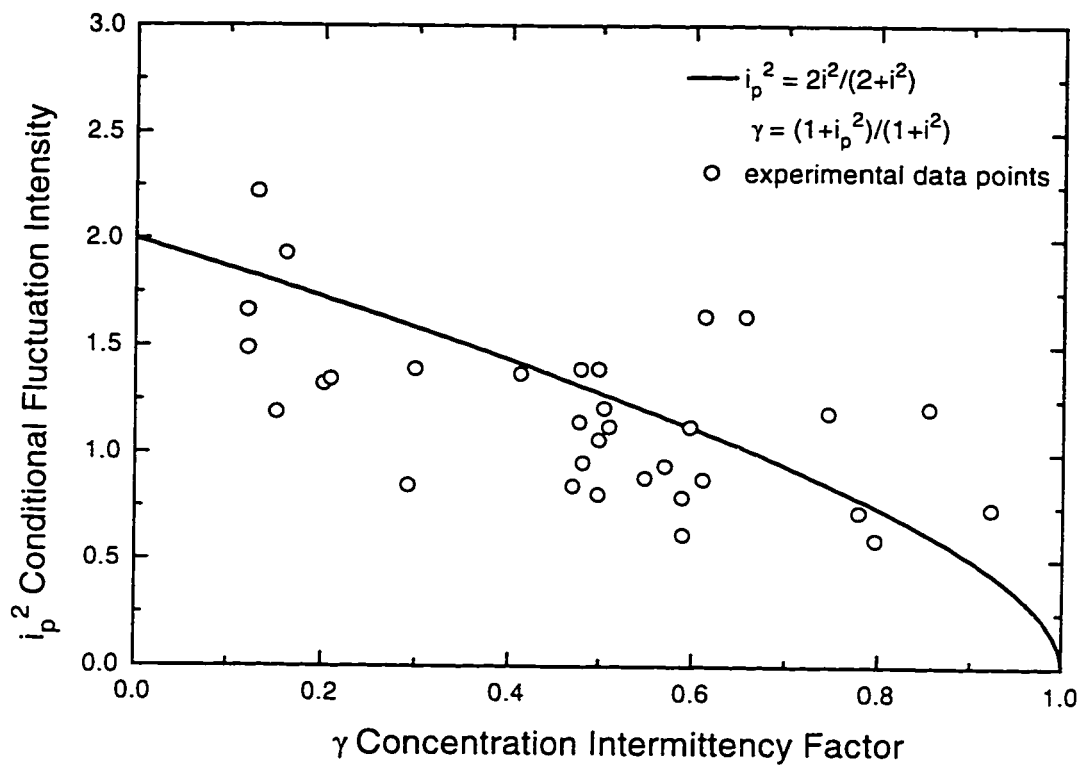


Figure 3.3: Empirical relationship between intermittency γ and the conditional fluctuation intensity i_p^2 , Wilson (1995). Experimental data points from Mylne and Mason (1991) and Fackrell and Robins (1982)

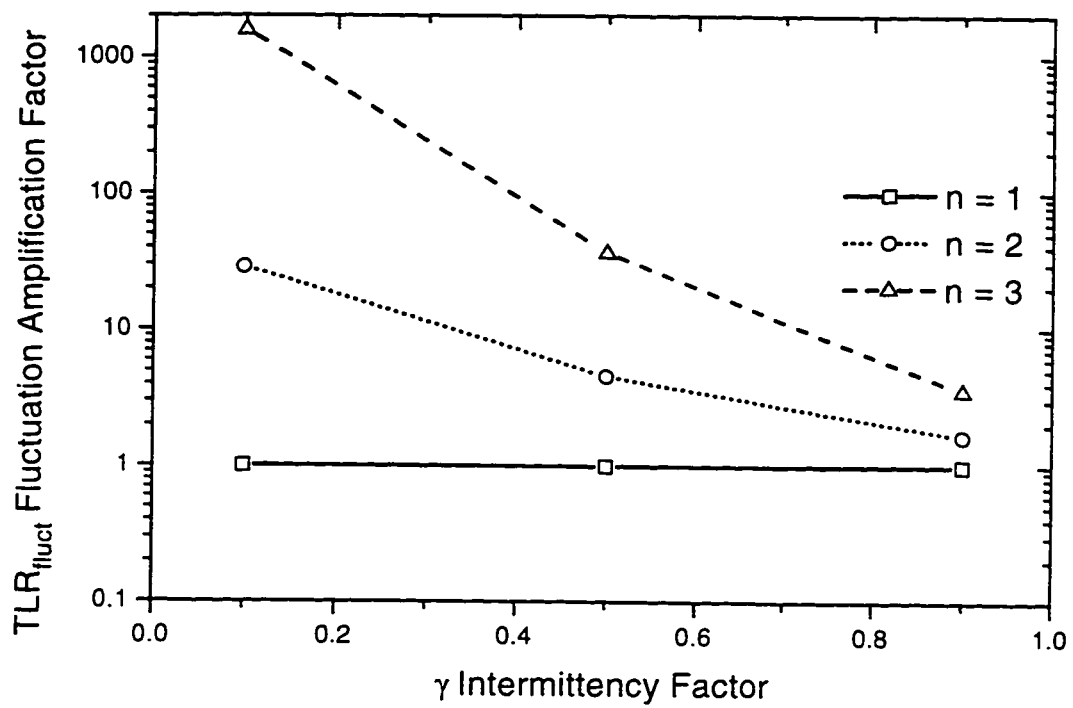


Figure 3.4: Fluctuation amplification factor TLR_{fluct} for the fluctuating exposure toxic load L .

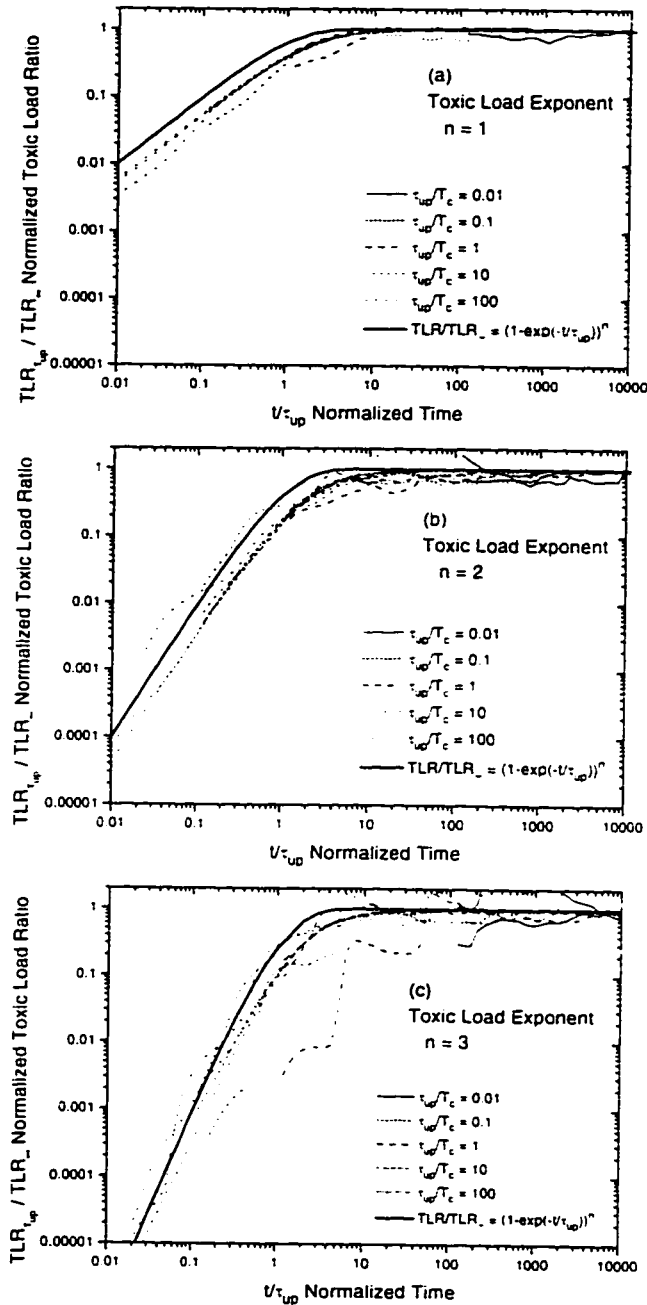


Figure 3.5: Ratio of $TLR_{\tau_{up}}/TLR_{\infty}$ for a range of 5 uptake time constants τ_{up}/T_c at normalized time t/τ_{up} . For each time constant value three different intermittency factor γ and conditional fluctuation intensity i_p combinations were tested (1) $\gamma = 0.1$ and $i_p = 1.4$ (2) $\gamma = 0.5$ and $i_p = 1.1$ (3) $\gamma = 0.9$ and $i_p = 0.7$. Each line is the ensemble average of 100 realizations with one combination of uptake time constant, intermittency factor and fluctuation intensity.

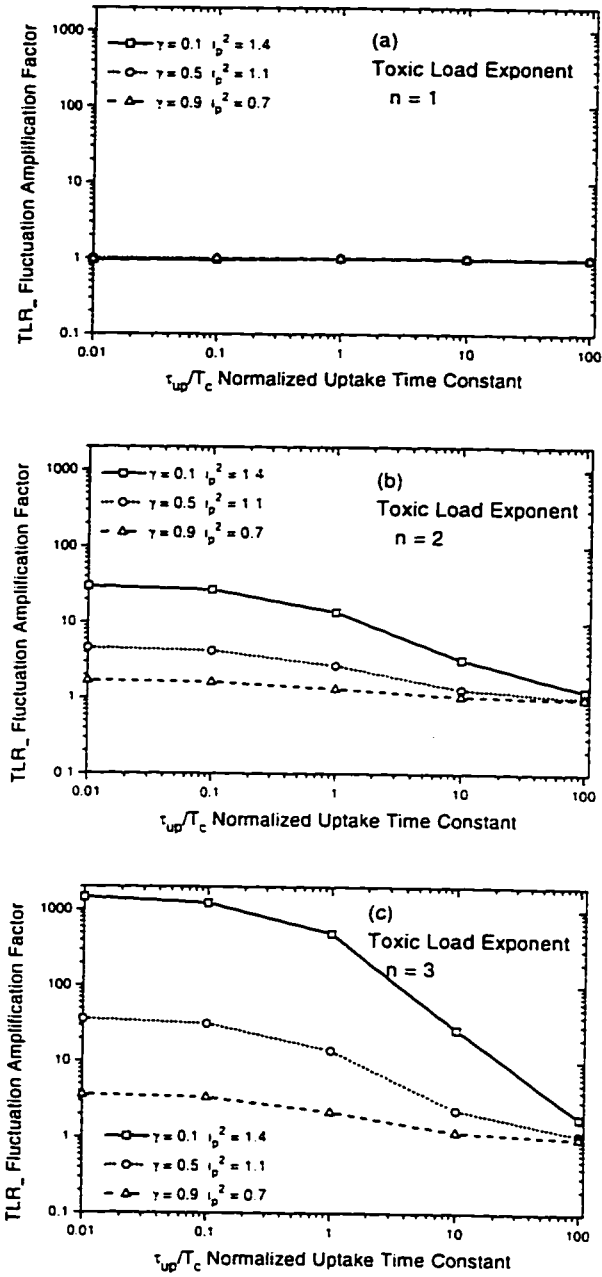


Figure 3.6: Fluctuation amplification factor TLR_{∞} of the effective toxic load model as $t \rightarrow \infty$ for a range of uptake time constants τ_{up}/T_c . Each point is the ensemble average of 100 realizations.

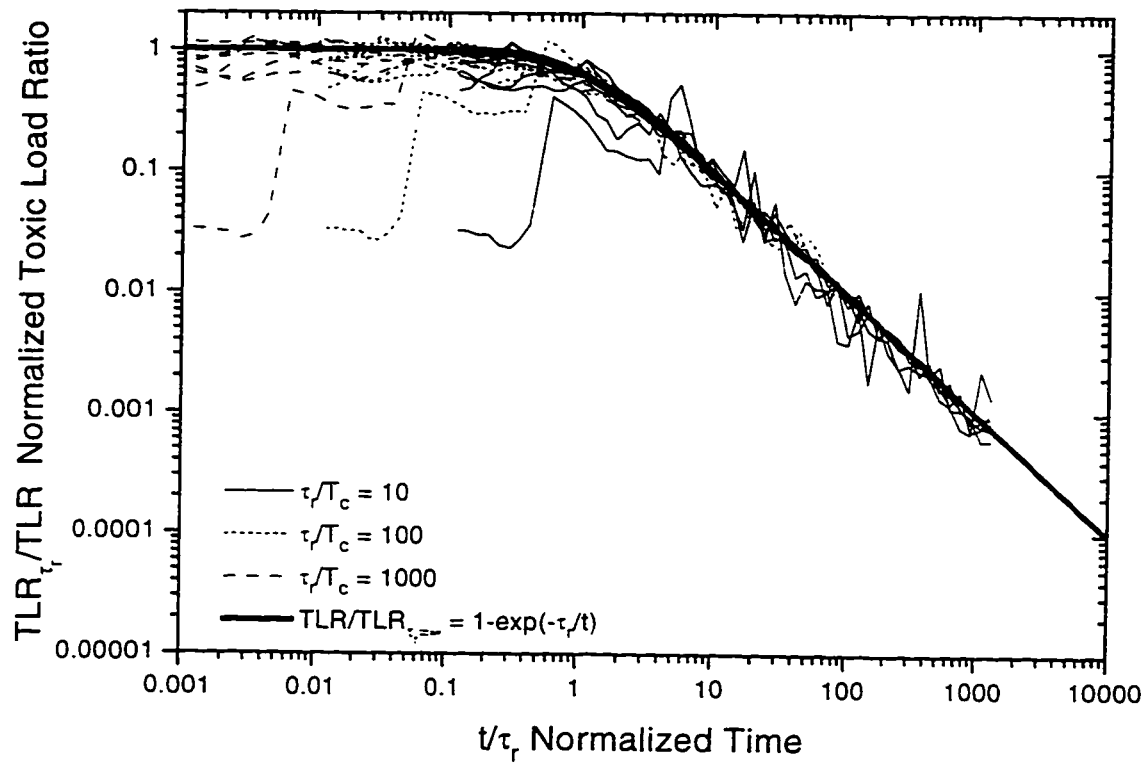


Figure 3.7: Ratio of $TLR_{\tau_r}/TLR_{\text{fluct}}$ for 3 recovery time constants τ_r/T_c at time t/τ_r . For each time constant value three different intermittency factor γ and conditional fluctuation intensity i_p combinations were tested (1) $\gamma = 0.1$ and $i_p = 1.4$ (2) $\gamma = 0.5$ and $i_p = 1.1$ (3) $\gamma = 0.9$ and $i_p = 0.7$. Each line is the ensemble average of 100 realizations with one combination of recovery time constant, intermittency factor and fluctuation intensity.

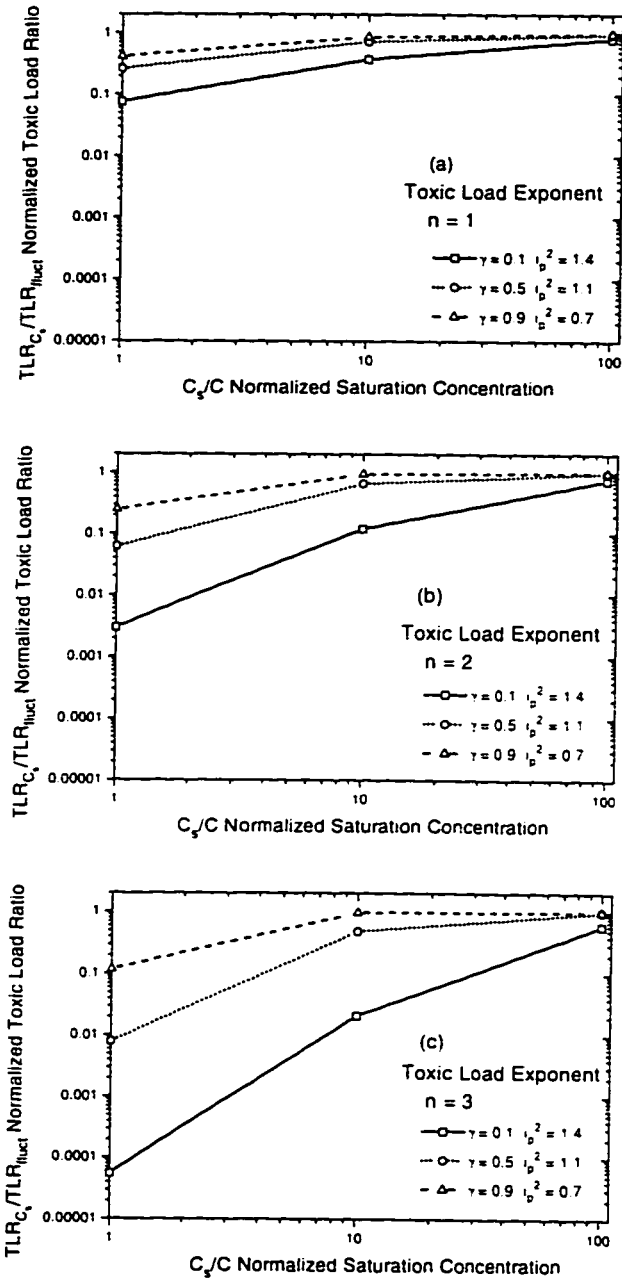


Figure 3.8: Ratio of TLR_{C_s}/TLR_{fluct} as $t \rightarrow \infty$ versus the normalized saturation concentration C_s/C and the intermittency γ fluctuation intensity i_p pair. Each point is the ensemble average of 100 random realizations.

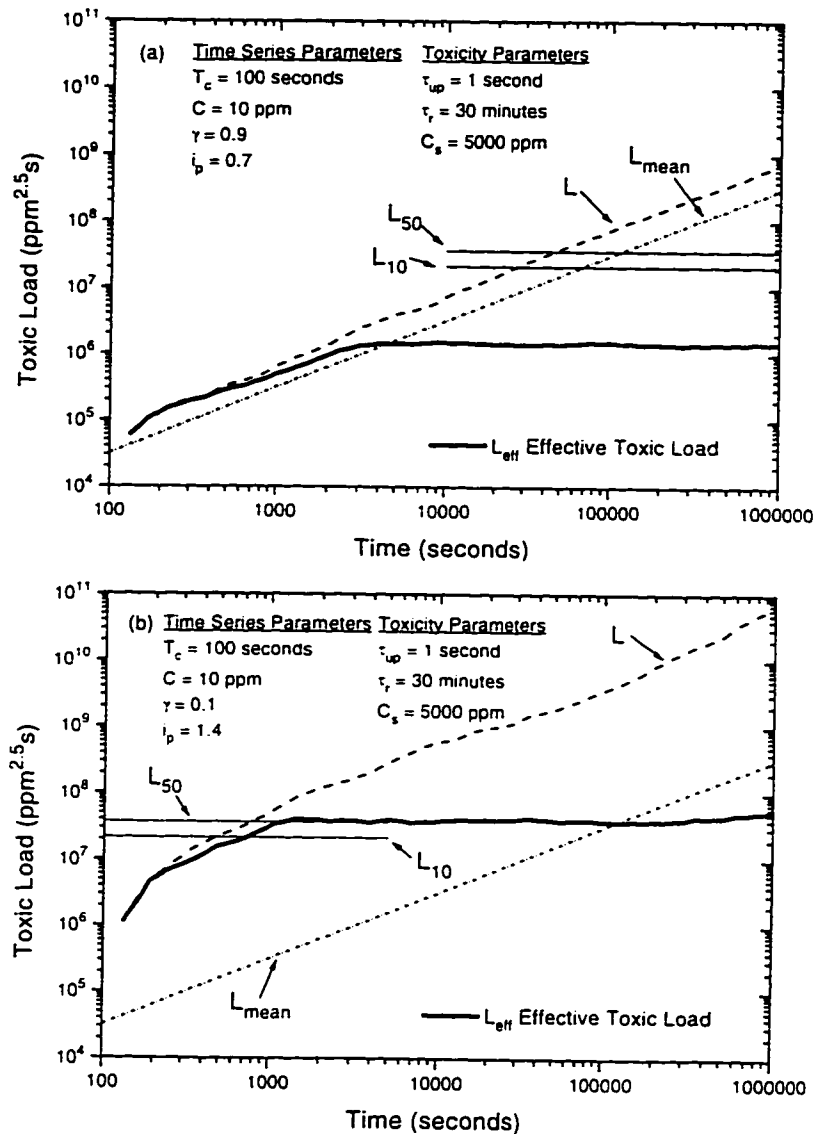


Figure 3.9: Example of the effective toxic load L_{eff} predicted for a hydrogen sulphide exposure (a) high intermittency factor $\gamma = 0.9$ with a corresponding low fluctuation intensity $i_p = 0.7$ and (b) low intermittency factor $\gamma = 0.1$ with a corresponding high fluctuation intensity $i_p = 1.4$. The L_{10} level is the toxic load predicted to cause 10% fatalities in the population and the L_{50} level is the toxic load predicted to cause 50% fatalities according to Rogers (1990). L is the fluctuating exposure toxic load and L_{mean} is the exposure toxic load calculated using the mean concentration. Each L_{eff} , L_{mean} , and L line is the smoothed through ensemble average of 10 realizations.

References

- Alberta Health (1988), *Report on H₂S Toxicity*, 65 pages.
- Bliss, C. I. (1934a), The Method of Probits. *Science*, 79(2037):38-39.
- Bliss, C. I. (1934b), The Method of Probits - A Correction. *Science*, 79(2053):409-410.
- Busvine, J. R. (1938), The toxicity of ethylene oxide to calandra oryzae. c. granaria triboleum castaneum, and cimex lectularius, *Annals of Applied Biology*. 25:605-32.
- CCPS (1989), *Guidelines for Chemical Process Quantitative Risk Analysis*. Center for Chemical Process Safety of the American Institute of Chemical Engineers.
- Cremer and Warner (1982), *Risk Analysis of Six Potentially Hazardous Industrial Objects in the Rijnmond Area. A Pilot Study*. Cremer and Warner Ltd.. published by D. Reidel Publishing Company. Dordrecht, Holland.
- Environmental Protection Service (1984), *Hydrogen Sulphide*. Technical Services Branch, Environmental Protection Programs Directorate. Ottawa. Ontario.
- Fackrell, J. E. and Robins, A. G. (1982). Concentration Fluctuations and Fluxes in Plumes from Point Sources in a Turbulent Boundary Layer. *Journal of Fluid Mechanics*. 117:1-26.
- Finney, D. J. (1971). *Probit Analysis*. Cambridge University Press. third edition.
- Gelzleichter, T. R., Witchi, H., and Last, J. A. (1992), Concentration-Response Relationships of Rat Lungs to Exposure to Oxidant Air Pollutant: A Critical Test of Haber's Law for Ozone and Nitrogen Dioxide. *Toxicology and Applied Pharmacology*. 112:73-80.
- Griffiths, R. F. (1991). The use of probit expressions in the assessment of acute population impact of toxic releases. *Journal of Loss Prevention in the Process Industry*. 4:49-57.
- Griffiths, R. F. and Harper, A. S. (1985). A Speculation on the Importance of Concentration Fluctuations in the Estimate of Toxic Response to Irritant Gases. *Journal of Hazardous Materials*. 11:369-372.
- Griffiths, R. F. and Megson, L. C. (1984). The Effect of Uncertainties in Human Toxic Response on Hazard Range Estimation for Ammonia and Chlorine. *Atmospheric Environment*, 18(6):1195-1206.
- Mylne, K. R. and Mason, P. (1991). Concentration fluctuation measurements in a dispersing plume at a range of up to 1000 m. *Quarterly Journal of the Royal Meteorological Society*, 117:177-206.

- Pratt, W. B. and Taylor, P. (1990), *Principles of Drug Action*. Churchill Livingstone. 3 edition.
- Ride, D. J. (1984), An Assessment of the Effects of Fluctuations on the Severity of Poisoning by Toxic Vapours, *Journal of Hazardous Materials*. 9:235–240.
- Ride, D. J. (1995), A Practical Method of Estimating Toxic Loads in the Presence of Concentration Fluctuations. *Environmetrics*. 6:643–650.
- Rogers, R. E. (1990). Toxicological Justification of the Triple Shifted Rijnmond Equation, Technical report, Alberta Energy Resources Conservation Board. Appendix B, Volume 7 of the Risk Approach: An Approach for Estimating Risk to Public Safety from Uncontrolled Sour Gas Releases.
- Saltzman, B. E. (1996). Assessment of Health Effects of Fluctuating Concentrations Using Simplified Pharmacokinetic Algorithms. *Journal of the Air and Waste Management Association*, 46:1022–1034.
- ten Berge, W. F., Zwart, A., and Appelman, L. M. (1986). Concentration-time mortality response relationship of irritant and systemically acting vapours and gases. *Journal of Hazardous Materials*. 13:301–309.
- Wilson, D. J. (1995). *Concentration Fluctuations and Averaging Time in Vapor Clouds*. Center for Chemical Process Safety of the American Institute of Chemical Engineers.
- Withers, R. M. J. and Lees, F. P. (1985a). The Assessment of Major Hazards: The Lethal Toxicity of Chlorine. Part 1. Review of Information on Toxicity. *Journal of Hazardous Materials*. 12:231–282.
- Withers, R. M. J. and Lees, F. P. (1985b). The Assessment of Major Hazards: The Lethal Toxicity of Chlorine. Part 2. Model of Toxicity to Man. *Journal of Hazardous Materials*. 12:283–302.
- Withers, R. M. J. and Lees, F. P. (1987). The Assessment of Major Hazards: The Lethal Toxicity of Chlorine. Part 3. Crosschecks from Gas Warfare. *Journal of Hazardous Materials*. 15:301–342.
- Young, M. R. (1983), Study Trip to Rotorua, New Zealand. Technical report. Amoco Canada Petroleum Company Ltd., in Hydrogen Sulphide and Health Report.

Chapter 4

Summary and Conclusions

The two unpublished papers in this thesis have presented modelling tools for more realistic evaluation of the effects of accidental gas releases. The first tool is a stochastic numerical simulation of intermittent concentration fluctuation time series and the second tool is an effective toxic load model for predicting fatalities from realistic fluctuating concentration exposures. These two tools complement each other because the effective toxic load model is designed to be applied directly to time series of concentration fluctuations that can be generated either experimentally, or with a simulation like the proposed stochastic model.

4.1 Summary of the Stochastic Simulation

The first paper “Stochastic Simulation of Intermittent Concentration Fluctuations” presented an extension of the stochastic model developed by Du (1995) to the simulation of realistic intermittent concentration fluctuation time series as a first order inertialess Markov process. The user inputs for the simulation are the intermittency

factor γ , the conditional fluctuation intensity i_p^2 and the probability density function (pdf) of concentration $p(c)$ for the intermittent fluctuations.

The stochastic simulation cannot handle intermittent periods directly so the fluctuation time series is first simulated in pseudo-concentration c_{\pm} coordinates using a lognormal pdf without intermittency. After a simulated time series is generated the concentrations are all shifted by a concentration c_{base} to give positive and negative concentrations. The key assumption is that the same physical mixing processes are responsible for both the intermittent periods of zero concentration and the non-zero concentration fluctuations. The negative concentrations are interpreted as zero concentrations where the magnitude of the negative concentration is inversely proportional to the probability of obtaining a non-zero concentration in the next time step. The final result is an intermittent concentration fluctuation time series represented by a clipped lognormal pdf.

The clipped lognormal was tested with experimental data from Wilson (Zelt and Pittman) water channel experiments and found to provide a good fit to the data. There was some evidence of evolution of the probability distribution with downstream distance, but the effect was small. No effect of intermittency, fluctuation intensity or cross stream distance on the pdf was observed.

The stochastic simulation accuracy was demonstrated by comparing the first derivative of concentration with respect to time and the upcrossing statistics of the simulation with the experimental data over a range of intermittency factors $\gamma = 0.7$ to 0.01 and fluctuation intensities $i_p^2 = 2.2$ to 7.5 . In all cases, the concentration derivative and the mean upcrossing rate from the simulation were within a factor of two of the experimental measurements.

4.1.1 Conclusions from the Stochastic Simulation

The stochastic simulation of intermittent concentration fluctuations produced realistic time series of fluctuations so it should be useful for generating time series to evaluate the hazardous effects from gas release. The advantages of the stochastic model are that it can be used to produce time series with any realistic combination of intermittency and fluctuation intensity and it can generate large ensembles of random time series with identical means, variances, and intermittencies. Each simulated time series represents an individual realization of the event and complex hazard models can be time stepped through simulated releases to observe the effects of realization to realization variability as well as large ensemble averages.

All the data used in this thesis were for fluctuations at the source emission height. Near ground level, where most receptor exposures occur, atmospheric mixing is complicated by large shearing forces and the present form of the stochastic simulation may not work as well. Additional experimental and theoretical work is required to further develop and validate this stochastic model for concentration fluctuations near ground level.

The information missing from this presentation of the stochastic model was the determination of the input fluctuation intensity i_p^2 and the intermittency factor γ for a real release. This information must come from other models of dispersion and fluctuating concentrations in plumes or from further research into the general behavior of dispersing gas plumes.

4.2 Summary of the Effective Toxic Load Model

The second paper "A Model for Effective Toxic Load from a Hazardous Gas Release" added three receptor response parameters to the standard exposure toxic load model: an uptake time constant τ_{up} , a recovery time constant τ_r , and a saturation concentration C_s . These additional factors are simplified approximations of the important biological processes that affect toxicity. The receptor response factors are used to correct the exposure toxic load model that is based on constant concentration and fixed duration exposures to laboratory animals for real exposure scenarios that include large fluctuations about the mean concentration and intermittent periods of zero concentration clean air.

The stochastic time series simulation model from the first paper was used to demonstrate that realistic values for the receptor response parameters cause the effective toxic load to be significantly different than either the exposure toxic load calculated using the mean exposure concentration, or the fluctuating exposure toxic load assuming instantaneous uptake, no recovery, and no saturation.

There is no direct experimental toxicology data for fluctuating exposures, so a simple hydrogen sulphide exposure simulation was used to demonstrate that the effective toxic load model provides predictions of fatalities consistent with information obtained from concentration exposure limits set by various regulatory agencies. Using this limited information, it seems that the effective toxic load model produces results that are more consistent with the experiences associated with simple concentration exposure limits than the results produced by the mean concentration exposure toxic load model or the fluctuating exposure toxic load model. The latter produce predictions which are seriously inconsistent with the exposure limits.

4.2.1 Conclusions from the Effective Toxic Load Model

The effective toxic load model is a significant advancement over the standard exposure toxic load calculations because it incorporates some simple, but physically realistic receptor response parameters and produces more realistic estimates of fatalities from a fluctuating exposure for the purposes of hazard assessment. Effective toxic load is a compromise between the very simple exposure toxic load model and the ideal toxicity model which would be a complete physiologically based pharmacokinetic model of the human response for each specific toxic gas.

The weakest link in the present model is the simplified recovery process which is difficult to justify in toxicological terms. Future work should include testing alternative models for recovery and application of the effective toxic load model to toxic gases other than hydrogen sulphide.

References

- Du, S. (1995). *Stochastic Models for Turbulent Diffusion*. PhD thesis, University of Alberta.
- Wilson, D. J., Zelt, B. W., and Pittman, W. E. (1991), *Statistics of Turbulent Fluctuation of Scalars in a Water Channel*. Technical report, Department of Mechanical Engineering, University of Alberta, Edmonton, Alberta.

Appendix A

Relationship between the Deterministic and Random Terms in the Stochastic Differential Equation

The stochastic model for intermittent time series of concentration fluctuation is based on the stochastic differential Langevin equation for a first order Markov process. Consider the simulation of the pseudo-concentrations c_{\pm} where the intermittency factor $\gamma_{\pm} = 1.0$. That is, there are no intermittent periods so all concentrations c_{\pm} are greater than zero. This process is represented by the stochastic differential equation:

$$\frac{dc_{\pm}}{dt} = a(c_{\pm}, t) + b(c_{\pm}, t) \frac{d\zeta}{dt} \quad (\text{A.1})$$

where $a(c_{\pm}, t)$ is the deterministic portion of the time derivative dependent on the concentration c_{\pm} and time t and $b(c_{\pm}, t)d\zeta$ is a random forcing function where $d\zeta$ is a Gaussian random number with a mean of zero and variance dt .

The one-dimensional Fokker-Planck equation that describes the time evolution of

the probability distribution of concentration in terms of a and b is:

$$\frac{\partial p}{\partial t} = -\frac{\partial(ap)}{\partial c_+} + \frac{1}{2} \frac{\partial^2(b^2 p)}{\partial c_+^2} \quad (\text{A.2})$$

It is assumed that the concentration fluctuation process is stationary. therefore $\partial p/\partial t = 0$ and the relationship for a and b in terms of the pdf p is:

$$b^2 = \frac{2}{p} \int_{c_+}^{\infty} -ap \, dc_+ \quad (\text{A.3})$$

The a term is the deterministic term in the fluctuation process. In the absence of fluctuating force, a determines the behavior of the derivative of concentration. It is assumed that in the absence of fluctuations the concentration will stabilize at some fixed value K . The functional form of the a term which includes the time scale of fluctuation process T_{c_+} is:

$$a = \frac{K - c_+}{T_{c_+}} \quad (\text{A.4})$$

where c_+ is the instantaneous concentration.

To find the b term, (A.4) is substituted into (A.3).

$$b^2 = \frac{2}{p} \int_{c_+}^{\infty} \frac{c_+ - K}{T_{c_+}} p \, dc_+ \quad (\text{A.5})$$

The probability distribution p was chosen to be the lognormal

$$p(c_+) = \frac{1}{\sqrt{2\pi}\sigma_{l_+}c_+} \exp\left(-\frac{\ln^2\left(\frac{c_+}{c_{50+}}\right)}{2\sigma_{l_+}^2}\right) \quad (\text{A.6})$$

where σ_{l_+} is the log standard deviation of the probability distribution of pseudo-concentrations, and c_{50+} is the median pseudo-concentration value.

Solving (A.5) for b^2 using (A.6) produces

$$b^2 = \frac{\sqrt{2\pi}\sigma_l c_+}{T_{c_+}} \exp\left(\frac{\ln^2\left(\frac{c_+}{c_{s0+}}\right)}{2\sigma_l^2}\right) \left[\frac{C_+}{2} \left(1 - \operatorname{erf}\left(\frac{\ln\left(\frac{c_+}{c_{s0+}}\right) - \sigma_l^2}{\sqrt{2}\sigma_l}\right)\right) - \frac{K}{2} \left(1 - \operatorname{erf}\left(\frac{\ln\left(\frac{c_+}{c_{s0+}}\right)}{\sqrt{2}\sigma_l}\right)\right) \right] \quad (\text{A.7})$$

where C_+ is the mean pseudo-concentration.

The range of acceptable values for the constant K is a problem of limits. As the pseudo-concentration c_+ approaches zero the value of b^2 goes to infinity if K is less than the mean pseudo-concentration C_+ . If $K < C_+$, the stochastic model will produce very large derivatives as the concentration c_+ becomes small and the pseudo-concentrations c_- can become negative. Negative c_+ concentrations are not acceptable because the pseudo-concentrations must be entirely positive and non-intermittent for the shifting and clipping process to produce the required intermittency and fluctuation intensity. The constant $K \geq C_+$ to avoid producing negative c_+ pseudo-concentrations.

If K is greater than C_+ , b^2 goes to negative infinity. The value of b is imaginary. Imaginary numbers cannot be utilized in the simulation calculations so $K \leq C_+$ in order to avoid this problem.

To satisfy both of the above conditions $K \geq C_+$ and $K \leq C_+$, the constant K must be equal to the mean pseudo-concentration C_+ . With $K = C_+$, b^2 from Equation (A.7) goes to zero as instantaneous pseudo-concentration c_+ goes to zero. No negative concentrations are produced by the stochastic model and the b^2 term always produces real values.

The only value of a that prevents the stochastic model from generating negative

c_+ concentrations or imaginary b values is

$$a = \frac{C_+ - c_+}{T_{c_+}} \quad (\text{A.8})$$

In the absence of a fluctuating component, Equation (A.8) causes the pseudo-concentration c_+ to return to the well-mixed mean pseudo-concentration C_+ .

Appendix B

Clipped Lognormal Distribution

A clipped lognormal probability distribution is used to describe the intermittent time series of concentration fluctuations. All of the steps required to work out the statistics of the clipped lognormal are presented in this appendix. Aitchison and Brown (1957) and Crow and Shimizu (1988) provide detailed information on the lognormal and include some discussion of clipped or truncated lognormal. Integrals of the lognormal distribution used in this analysis are contained in appendix C.

All of the concentrations will be nondimensionalized by normalizing by the median concentration c_{50} including all of the zero periods. The dimensionless concentrations will be denoted by ϕ to avoid confusion with the dimensioned concentration c . Capital letters denote mean values and the subscript “p” indicates conditional in-plume values that exclude intermittent periods of zero concentration. These normalized

concentrations are:

$$\phi = \frac{c}{c_{50}} \quad (\text{B.1})$$

$$\Phi = \frac{C}{c_{50}} \quad (\text{B.2})$$

$$\Phi_p = \frac{C_p}{c_{50}} \quad (\text{B.3})$$

$$\phi' = \frac{c'}{c_{50}} \quad (\text{B.4})$$

$$\phi'_p = \frac{c'_p}{c_{50}} \quad (\text{B.5})$$

where ϕ is the instantaneous dimensionless concentration. Φ is the mean dimensionless concentration. Φ_p is the conditional (in-plume) mean concentration. ϕ' is the standard deviation of the dimensionless concentration, and ϕ'_p is the conditional standard deviation of concentration excluding the zero periods. By definition, $c_{50} = 1$ is the median dimensionless concentration.

The subscript “+” indicates the shifted values of concentration that are used for the purposes of the stochastic simulation where:

$$\tilde{\phi} = \phi_+ - \phi_{\text{base}} \quad (\text{B.6})$$

The $\tilde{\phi}$ concentrations can be positive or negative. To obtain the real concentrations ϕ all of the negative $\tilde{\phi}$ concentrations are transformed to a zero concentration delta function.

In pseudo-concentration “+” coordinates all concentrations are normalized by the median concentration c_{50+} of the pseudo-concentration time series:

$$\phi_+ = \frac{c_+}{c_{50+}} \quad (\text{B.7})$$

$$\Phi_+ = \frac{C_+}{c_{50+}} \quad (\text{B.8})$$

$$\phi'_+ = \frac{c'_+}{c_{50+}} \quad (\text{B.9})$$

where ϕ_+ is the instantaneous dimensionless pseudo-concentration, Φ_+ is the mean dimensionless pseudo-concentration, ϕ'_+ is the standard deviation of the dimensionless pseudo-concentration, and by definition the median dimensionless pseudo-concentration is $\phi_{50+} = 1$.

B.1 Lognormal Distribution in “+” Coordinates

The lognormal density function in “+” coordinates is:

$$p(\phi_+) = \frac{1}{\sqrt{2\pi}\sigma_{l+}\phi_+} \exp\left(-\frac{\ln^2\left(\frac{\phi_+}{\phi_{50+}}\right)}{2\sigma_{l+}^2}\right) \quad (\text{B.10})$$

The mean of the distribution is

$$\Phi_+ = \int_0^{\infty} \phi_+ p(\phi_+) d\phi_+ \quad (\text{B.11})$$

Which is

$$\Phi_+ = \phi_{50+} \exp\left(\frac{\sigma_{l+}^2}{2}\right) \quad (\text{B.12})$$

The variance of the distribution is

$$\phi_+^{\prime 2} = \int_0^{\infty} (\phi_+ - \Phi_+)^2 p(\phi_+) d\phi_+ \quad (\text{B.13})$$

$$= \int_0^{\infty} \phi_+^2 p(\phi_+) d\phi_+ - 2\Phi_+ \int_0^{\infty} \phi_+ p(\phi_+) d\phi_+ + \Phi_+^2 \int_0^{\infty} p(\phi_+) d\phi_+ \quad (\text{B.14})$$

which is

$$\phi_+^{\prime 2} = \phi_{50+}^2 \exp(2\sigma_{l+}^2) - 2\Phi_+ \phi_{50+} \exp\left(\frac{\sigma_{l+}^2}{2}\right) + \Phi_+^2 \quad (\text{B.15})$$

and simplifies to:

$$\phi_+^{\prime 2} = \Phi_+^2 (\exp(\sigma_{l+}^2) - 1) \quad (\text{B.16})$$

B.2 Concentration Shift ϕ_{base}

The strictly positive concentrations of the lognormal distribution in “+” coordinates are shifted by a value of ϕ_{base} to give positive and negative concentrations. The clipped distribution is formed by removing all of the negative concentrations and replacing them with a delta function at zero concentration. The ϕ_{base} value must be chosen such that the probability of getting a concentration greater than zero is equal to the intermittency factor γ . Therefore,

$$\gamma = \int_{\phi_{\text{base}}}^{\infty} p(\phi_+) d\phi_+ \quad (\text{B.17})$$

Solving this gives

$$\gamma = \frac{1}{2} \left(1 - \text{erf} \left(\frac{\ln \left(\frac{\phi_{\text{base}}}{\phi_{50\%}} \right)}{\sqrt{2}\sigma_{l+}} \right) \right) \quad (\text{B.18})$$

B.3 Clipped Lognormal

Now we solve for the parameters of the clipped distribution in ϕ coordinates. (Note the absence of the subscript “+”). The total mean Φ of the clipped lognormal is:

$$\Phi = \int_0^{\phi_{\text{base}}} 0p(\phi_+)d\phi_+ + \int_{\phi_{\text{base}}}^{\infty} (\phi_+ - \phi_{\text{base}})p(\phi_+)d\phi_+ \quad (\text{B.19})$$

These integrals are easily solved to give:

$$\begin{aligned}
\Phi &= \frac{\phi_{50+} \exp\left(\frac{\sigma_{l+}^2}{2}\right)}{2} \left(1 - \operatorname{erf}\left(\frac{\ln\left(\frac{\phi_{\text{base}}}{\phi_{50+}}\right) - \sigma_{l+}^2}{\sqrt{2}\sigma_{l+}}\right)\right) \\
&\quad - \frac{\phi_{\text{base}}}{2} \left(1 - \operatorname{erf}\left(\frac{\ln\left(\frac{\phi_{\text{base}}}{\phi_{50+}}\right)}{\sqrt{2}\sigma_{l+}}\right)\right) \\
&= \frac{\Phi_+}{2} \left(1 - \operatorname{erf}\left(\frac{\ln\left(\frac{\phi_{\text{base}}}{\phi_{50+}}\right) - \sigma_{l+}^2}{\sqrt{2}\sigma_{l+}}\right)\right) \\
&\quad - \frac{\phi_{\text{base}}}{2} \left(1 - \operatorname{erf}\left(\frac{\ln\left(\frac{\phi_{\text{base}}}{\phi_{50+}}\right)}{\sqrt{2}\sigma_{l+}}\right)\right)
\end{aligned} \tag{B.20}$$

The total second moment is

$$\overline{o^2} = \int_0^{\phi_{\text{base}}} o^2 p(o) do + \int_{\phi_{\text{base}}}^{\infty} (o - \phi_{\text{base}})^2 p(o) do \tag{B.21}$$

which when integrated gives

$$\overline{o^2} = \frac{\phi_{50+}^2 \exp(2\sigma_{l+}^2)}{2} \left(1 - \operatorname{erf}\left(\frac{\ln\left(\frac{\phi_{\text{base}}}{\phi_{50+}}\right) - 2\sigma_{l+}^2}{\sqrt{2}\sigma_{l+}}\right)\right) - \tag{B.22}$$

$$\begin{aligned}
&\phi_{\text{base}} \phi_{50+} \exp\left(\frac{\sigma_{l+}^2}{2}\right) \left(1 - \operatorname{erf}\left(\frac{\ln\left(\frac{\phi_{\text{base}}}{\phi_{50+}}\right) - \sigma_{l+}^2}{\sqrt{2}\sigma_{l+}}\right)\right) \\
&\quad + \frac{\phi_{\text{base}}^2}{2} \left(1 - \operatorname{erf}\left(\frac{\ln\left(\frac{\phi_{\text{base}}}{\phi_{50+}}\right)}{\sqrt{2}\sigma_{l+}}\right)\right) \\
&= \frac{\Phi_+^2 \phi_{50+}^2}{2} \left(1 - \operatorname{erf}\left(\frac{\ln\left(\frac{\phi_{\text{base}}}{\phi_{50+}}\right) - 2\sigma_{l+}^2}{\sqrt{2}\sigma_{l+}}\right)\right) \\
&\quad - \phi_{\text{base}} \Phi_+ \left(1 - \operatorname{erf}\left(\frac{\ln\left(\frac{\phi_{\text{base}}}{\phi_{50+}}\right) - \sigma_{l+}^2}{\sqrt{2}\sigma_{l+}}\right)\right) \\
&\quad + \frac{\phi_{\text{base}}^2}{2} \left(1 - \operatorname{erf}\left(\frac{\ln\left(\frac{\phi_{\text{base}}}{\phi_{50+}}\right)}{\sqrt{2}\sigma_{l+}}\right)\right)
\end{aligned} \tag{B.23}$$

With the total mean Φ and the total second moment $\overline{\phi^2}$ we can use the definition for relating the conditional moments to the total moments. Conditional statistics include only the non-zero concentrations.

$$\gamma \overline{\phi_p^n} = \overline{\phi^n} \quad (\text{B.24})$$

therefore

$$\Phi_p = \frac{\Phi}{\gamma} \quad (\text{B.25})$$

and

$$\overline{\phi_p^2} = \frac{\overline{\phi^2}}{\gamma} \quad (\text{B.26})$$

By definition the total second moment $\overline{\phi^2}$ is

$$\overline{\phi^2} = \Phi^2 + \sigma^2 \quad (\text{B.27})$$

and the conditional second moment is

$$\overline{\phi_p^2} = \Phi_p^2 + \phi_p'^2 \quad (\text{B.28})$$

Therefore using (B.26) with (B.27) and (B.28) we get

$$\gamma(\Phi_p^2 + \phi_p'^2) = \overline{\phi^2} \quad (\text{B.29})$$

dividing through by Φ_p^2

$$\gamma\left(1 + \frac{\phi_p'^2}{\Phi_p^2}\right) = \frac{\overline{\phi^2}}{\Phi_p^2} \quad (\text{B.30})$$

then dividing by γ

$$\left(1 + \frac{\phi_p'^2}{\Phi_p^2}\right) = \frac{\overline{\phi^2}}{\Phi^2} \quad (\text{B.31})$$

and subtracting 1

$$\frac{\phi_p'^2}{\bar{\Phi}_p^2} = \frac{\bar{\phi}^2}{\bar{\Phi}^2} - 1 \quad (\text{B.32})$$

The conditional fluctuation intensity i_p^2 is defined as

$$i_p^2 = \frac{\phi_p'^2}{\bar{\Phi}_p^2} \quad (\text{B.33})$$

and using (B.32) we have

$$i_p^2 = \frac{\bar{\phi}^2}{\bar{\Phi}^2} - 1 \quad (\text{B.34})$$

Equation (B.34) is solved using the definitions of the total second moment $\bar{\phi}^2$ from (B.23) and the definition of the total mean $\bar{\Phi}$ from (B.20).

References

- Aitchison. J. and Brown. J. A. C. (1957). *The Lognormal Distribution*. Cambridge University Press.
- Crow. E. L. and Shimizu. K. (1988). *Lognormal Distributions: Theory and Applications*. Marcel Dekker Inc.

Appendix C

Integrals of the Lognormal

Integration of the lognormal probability density function is required to evaluate the moments of the density function. The easiest method to solve for these definite integrals is to find the solution in terms of the error function. Tables of the error function or numerical approximations can then be used to determine the value of the integral.

The lognormal probability density function that is used to describe concentration fluctuations is $p(c)$.

$$p(c) = \frac{1}{\sqrt{2\pi}\sigma_l c} \exp\left(-\frac{\ln^2\left(\frac{c}{c_{50}}\right)}{2\sigma_l^2}\right) \quad (\text{C.1})$$

The general form of the integral that is required in order to calculate moments of the lognormal distribution is $c^a p(c)$.

$$\int_m^n c^a p(c) dc = \int_m^n \frac{c^a}{\sqrt{2\pi}\sigma_l c} \exp\left(-\frac{\ln^2\left(\frac{c}{c_{50}}\right)}{2\sigma_l^2}\right) dc \quad (\text{C.2})$$

$$= \frac{1}{\sqrt{2\pi}\sigma_l} \int_m^n c^{a-1} \exp\left(-\frac{\ln^2\left(\frac{c}{c_{50}}\right)}{2\sigma_l^2}\right) dc \quad (\text{C.3})$$

To solve this integral the following substitution is required. Let

$$t = \frac{\ln\left(\frac{c}{c_{50}}\right) - a\sigma_l^2}{\sqrt{2}\sigma_l} \quad (\text{C.4})$$

therefore

$$dt = \frac{dc}{\sqrt{2}\sigma_l c} \quad (\text{C.5})$$

Changing the limits on the integral

$$\textcircled{c} \quad c = \begin{cases} m & t = \frac{\ln\left(\frac{m}{c_{50}}\right) - a\sigma_l^2}{\sqrt{2}\sigma_l} \\ n & t = \frac{\ln\left(\frac{n}{c_{50}}\right) - a\sigma_l^2}{\sqrt{2}\sigma_l} \end{cases} \quad (\text{C.6})$$

Putting (C.4),(C.5),and (C.6). into (C.3)

$$\int_m^n c^a p(c) dc = \frac{1}{\sqrt{2\pi}\sigma_l} \int_{\frac{\ln\left(\frac{m}{c_{50}}\right) - a\sigma_l^2}{\sqrt{2}\sigma_l}}^{\frac{\ln\left(\frac{n}{c_{50}}\right) - a\sigma_l^2}{\sqrt{2}\sigma_l}} c^{a-1} \exp\left(\frac{a^2\sigma_l^4}{2\sigma_l^2}\right) \exp\left(\frac{-2a\sigma_l^2 \ln\left(\frac{c}{c_{50}}\right)}{2\sigma_l^2}\right) \exp(-t^2) \sqrt{2}\sigma_l c dt \quad (\text{C.7})$$

Canceling out terms in (C.7) gives

$$\int_m^n c^a p(c) dc = \frac{c_{50}^a \exp\left(\frac{a^2\sigma_l^2}{2}\right)}{\sqrt{\pi}} \int_{\frac{\ln\left(\frac{m}{c_{50}}\right) - a\sigma_l^2}{\sqrt{2}\sigma_l}}^{\frac{\ln\left(\frac{n}{c_{50}}\right) - a\sigma_l^2}{\sqrt{2}\sigma_l}} \exp(-t^2) dt \quad (\text{C.8})$$

Given that

$$\operatorname{erf} z = \frac{2}{\sqrt{\pi}} \int_0^z \exp(-t^2) dt \quad (\text{C.9})$$

then using (C.9) in (C.8) the solution is

$$\int_m^n c^a p(c) dc = \frac{c_{50}^a \exp\left(\frac{a^2\sigma_l^2}{2}\right)}{2} \left(\operatorname{erf}\left(\frac{\ln\left(\frac{n}{c_{50}}\right) - a\sigma_l^2}{\sqrt{2}\sigma_l}\right) - \operatorname{erf}\left(\frac{\ln\left(\frac{m}{c_{50}}\right) - a\sigma_l^2}{\sqrt{2}\sigma_l}\right) \right) \quad (\text{C.10})$$

Appendix D

Random Number Generation

A large number of random numbers must be generated to implement a numerical stochastic model. Unfortunately, most random number generators included in compilers and other numerical programs are inadequate for large scale simulations. For example, the ANSI C standard only requires that the period of the generator is at least 32767 (Press et al., 1992). This means that after generating 32767 numbers with a given seed, the sequence repeats itself. Repeating the same sequence of numbers within a stochastic simulation is not the same as generating several million independent random numbers with no repetition.

D.1 Uniform Random Number Generators

In this study two long period random number generators were examined:

ran2 A combination of two linear congruential generators implemented by Press et al. (1992) with a period of approximately 2×10^{18} .

R250 A shift register sequence generator implemented by Maier (1991) and Carter

(1994). The period of the R250 generator is approximately 9×10^7 .

A linear congruential generator, such as that used by `ran2`, generates a random sequence of integers I_1, I_2, I_3, \dots with the recurrence relationship given by Press et al. (1992):

$$I_{j+1} = (aI_j + c) \pmod{m} \quad (\text{D.1})$$

where a is the multiplier, c is the increment, m is the modulus. The values of a, c and m are constants that are carefully chosen to give a random sequence with a period that can be at most m .

A shift register generator is comprised of a 1-bit random number generator of the form:

$$I_k = c_1 I_{k-1} + c_2 I_{k-2} + \dots + c_{p-1} I_{k-p+1} + I_{k-p} \pmod{2} \quad (\text{D.2})$$

where $p = 250$ for the R250 generator and most of the c_i terms are chosen to be zero. From Carter (1994)

$$I_k = I_{k-q} + I_{k-p} \quad (\text{D.3})$$

with $q = 103$. A random bit I_k is generated by adding the previously calculated 103rd and 250th bits that were generated. To implement this generator it is first seeded with another random number generator. Each bit in a random integer is calculated using equation (D.3).

Both the `ran2` and R250 random number generators were tested and there was no discernible difference in the output from the stochastic model. The R250 generator was used for all of the modelling because it proved to be marginally faster than the `ran2` generator.

D.2 Converting to a Gaussian Random Number

The ran2 and R250 random number generators produce integer outputs that are converted to a uniform series of floating point numbers between zero and one by normalizing by the maximum possible integer. For the stochastic simulation a Gaussian distribution of random numbers with a mean of zero and a variance of one is required. The Box-Muller (1958) transformation allows the conversion of uniformly distributed random variables to a Gaussian distribution.

Following Box and Muller (1958) if two random numbers x_1 and x_2 , that come from a uniform distribution between 0 and 1 are chosen they can be converted to two random numbers y_1 and y_2 from a Gaussian distribution by the following equations:

$$\begin{aligned}y_1 &= \sqrt{-2 \ln x_1} \cos 2\pi x_2 \\y_2 &= \sqrt{-2 \ln x_1} \sin 2\pi x_2\end{aligned}\tag{D.4}$$

References

- Box, G. E. P. and Muller, M. F. (1958). A note on the generation of random normal deviates, *Annals of Mathematical Statistics*, 29:610–611.
- Carter, E. F. (1994). The Generation and Application of Random Numbers. *Forth Dimensions*, 16(1.2):67–72.
- Maier, W. L. (1991). A Fast Pseudo Random Number Generator. *Dr. Dobb's Journal*, pages 152–157.
- Press, W. H., Teukolsky, S. A., Vetterling, W. T., and Flannery, B. P. (1992). *Numerical Recipes in C: The Art of Scientific Computing*. Cambridge University Press. second edition.

Appendix E

Experimental Data Compared to the Clipped Lognormal pdf

The choice of the clipped lognormal pdf to describe concentration fluctuations was tested by comparison with the water channel experimental data. For this comparison only conditional (in-plume) concentrations were considered so all concentrations were normalized by the conditional mean concentration C_p . The theoretical clipped lognormal distributions were given the same intermittency γ and conditional fluctuation intensity i_p^2 as the experimental data sets.

The evidence presented in Figures E.1 through E.6 demonstrates that the clipped lognormal is a reasonable distribution to describe the concentration fluctuations at source height. The clipped lognormal fits well over a wide range of intermittency factors from $\gamma = 0.7$ to $\gamma = 0.012$ and for a range in fluctuation intensities from $i_p^2 = 2.2$ to $i_p^2 = 7.5$. The plots show some evidence that the shape of the probability distribution of concentration evolves slowly with downstream distance, but the effect is small.

E.1 Probability Density

Figures E.1 and E.2 are the normalized conditional probability densities $p_p(c/C_p)$ where:

$$\int_0^{\infty} p_p\left(\frac{c}{C_p}\right) d\left(\frac{c}{C_p}\right) = 1.0 \quad (\text{E.1})$$

The clipped lognormal pdf in Figures E.1 and E.2 fits the data well over a wide range of intermittencies with a maximum error of about a factor of 2. There is little apparent difference in these plots between the clipped lognormal and unclipped lognormal. A lognormal and a clipped lognormal pdf should look different at very low concentrations $c < 0.1C_p$ because the lognormal goes to zero at $c = 0$ while the clipped lognormal pdf has some value greater than zero. The probe background noise level intermittency cutoff of the experimental data eliminated concentrations less than $0.1C_p$ so the fit of this portion of the pdf cannot be evaluated.

E.2 Cumulative Probability

Figures E.3 and E.4 are the normalized conditional cumulative probability distributions (cdf) $P_p(c/C_p)$ defined as the probability of finding a concentration less than c/C_p

$$P_p\left(\frac{c}{C_p}\right) = \int_0^{\frac{c}{C_p}} p_p\left(\frac{c}{C_p}\right) d\left(\frac{c}{C_p}\right) \quad (\text{E.2})$$

The log-log cdf plots emphasize the low concentrations $c < C_p$ where the difference between the lognormal and the clipped lognormal are apparent.

In Figures E.3 and E.4 there is some evidence that the probability distribution evolves with downstream distance although it seems to be independent of intermittency and fluctuation intensity. At $x/h_s \leq 19$ the clipped lognormal fits the data

better than the lognormal, but at $x/h_s = 29$ the clipped lognormal overestimates the cdf of concentration and the lognormal provides a better fit. A similar effect is reported in Yee, Wilson and Zelt (1993) who found that a clipped normal distribution provides a good fit to low dilutions near the source while the lognormal fits better far downwind. Although the initial assumption that the shape of the pdf is independent of location may not be true, a clipped lognormal provides a reasonable fit to the data in the present study at downstream locations from $x/h_s = 9.0$ to 29.

E.3 Exceedance Probability

Figures E.5 and E.6 show the normalized conditional exceedance probability $E_p(c/C_p)$ defined as the probability of finding a concentration greater than c/C_p

$$E_p\left(\frac{c}{C_p}\right) = \int_{\frac{c}{C_p}}^{\infty} p_p\left(\frac{c}{C_p}\right) d\left(\frac{c}{C_p}\right) = 1 - P_p\left(\frac{c}{C_p}\right) \quad (\text{E.3})$$

The log-log plots of exceedance probability emphasize the high concentrations $c > C_p$ and complement the information presented by the cdf. Agreement with the experimental data is within a few percent up to $E_p = 0.1$, that is the 90th percentile concentration. At the 99th percentile concentration or $E_p = 0.01$, the error is within a factor of two, even when the intermittency factor γ is very small and there are measurable concentrations only 1% of the total time. All of the plots go to $E_p = 0.00001$ that gives the concentration that is exceeded only 0.001% of the time during which there is a measurable concentration. This low probability means that there are at only 1 or 2 events in the entire experimental data set that exceeded that concentration. It is difficult to evaluate the fit at these high concentration, low probability values, because only 125,000 data points were recorded in each experimental time series.

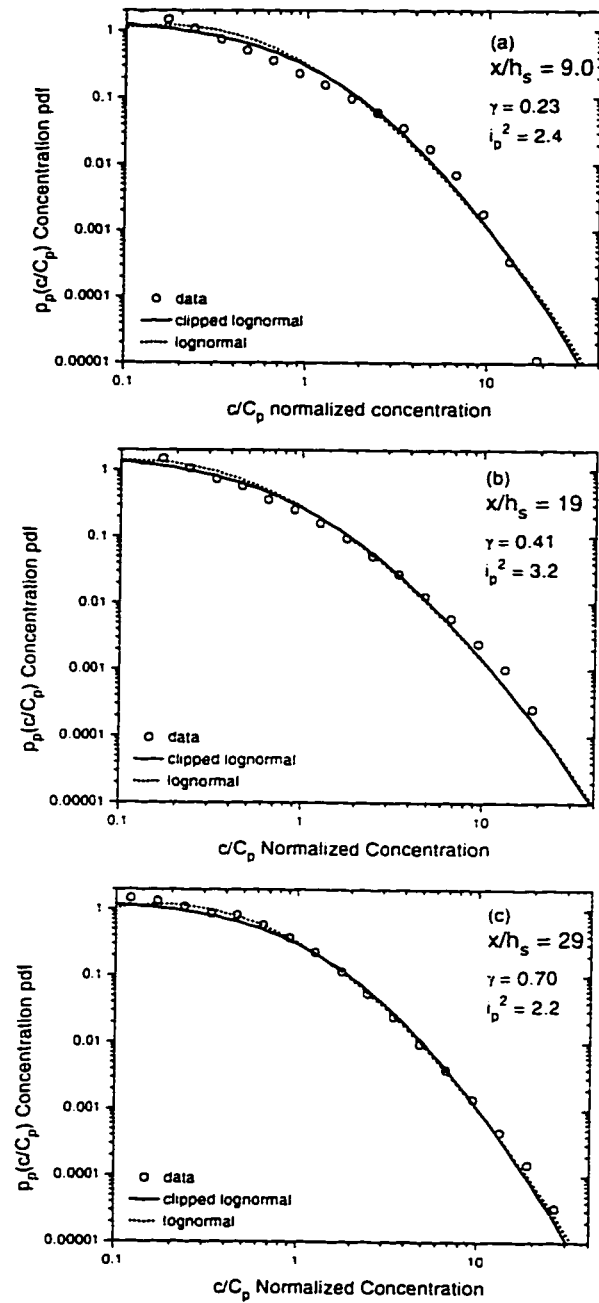


Figure E.1: Conditional probability density p_p for moderately intermittent fluctuations of the concentration c/C_p near the centreline of the plume. Cross stream distance from source (a) $y/\sigma_y = 0.3$ (b) $y/\sigma_y = 0.25$ (c) $y/\sigma_y = 0.18$

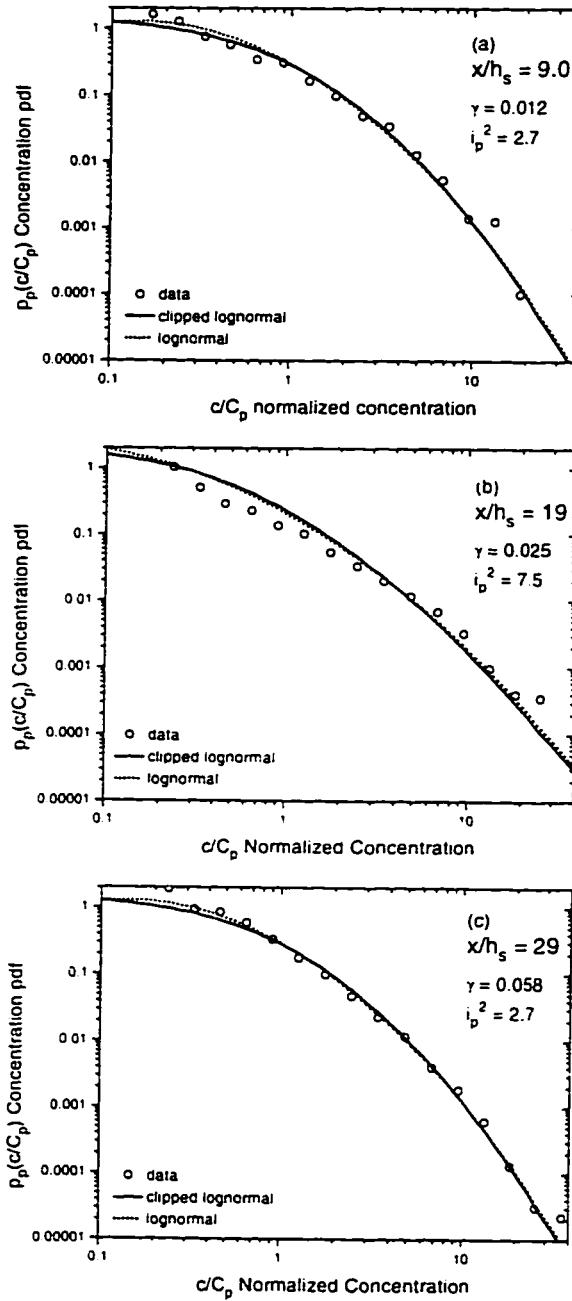


Figure E.2: Conditional probability density p_p for highly intermittent fluctuations of the concentration c/C_p on the outside edge of the plume. Cross stream distance from source (a) $y/\sigma_y = 4.1$ (b) $y/\sigma_y = 4.8$ (c) $y/\sigma_y = 2.8$

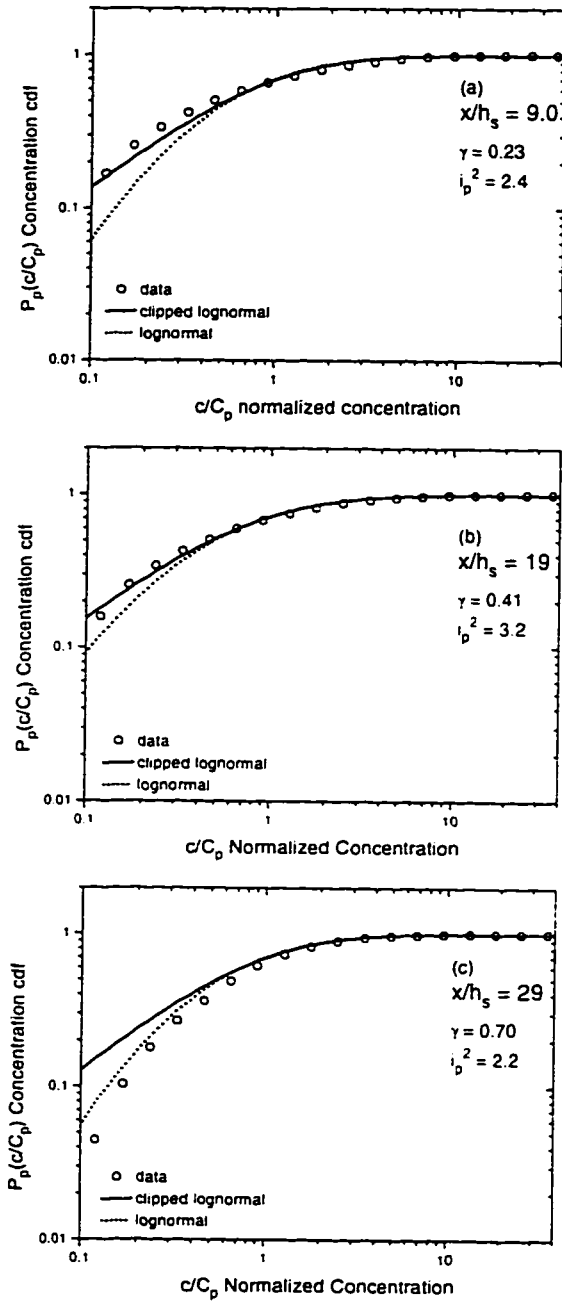


Figure E.3: Conditional cumulative probability distribution P_p for moderately intermittent fluctuations of the concentration c/C_p near the centreline of the plume. Cross stream distance from source (a) $y/\sigma_y = 0.3$ (b) $y/\sigma_y = 0.25$ (c) $y/\sigma_y = 0.18$

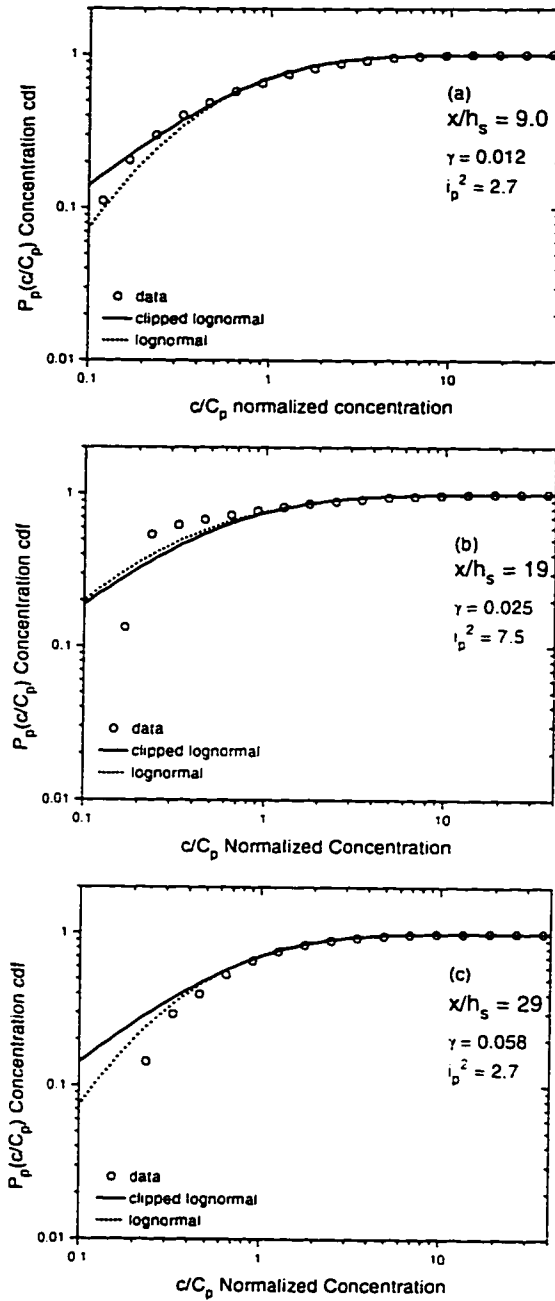


Figure E.4: Conditional cumulative probability distribution P_p for highly intermittent fluctuations of the concentration c/C_p on the outside edge of the plume. Cross stream distance from source (a) $y/\sigma_y = 4.1$ (b) $y/\sigma_y = 4.8$ (c) $y/\sigma_y = 2.8$

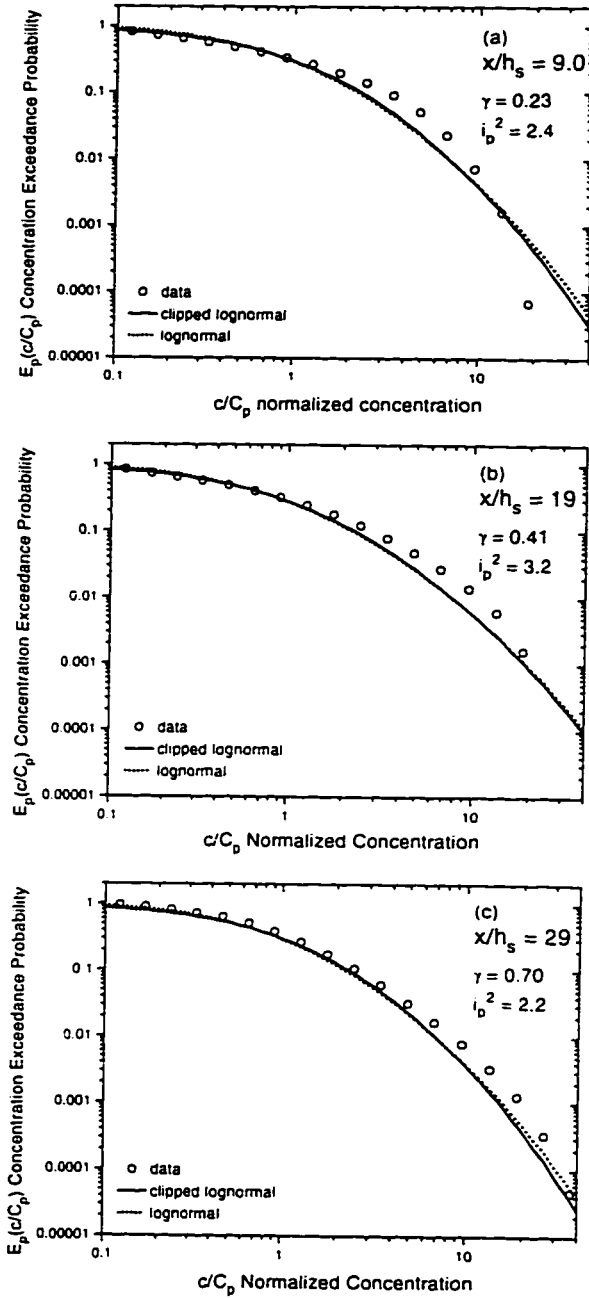


Figure E.5: Conditional exceedance probability E_p for moderately intermittent fluctuations of the concentration c/C_p near the centreline of the plume. Cross stream distance from source (a) $y/\sigma_y = 0.3$ (b) $y/\sigma_y = 0.25$ (c) $y/\sigma_y = 0.18$

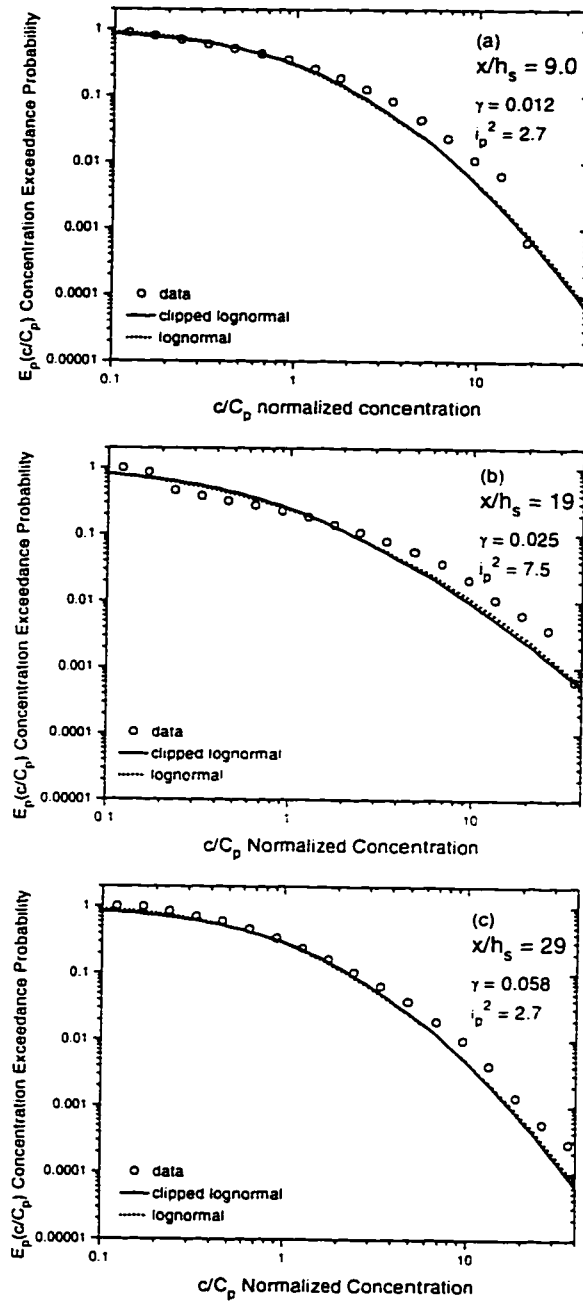


Figure E.6: Conditional exceedance probability E_p for highly intermittent fluctuations of the concentration c/C_p on the outside edge of the plume. Cross stream distance from source (a) $y/\sigma_y = 4.1$ (b) $y/\sigma_y = 4.8$ (c) $y/\sigma_y = 2.8$

References

Yee, E., Wilson, D. J., and Zelt, B. W. (1993), Probability distributions of concentration fluctuations of a weakly diffusive passive plume in a turbulent boundary layer. *Boundary-Layer Meteorology*, 64:321–354.